Cross-kingdom RNA interference in the *Botrytis*-plant interaction

Dissertation der Fakultät für Biologie
der Ludwig-Maximilians-Universität München

An-Po Cheng (M. Sc.)

München, 2025

Diese Dissertation wurde angefertigt

unter der Leitung von Dr. habli. Arne Weiberg

am Lehrstuhl für Genetik, Fakultät für Biologie

der Ludwig-Maximilians-Universität München

Erstgutachter: Dr. habli. Arne Weiberg

Zweitgutachter: Prof. Dr. Martin Parniske

Tag der Abgabe: 30. Juni 2025

Tag der mündlichen Prüfung: 4. November 2025

Eigenständigkeitserklärung

Hiermit versichere ich an Eides statt, dass die vorliegende schriftliche Dissertation mit dem Titel

Cross-kingdom RNA interference in the *Botrytis*-plant interaction

von mir selbstständig verfasst wurde und dass keine anderen als die angegebenen Quellen und Hilfsmittel benutzt wurden. Die Stellen der Arbeit, die anderen Werken dem Wortlaut oder dem Sinne nach entnommen sind, wurden in jedem Fall unter Angabe der Quellen (einschließlich des World Wide Web und anderer elektronischer Text- und Datensammlungen) kenntlich gemacht. Weiterhin wurden alle Teile der Arbeit, die mit Hilfe von Werkzeugen der künstlichen Intelligenz de novo generiert wurden, durch Fußnote/Anmerkung an den entsprechenden Stellen kenntlich gemacht und die erwendeten Werkzeuge der künstlichen Intelligenz gelistet. Die genutzten Prompts befinden sich im Anhang. Diese Erklärung gilt für alle in der Arbeit enthaltenen Texte, Graphiken, Zeichnungen, Kartenskizzen und bildliche Darstellungen.

München, 21.11.2025

_____

An-Po Cheng

Affidavit

Herewith I certify under oath that I wrote the accompanying Dissertation thesis myself.

Title: Cross-kingdom RNA interference in the *Botrytis*-plant interaction

In the thesis no other sources and aids have been used than those indicated. The passages of the thesis that are taken in wording or meaning from other sources have been marked with an indication of the sources (including the World Wide Web and other electronic text and data collections). Furthermore, all parts of the thesis that were de novo generated with the help of artificial intelligence tools were identified by footnotes/annotations at the appropriate places and the artificial intelligence tools used were listed. The prompts used were listed in the appendix. This statement applies to all text, graphics, drawings, sketch maps, and pictorial representations contained in the Work.

München, 21.11.2025

_____

An-Po Cheng

Table of Contents

General abbreviation index

Argonaute	AGO
Botrytis cinerea	*B. cinerea*
cross-kingdom RNA interference	ckRNAi
double-stranded RNA	dsRNA
effect-triggered immunity	ETI
host-induced gene silencing	HIGS
Hyaloperonospora arabidopsidis	*Hpa*
knock-out	ko
microRNA	miRNA
meiotic silencing by unpaired DNA	MSUD
pattern-triggered immunity	PTI
quantitative real-time polymerase chain reaction	qRT-PCR
RNA-dependent RNA polymerase	RDR
RNA-induced silencing complexes	RISC
RNA interference	RNAi
small interfering RNA	siRNA
small RNA	sRNA
short tandem target mimics	STTM

List of publications

Publications provided in this thesis

1. Cheng, An-Po, Bernhard Lederer[*], Lorenz Oberkofler[*], Lihong Huang, Nathan R Johnson, Fabian Platten, Florian Dunker, Constance Tisserant, and Arne Weiberg. 2023. A fungal RNA-dependent RNA polymerase is a novel player in plant infection and cross-kingdom RNA interference, *PLoS pathogens*, 19: e1011885**.**

   [*] These authors contributed equally to the work.
2. Cheng, An-Po, Lihong Huang, Lorenz Oberkofler, Nathan R Johnson, Adrian-Stefan Glodeanu, Kyra Stillman, and Arne Weiberg. 2025. Fungal Argonaute proteins act in bidirectional cross-kingdom RNA interference during plant infection, *Proceedings of the National Academy of Sciences*, 122: e2422756122.

Additional publications/articles (not included in this thesis)

- **Unpublished paper**

1. Baoye He[*], Qiang Cai[*], Arne Weiberg[*], Wei Li, An-Po Cheng, Shouqiang Ouyang, Katherine Borkovich, Jason Stajich, Cei Abreu-Goodger, Hailing Jin. *Botrytis cinerea* small RNAs are associated with tomato AGO1 and silence tomato defense-related target genes supporting cross-kingdom RNAi. 2023. *bioRxiv*.

   [*] These authors contributed equally to the work.
2. Annika Lubbe[*], Manisha Haag[*], An-Po Cheng[*], Bernhard Lederer, Jin Yan Khoo, Florian Dunker, Arne Weiberg[#], Caroline Gutjahr[#]. Cross-kingdom RNA interference promotes arbuscular mycorrhiza development. 2025. *Nature Plants (under review).*

   [*] These authors contributed equally to the work. [#]Corresponding authors

- **Review article**

1. An-Po Cheng, Seomun Kwon, Trusha Adeshara, Vera Göhre, Michael Feldbrügge, Arne Weiberg. 2023. Extracellular RNAs released by plant-associated fungi: from fundamental

mechanisms to biotechnological applications. *Applied Microbiology and Biotechnology,* 107(19):5935-5945.

Declaration of contribution as co-author

Publication 1

Cheng, An-Po, Bernhard Lederer, Lorenz Oberkofler, Lihong Huang, Nathan R Johnson, Fabian Platten, Florian Dunker, Constance Tisserant, and Arne Weiberg. 2023. A fungal RNA-dependent RNA polymerase is a novel player in plant infection and cross-kingdom RNA interference, *PLoS pathogens*, 19: e1011885.

In this publication, I designed and performed all experiments and contributed all data, if they are not listed below.

Lihong Huang generated the construct and performed the fungal transformation of bc*rdr1* ko mutant. Constance Tisserant performed the first selection of single spore isolation for accurate transformants. I performed the single spore isolation for homokaryotic *bcrdr1*. I generated all the constructs and mutans for all the other *Botrytis* strains. Fabian Platten and I contributed to the pathoassay and qRT-PCR. The next generation sequencing data was together performed by Arne Weiberg, Nathan R Johnson and me. Florian Dunker generated the transformation of STTM transgenic plants. Bernhard Lederer performed the selection of homozygous STTM transgenic plants and *Hpa* infection. Lorenz Oberkofler performed the reporter plant imaging and generated video from Thunder microscope. Arne Weiberg was responsible for the formulation of the study, contributed to the experimental design, obtained funding, and project supervision.

Publication 2

Cheng, An-Po, Lihong Huang, Lorenz Oberkofler, Nathan R Johnson, Adrian-Stefan Glodeanu, Kyra Stillman, and Arne Weiberg. 2025. Fungal Argonaute proteins act in bidirectional cross-kingdom RNA interference during plant infection, *Proceedings of the National Academy of Sciences*, 122: e2422756122.

In this publication, I designed and performed all experiments and contributed all data, if they are not listed below.

Lihong Huang generated *bcago2*, *bcago3*, *bcago4* single mutant and performed the sRNA-seq from total BcsRNA. The next generation sequencing data was together analyzed by Arne Weiberg, Nathan R Johnson and me. Lorenz Oberkofler performed the reporter plant imaging from Thunder microscope. Adrian-Stefan Glodeanu and I performed the stem-loop RT PCR assay. Kyra Stillman and I performed the qRT-PCR experiments. Arne Weiberg was responsible for the formulation of the study, contributed to the experimental design, obtained funding, and project supervision.

München, 21.November.2025

_____

An-Po Cheng

License and permission

1. Cheng, An-Po, Bernhard Lederer, Lorenz Oberkofler, Lihong Huang, Nathan R Johnson, Fabian Platten, Florian Dunker, Constance Tisserant, and Arne Weiberg. 2023. 'A fungal RNA-dependent RNA polymerase is a novel player in plant infection and cross-kingdom RNA interference', *PLoS pathogens*, 19: e1011885.

2. Cheng, An-Po, Lihong Huang, Lorenz Oberkofler, Nathan R Johnson, Adrian-Stefan Glodeanu, Kyra Stillman, and Arne Weiberg. 2025. 'Fungal Argonaute proteins act in bidirectional cross-kingdom RNA interference during plant infection', *Proceedings of the National Academy of Sciences*, 122: e2422756122.

Summary

Cross-kingdom RNA interference (ckRNAi) represents a novel and rapidly advancing frontier in the study of host–pathogen interactions. In previous studies, it was shown that the fungal pathogen *Botrytis cinerea* (*B. cinerea*) could deliver small RNAs (sRNAs) into plant host cells. It was observed that the fungal sRNAs were able to hijack the plant RNAi machinery, which resulted in the suppression of immune-related gene expression and the promotion of infection (Wang *et al.*, 2016; Weiberg *et al.*, 2013). However, the fungal RNA interference (RNAi) components that mediate this cross-kingdom RNA trafficking have not yet been fully identified.

Me and my colleague developed a novel GFP-based "switch-on" reporter system to monitor ckRNAi in real-time during infection. Based on this reporter tool, I identified key fungal components required for ckRNAi, including *Botrytis* RNA-dependent RNA polymerase 1 (BcRDR1), Argonaute 1 (BcAGO1), and Argonaute 2 (BcAGO2). BcRDR1 and BcAGO1 showed to be involved in the accumulation of *B. cinerea* sRNAs, while BcAGO2 is crucial for the translocation of these sRNAs into host cells. I confirmed our candidate fungal sRNAs, which derived from fungal transposon elements, mediated silencing of plant defense-related genes.

Co-immunoprecipitation of BcAGOs and sRNA sequencing revealed a mutual RNA exchange, in which host-derived sRNAs are transported into fungal cells and loaded into BcAGOs. Functional analysis has demonstrated that these plant sRNAs have the capacity to suppress fungal virulence gene expression. My findings supported that ckRNAi is a bidirectional process that influenced both fungal pathogenicity and plant defense.

My works offered a deeper insight into the significant roles of *B. cinere*a argonaute and RNA-dependent RNA polymerase proteins in ckRNAi. I provided molecular evidence that suggested the RNA-based bidirectional communication between fungal pathogens and their plant hosts. These insights could potentially broaden our understanding of RNA-mediated host–pathogen interactions and may suggest new avenues for RNAi-based disease management strategies in agriculture.

Introduction

Botrytis cinerea: overviews and impact to the global food resources

Botrytis cinerea, commonly called as "gray mold", is a devastating plant pathogen that affects numerous of economically important crops worldwide (Elmer & Reglinski, 2006). The necrotrophic fungus has the remarkable ability to infect over 200 different plant species, including fruits and vegetables. This lead to a great significant economic losses, with estimated annual around $10 to $100 billion (Dean *et al.*, 2012). However, developing effective control strategies often requires a comprehensive understanding of the complex interactions between the pathogen and its various plant hosts growing under different environmental conditions.

Life cycle of *B. cinerea* involves the production of sclerotia, which are the structures that last in the soil or on plant debris overwinter. The sclerotia serve as a source of primary inoculum for new infections. During the growing season, sclerotia will germinate and produce conidiophores, which in turn release asexual spores (conidia) that can be spread by wind or water splash to another new host plant. Once a plant is infected, *B. cinerea* secretes a variety of chemical compounds and virulence factors that enable the pathogen to colonize and kill host tissues. This leads to the growth of grey, fuzzy fungal colonies on the infected plant tissue (van Kan, 2006; Williamson *et al.*, 2007).

B. cinerea has evolved a multifaceted virulence factor that enable it to break through the plant's physical and chemical defenses, manipulate host cellular processes, and ultimately establish a successful infection (Amselem *et al.*, 2011; Choquer *et al.*, 2007). Studies showed that *B. cinerea* produces cell wall-degrading enzymes which effectively break the physical barrier of the plant cell wall, allowing *Botrytis* for host tissue entry. Additionally, *B. cinerea* secretes phytotoxins and other effector molecules, making the fungus manipulate and affect host cellular signaling pathways, suppress immune responses, and create an suitable environment for fungal colonization and nutrient acquisition (Laluk & Mengiste, 2010; van Kan, 2006). This multifaceted virulence strategy enables *B. cinerea* to successfully infect and cause disease in a wide range of plant hosts, posing a significant challenge to agricultural disease management efforts.

The plant immune response to *Botrytis* infection

In nature, plants are constantly exposed to a huge variety of biotic stresses, including fungi, bacteria, nematodes, viruses, and oomycetes. Plants have therefore through a long period of time developed complex and comprehensive immune systems to detect and defend against these threats. Plants have a variety of strategies to defend against microbial invasion, including physical barriers, synthesis of antimicrobial compounds, and activation of signaling pathways that trigger downstream defense responses. Defense mechanisms can be roughly divided into two main branches: "pattern-triggered immunity (PTI)" and "effect-triggered immunity (ETI)". PTI is activated when plant pattern recognition receptors recognize conserved microbial molecules, called pathogen-associated molecular patterns. On the other hand, ETI is initiated when plants recognize pathogen-derived effector proteins that are delivered into plant cells to suppress host defenses or manipulate host cellular processes. In addition to these two major classes of plant immunity, plants have developed systemic acquired resistance, which is a long-lasting, broad-spectrum resistance response triggered by an initial local infection (Jones & Dangl, 2006; Jones *et al.*, 2024).

For the case of plant infected by *B. cinerea*, plants actively try to prevent pathogen invasion by activating multiple defense pathways, including the production of antifungal metabolites and pathogenesis-related proteins. Plant-*Botrytis* interaction has been reported triggers oxidative burst, involving the production of hydrogen peroxide and nitric oxide, and the formation of proteolytic vesicles at the host–pathogen interface (Williamson *et al.*, 2007). Plants utilize pre-existing structural defenses, such as the cuticle and cell wall, to impede the initial stages of pathogen entry and colonization (Bi *et al.*, 2023; Laluk & Mengiste, 2010). Upon recognition of pathogen-associated molecular patterns, plants activate pattern-triggered immunity, resulting in the production of reactive oxygen species, the expression of defense genes, and the reinforcement of cell walls (Jeblick *et al.*, 2023).

Furthermore, plants produce polygalacturonase-inhibiting proteins. These proteins have been shown to inhibit endopolygalacturonases of plant pathogenic fungi through a direct physical interaction between the two proteins. The endopolygalacturonases are leucine-rich repeat-containing proteins. The outcome of the interaction between *B. cinerea* virulence factors and plant defense responses determines the interaction's result, with successful infection

occurring when the pathogen overcomes or suppresses plant immunity (Bi *et al.*, 2023; Williamson *et al.*, 2007).

The pathogenicity of *Botrytis cinerea*

Fungal pathogens, in contrast, secrete various types of virulence molecules into host plants to manipulate plant immunity and promote colonization. These effectors can be proteins, RNAs, or metabolites that target different cellular processes in the host, including immune signaling, hormonal regulation, and gene expression. Fungal pathogens secrete a variety of "effector" proteins that are able to overcome host defenses to enable successful colonization (Greenshields & Jones, 2008; Lovelace *et al.*, 2023). Effector proteins produced by fungal pathogens play crucial roles in manipulating plant immunity and promoting colonization. During host-pathogen interactions, studies have shown that effector proteins can either suppress the host immune response or reprogram the host's metabolism to benefit the pathogen. According to literatures, fungi secrete effectors into the apoplast region or to be transmitted directly into the cytoplasm of plant cells via endocytosis (Tanaka & Kahmann, 2021; Wang *et al.*, 2023). Effectors secreted into the apoplast interfere with plant defense signaling pathways or degrade the plant cell wall, while effectors delivered into the cytoplasm have the capacity to directly target host proteins involved in immunity or metabolism (Rocafort *et al.*, 2020; Selin *et al.*, 2016).

Botrytis cinerea is a necrotrophic pathogen that produces many kinds of effectors to facilitate its infection process. During the early stages of infection, *Botrytis* secretes effector molecules which play key roles in regulating host cell death reaction, including inhibit the formation of autophagy, a key defense mechanism employed by plants (Veloso & van Kan, 2018). With the help of blocking this critical defense mechanism, *B. cinerea* can successfully infect and colonize into plant tissues (Bi *et al.*, 2023). Despite tons of the research have been conducted, conclusively identifying specific protein effectors in *B. cinerea* that can directly interact with and counteract the plant's complex defense machinery remains a major challenge. The difficulties may be caused by technical challenges associated with the isolation of these elusive molecules or the extensive host range of this necrotrophic pathogen. The latter can

result in a reduction in the efficiency of classical effectors or mask their contribution due to the involvement of other complicating factors (Bi *et al.*, 2023).

RNA interference in plants

Plants produce two class of sRNAs, microRNAs (miRNAs) and short interfering RNAs (siRNA), with normally 20-27 nt in length. miRNAs are derived from long single-stranded RNA (pro-miRNA) that carried stem-loop secondary structures. The sRNA precursors are processed by Dicer-like proteins and typically form 21 nt sRNAs (Bartel, 2004; Jones-Rhoades *et al.*, 2006; Mallory & Vaucheret, 2006). Plant miRNAs regulate plant development, hormone signaling, and environmental stress response. They bind to complementary sequences in mRNAs, resulting in mRNA cleavage and translational repression (Mallory & Vaucheret, 2006; Voinnet, 2009). On the other hand, siRNAs are typically derived from endogenous mRNA, viral RNA, or transposons. The templates bind to RNA-dependent RNA polymerases to form double-stranded RNA (dsRNA) precursors and then processed by Dicer-like proteins. siRNAs in plants have been reported to function for genome defense and epigenetic regulation (Baulcombe, 2004; Carthew & Sontheimer, 2009). Both miRNAs and siRNAs are loaded into Argonaute proteins, which form the core component of the RNA-induced silencing complex (Ender & Meister, 2010; Hutvagner & Simard, 2008).

Plant miRNAs and siRNAs regulate gene expression has been demonstrated to play a crucial role in the regulation of plant innate immune responses. For example, miRNAs modulate PTI and ETI by targeting hormone signaling pathway, reactive oxygen species production, and nucleotide-binding site-leucine-rich repeat (NBS-LRR) disease resistance genes (Luo *et al.*, 2024; Peláez & Sanchez, 2013; Tang *et al.*, 2021). Similarly, siRNAs in plants can target to viral genome or reprogram endogenous genes involved in plant immunity (Katiyar-Agarwal *et al.*, 2006; Kong *et al.*, 2022; Liu *et al.*, 2021).

RNA interference in Fungi

Fungi have also developed complex RNAi machinery. The RNAi system in fungi plays important roles in regulating biology and interactions with other living organisms (Dang *et al.*, 2011;

Nicolás & Garre, 2017). The RNAi machinery consists of several essential components, such as RNA-dependent RNA polymerases, Dicer-like proteins, and Argonaute proteins. These RNAi components are responsible for creating, processing, and regulating small regulatory RNA molecules. These sRNAs have different functions in fungi, including regulating genes involved in cell growth, pathogenicity, defense against viral infections, and the control of transposable elements (Nicolás & Garre, 2017). RNAi-mediated regulation of these different cellular processes can have a significant impact on the growth, development and ecological interactions of fungal organisms.

Fungi are distinct from plants in that they own unique biosynthesis and RNAi regulation pathways. One of the RNA interference pathways in fungi is known as "quelling". Quelling was first discovered in the filamentous fungus *Neurospora crassa*. The quelling pathway is triggered by the presence of dsRNAs, which can be derived from endogenous overlapping transcripts; or from exogenous sources, such as viral infections or the introduction of transgenes. Quelling typically regulates gene expression during the vegetative growth and developmental stages of fungi. The quelling pathway shows to suppress repetitive sequences or transgenes introduced into the genome, such as transposable genetic elements Quelling contributes to the maintenance of genomic stability in *Neurospora crassa* and other filamentous fungi (Espino *et al.*, 2014; Fulci & Macino, 2007; Galagan & Selker, 2004). Another RNAi pathway in fungi is known as “meiotic silencing by unpaired DNA (MSUD)”. MSUD was found mainly regulates during fungal sexual stage. It is triggered by unpaired DNA regions during homologous chromosome pairing which mainly function to protect genome integrity during meiosis (Chang *et al.*, 2012; Dang *et al.*, 2011; Honda *et al.*, 2020).

Cross-Kingdom RNA Interference in Plant-Pathogen Interactions

In recent years, a fascinating and growing field called cross-kingdom RNA interference (ckRNAi) has gained attention to scientists who study plant-microbe interactions. The process refers to sRNAs moving between two different species, including plants and their associated pathogens or beneficial microbes, and regulate the gene expression in the recipient species. *B. cinerea* has revealed as a pioneering model in the field of ckRNAi, that it evolved the capacity to deliver fungal sRNAs into host cells and hijack the plant RNAi machinery, especially plant

AGOs, to suppress plant immune genes, promoting fungal infection. Among the identified sRNAs, BcsRNA3.1, BcsRNA3.2, BcsRNA5, and BcsRNA20 have been functionally characterized as virulence effectors. These *Botrytis* sRNAs were derived from retrotransposon-rich genomic loci and were delivered into Arabidopsis cells during infection. These BcsRNAs selectively loaded into plant AGO1 and guided the silencing critically against Arabidopsis defense-related genes such as *AtMPK1*, *AtMPK2*, *AtPERK1*, *AtWAK*, and *AtPRXIIF* (Porquier *et al.*, 2021; Weiberg *et al.*, 2013). Plants on the other site sent plant-derived miRNAs and siRNAs into *B. cinerea*'s cells. These plant sRNAs targeted and silenced virulence genes such as *Bcvps51D*, *Bcdctn1D*, and *Bcsac1D*, which led to the reduction of fungal infection (Cai *et al.*, 2018a; Cai *et al.*, 2018b; Wang *et al.*, 2016; Weiberg *et al.*, 2013).

It is notable that ckRNAi has been observed to be a common natural phenomenon in diverse plant-biotic interactions. Additional examples have been observed not only in interactions with *Botrytis* but also with other fungal pathogens such as *Sclerotinia sclerotium*, *Puccinia striiformis* f. sp. *tritici*, *Verticilium dahliae*, *Fusarium graminearum* (Cheng *et al.*, 2023a; Derbyshire *et al.*, 2019; Jian & Liang, 2019; Weiberg *et al.*, 2015). Studies suggested other biological systems, including oomycetes, beneficial fungal, as well as bacteria, have evolved the ckRNAi process during the host-microbe interaction (Dunker *et al.*, 2020; Ren *et al.*, 2019; Silvestri *et al.*, 2025; Wong-Bajracharya *et al.*, 2022).

A major topic in recent studies focus on how sRNAs are transported between host and microbe. Extracellular vesicles (EVs) at this stage draw a widespread of attention. EVs are lipid-bilayer nanoparticles which carry cytoplasmic molecules such as proteins, compounds, DNAs, RNAs (Colombo *et al.*, 2014; Van Niel *et al.*, 2018). In plants, EVs have been shown to participate in defense responses by delivering small RNAs to pathogens (Cai *et al.*, 2018b; He *et al.*, 2021; Rutter & Innes, 2017). Conversely, fungi release EVs with effectors or RNAs to modulate host immunity for promoting colonization or suppressing defense mechanisms (He *et al.*, 2023; Kwon *et al.*, 2021; Oliveira-Garcia *et al.*, 2023). An increasing number of studies analyzing EVs released by both plants and microbes suggesting there potential for the future agricultural application. Understanding their content and function offers promising insights into plant health and disease resistance strategies (Cheng *et al.*, 2023a).

The discovery of ckRNAi opened an era for understanding the complicated molecular communication between plants and microbes. However, the roles of fungal RNAi component

in ckRNAi regulation remain unclear. Uncover the knowledge may help develop new strategies for disease control that could benefit agricultural production and food security (Cheng *et al.*, 2023a).

Aim of the thesis

My doctoral study elucidated the molecular mechanisms of cross-kingdom RNA interference (ckRNAi) between the fungal pathogen *Botrytis cinerea* and its plant hosts. Although previous studies have shown that *B. cinerea* delivers sRNAs into host plant cells to suppress immunity-related genes, the roles of the fungal factors mediating this process have remained unclear. To address the knowledge gap, I evaluated in my study whether fungal RNAi components are involved in ckRNAi and what active functions do they regulate in the target species.

I focused on *B. cinerea* RNA-dependent RNA polymerase (RDR) and Argonaute proteins. My study first validated how the two proteins contributed to fungal sRNA production. I next investigated whether plants uptake *B. cinerea* sRNAs. To make this ckRNAi activity visual and trackable, me and my colleagues established a reporter system in transgenic plants, enabling real-time live tracking of sRNA-mediated gene silencing during fungal invasion. On top of the reporter plants, I studied how the fungal sRNAs functioned in host cells, particularly focused on the suppression of plant immunity during infection.

In the direction from plant host to fungus, I explored whether host sRNAs could be taken up by fungal cells and hijacked *B. cinerea* Argonaute proteins. I wanted to uncover if host sRNAs downregulate fungal virulence genes. In parallel, the functional divergence between *Botrytis* Argonaute proteins was investigated. I wanted to further evaluate the feasibility of strategies to block ckRNAi. The goal is to find new possibilities to enhance crop protection against fungal pathogens.

My doctoral study aimed to provide a comprehensive view of bidirectional sRNA-mediated communication between fungal pathogens and their plant hosts. By revealing the key molecular players in ckRNAi and their roles, this work contributed to the broader understanding of host-pathogen interactions and provides a promising route for developing RNA-based disease control strategies in agriculture.

Results

I. A fungal RNA-dependent RNA polymerase is a novel player in plant infection and cross-kingdom RNA interference

PLOS PATHOGENS

RESEARCH ARTICLE

A fungal RNA-dependent RNA polymerase is a novel player in plant infection and cross-kingdom RNA interference

An-Po Cheng[1], Bernhard Lederer[1☯], Lorenz Oberkofler[1☯], Lihong Huang[1¤], Nathan R. Johnson[2,3], Fabian Platten[1], Florian Dunker[1], Constance Tisserant[1], Arne Weiberg[1]*

1 Institute of Genetics, Faculty of Biology, Ludwig Maximilian University of Munich, Martinsried, Germany, **2** Centro de Genómica y Bioinformática, Facultad de Ciencias, Ingeniería y Tecnología, Universidad Mayor, Santiago, Chile, **3** ANID-Millennium Science Initiative Program-Millennium Institute for Integrative Biology (iBio), Santiago, Chile

☯ These authors contributed equally to this work.
¤ Current address: GMU-GIBH Joint School of Life Sciences, The Guangdong-Hong Kong-Macau Joint Laboratory for Cell Fate Regulation and Diseases, Guangzhou Medical University, Guangzhou, China
* a.weiberg@lmu.de

OPEN ACCESS

Citation: Cheng A-P, Lederer B, Oberkofler L, Huang L, Johnson NR, Platten F, et al. (2023) A fungal RNA-dependent RNA polymerase is a novel player in plant infection and cross-kingdom RNA interference. PLoS Pathog 19(12): e1011885. https://doi.org/10.1371/journal.ppat.1011885

Editor: Eva H. Stukenbrock, CAU: Christian-Albrechts-Universitat zu Kiel, GERMANY

Received: June 5, 2023

Accepted: December 5, 2023

Published: December 20, 2023

Peer Review History: PLOS recognizes the benefits of transparency in the peer review process; therefore, we enable the publication of all of the content of peer review and author responses alongside final, published articles. The editorial history of this article is available here: https://doi.org/10.1371/journal.ppat.1011885

Data Availability Statement: Sequencing data have been deposited in NCBI SRA (BioProject ID PRJNA978613).

Abstract

Small RNAs act as fungal pathogen effectors that silence host target genes to promote infection, a virulence mechanism termed cross-kingdom RNA interference (RNAi). The essential pathogen factors of cross-kingdom small RNA production are largely unknown. We here characterized the RNA-dependent RNA polymerase (RDR)1 in the fungal plant pathogen *Botrytis cinerea* that is required for pathogenicity and cross-kingdom RNAi. *B. cinerea bcrdr1* knockout (ko) mutants exhibited reduced pathogenicity and loss of cross-kingdom small RNAs. We developed a "switch-on" GFP reporter to study cross-kingdom RNAi in real-time within the living plant tissue which highlighted that *bcrdr1* ko mutants were compromised in cross-kingdom RNAi. Moreover, blocking seven pathogen cross-kingdom small RNAs by expressing a short-tandem target mimic RNA in transgenic *Arabidopsis thaliana* led to reduced infection levels of the fungal pathogen *B. cinerea* and the oomycete pathogen *Hyaloperonospora arabidopsidis*. These results demonstrate that cross-kingdom RNAi is significant to promote host infection and making pathogen small RNAs an effective target for crop protection.

Author summary

Botrytis cinerea is a notorious plant pathogen that can only be effectively controlled by chemical fungicides. With the aim to reduce fungicide application, new control strategies are in need. Cross-kingdom RNA interference (RNAi) is an emerging field in plant-pathogen research. Uncovering the key factors to understand the molecular mechanisms and functions in cross-kingdom RNAi is fundamental to develop innovative RNA-based strategies for crop protection. *B. cinerea* produces extracellular small RNAs to induce natural cross-kingdom RNAi in plant hosts for infection. In this study, we describe the *B. cinerea*

[11]. While such reports have indicated that distinct fungal RDRs are involved in pathogenicity, their mode of action remains unclear.

In this study, we investigated the role of the *BcRDR1* gene in the fungus *Botrytis cinerea*, a multi-host plant pathogen infecting more than 1,000 different plant species and causing the devastating grey mold disease. As part of its pathogenicity, *B. cinerea* releases extracellular small RNAs (Bc-sRNAs) that enter plant cells during infection and recruit the plant's own AGO1/RISC to induce host gene silencing for promoting infection [12,13]. This virulence phenomenon has been termed cross-kingdom RNAi and is a general infection strategy of diverse plant and animal pathogenic as well as symbiotic microbes, including fungi, oomycetes, and bacteria [14–16]. Most Bc-sRNAs inducing cross-kingdom RNAi are encoded by GYPSY-class of long terminal repeat retrotransposons and are produced by *B. cinerea* BcDCL1 and BcDCL2 [13,15,17]. We herein discovered that the *B. cinerea* BcRDR1 is a pathogenicity factor and is required for *B. cinerea*-induced cross-kingdom RNAi.

Results

B. cinerea BcRDR1 is a pathogenicity factor

In order to identify unknown genes involved in cross-kingdom RNAi, we analyzed the family of BcRDRs in *B. cinerea*. Through a homology search with the *N. crassa* RDR, SAD-1, we identified three genes encoding conserved RDRs in the genome of the *B. cinerea* strain B05.10, thereafter named *BcRDR1* (*Bcin01g01810*), *BcRDR2* (*Bcin08g02220*), and *BcRDR3* (*Bcin07g01750*). Phylogenetic analysis of full-length amino acid sequences revealed that BcRDR1 is the orthologue of the *N. crassa* SAD-1 involved in MSUD [18], and BcRDR2 is the orthologue of *N. crassa* quelling RDR, QDE-1 [19]. BcRDR3 is another conserved RDR with unknown function (S1A Fig). All three BcRDRs comprised a conserved DxDGD motif indicating that they function as RNA polymerases (S1B Fig). We detected transcripts of *BcRDR1*, *BcRDR2* and *BcRDR3* when growing *B. cinerea* in liquid culture or during infection of *Solanum lycopersicum* (tomato) leaves; however, there was no consistent up-regulation of any of the *BcRDR*s measured during infection (S2 Fig).

In order to investigate potential functions of BcRDRs in *B. cinerea* pathogenicity, we generated targeted gene knockout (ko) mutant strains by homologous recombination. We isolated two independent *bcrdr1* ko and two independent *bcrdr2* ko isolates (S3 Fig), while we obtained only heterozygous isolates when attempting to generate *bcrdr3* ko mutants. Therefore, we continued analyzing *bcrdr1* and *bcrdr2* ko mutants. Infection assays using detached *S. lycopersicum* or *A. thaliana* leaves revealed that *bcrdr1* ko mutants induced smaller lesion sizes compared to the *B. cinerea* wild type (WT) strain (Fig 1A and 1B). This phenotype was accompanied with lower fungal biomass, as estimated by quantification of *B. cinerea* genomic DNA, while genetic complemented BcRDR1 (cBcRDR1) strains in the *bcrdr1* ko background were reverted to full virulence (Figs 1C and S4). Both *bcrdr1* ko mutants and cBcRDR1 strains showed a WT-like growth and development phenotype under axenic culture condition (Figs 1A and S5). The *bcrdr1* ko mutants were not affected in the expression of other known virulence genes [20] (S6 Fig). Based on these results, we concluded that BcRDR1 is a pathogenicity factor in *B. cinerea* which was likely related to Bc-sRNAs.

Biogenesis of retrotransposon-derived Bc-sRNAs requires BcRDR1

Some plant, nematode, and fungal RDRs are required for siRNA biogenesis, and abolished Bc-sRNA production in a *B. cinerea bcdcl1dcl2* ko mutant led to reduced pathogenicity due to impaired cross-kingdom RNAi [13]. To investigate the role of BcRDR1 in Bc-sRNA biogenesis, we performed comparative small RNA-seq analysis. *B. cinerea* WT and two independent

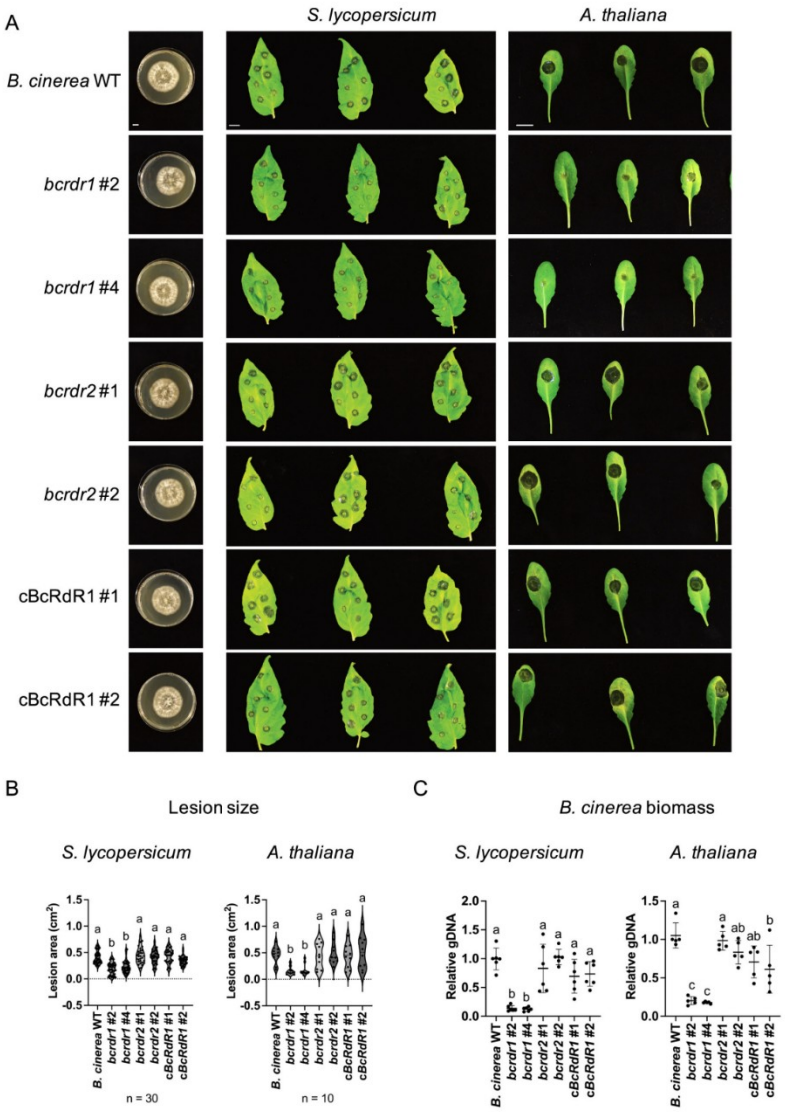

Fig 1. *B. cinerea bcrdr1* ko mutants are compromised in pathogenicity. A) Infection series on *S. lycopersicum* or *A. thaliana* detached leaves using *B. cinerea* WT, two *bcrdr1* ko mutants #2 and #4, two *bcrdr2* ko mutants #1 and #2, as well as two cBcRDR1 complementation strains #1 and #2. For each strain, a 20 μl drop of 5 x 10^4/ml or 2 x 10^5/ml conidiospore suspension was placed onto *S. lycopersicum* or *A. thaliana* leaves, respectively. B) Lesion size induced by *B. cinerea* infection was measured at 48 hpi for *S. lycopersicum* or 60 hpi for *A. thaliana*. 30 lesions on *S. lycopersicum* and 10 lesions on *A. thaliana* were

measured and statistical analysis was performed using ANOVA followed by a Tukey post-hoc test with *p*-value threshold $p < 0.05$. The scale bars represent 1 cm. C) *B. cinerea* biomass was estimated by measuring genomic DNA using primers of the *Bc-Tubulin (BcTub)A* and related to plant genomic DNA measured with *SlActin2* or *AtActin2* primers in five or six biological replicates. Statistical analysis was performed using ANOVA followed by a Tukey post-hoc test with *p*-value threshold $p < 0.05$. The scale bars represent 1 cm.

https://doi.org/10.1371/journal.ppat.1011885.g001

bcrdr1 ko mutants were cultured for two days in liquid medium, and mycelium was collected to extract total RNA. Upon small RNA isolation via PAGE, RNA libraries were cloned for Illumina sequencing. In total, sequencing depth among the small RNA libraries were in the range of 1.3–4.9 millions that were mapped to the *B. cinerea* reference genome either unique or multiple times, as to the same read mapped to multiple chromosomal regions. The fraction of multiple mapping reads was reduced in both *bcrdr1* ko mutants (Fig 2A). Plotting read numbers by size revealed a reduction of 21–22 nucleotides (nt) long Bc-sRNAs in both *bcrdr1* ko mutants, mostly representing 5'prime Uracil nucleobase, retrotransposon (RT)-derived Bc-sRNAs (Figs 2B–2D and S7). This result indicated that production of Bc-sRNAs that mostly mapped to RTs was dependent on BcRDR1. The long-terminal repeat RT *BcGypsy3* was previously found to be a major source of Bc-sRNAs that were induced during plant infection and was a pathogenicity factor of *B. cinerea* [17]. Accordingly, reduced accumulation of RT-derived Bc-sRNAs in *bcrdr*1 ko mutants resulted in increased mRNA levels of *BcGypsy3* (S7C Fig) and upregulation of BcGypsy mRNAs during tomato infection was only measured with *B. cinerea* WT, but not with *bcrdr1* ko mutants (S7D–S7E Fig), suggesting a potential role of BcRDR1 in post-transcriptional silencing of RTs.

B. cinerea bcrdr1 ko mutants are compromised in cross-kingdom RNAi

RT-derived Bc-sRNAs were previously found to induce cross-kingdom RNAi [13,17]. In particular, the four Bc-sRNAs, Bc-sRNA3.1, Bc-sRNA3.2, Bc-sRNA5, and Bc-sRNA20 induced silencing of the *S. lycopersicum* host genes *Vacuolar sorting protein* (*SlVPS*) (*Solyc09g014790*), *Mitogen-activated protein kinase kinase kinase* (*SlMPKKK)4* (*Solyc08g081210*), and *C2H2 zinc-finger transcription factor SlBhlh63* (*Solyc03g120530*), and the *A. thaliana* host genes *Mitogen-activated protein kinase* (*AtMPK)1* (*AT1G10210*), *AtMPK2* (*AT1G59580*), a *Cell Wall kinase* (*WAK*) (*AT5G50290*), and the *Peroxiredoxin PRXIIF* (*AT3G06050*) (Fig 3A). We confirmed that *bcrdr1* ko mutants lost accumulation of these Bc-sRNAs, while they were produced in the *B. cinerea* WT and the cBcRDR1 strains during tomato infection as revealed by stem-loop reverse transcriptase PCR (Figs 3B and S8). When inoculating *S. lycopersicum* or *A. thaliana* with *B. cinerea* WT or *bcrdr1* ko mutants, we observed significant down-regulation of Bc-sRNA target genes in WT-infected plants compared to non-inoculated plants. The target gene down-regulation was abolished or less strong in *bcrdr1*-infected plants (Figs 3C and S9). Successful infection of plants and induced host defense response due to *B. cinerea* infection was validated by measured up-regulation of *S. lycopersicum Proteinase inhibitor* (*SlPI*)*-I* and *SlPI-II* or *A. thaliana Plant Defensin* (*AtPDF*)*1.2* immunity genes (Fig 3D). These results indicated that *bcrdr1* mutants might be compromised in inducing cross-kingdom RNAi, which would explain the reduced pathogenicity observed in *S. lycopersicum* and *A. thaliana*.

To further inspect whether *bcrdr1* mutant strains were indeed compromised in inducing cross-kingdom RNAi, we designed a GFP "switch-on" cross-kingdom RNAi reporter that exclusively responded to the translocation of Bc-sRNA3.1 and Bc-sRNA3.2 from *B. cinerea* into the plant host (Fig 4A). In this reporter construct, the CRISPR-type RNA endonuclease Csy4 [21] is co-expressed with a GFP version that is fused to the Csy4 recognition motif at its N-terminus, in adaptation to a previously designed cross-kingdom RNAi reporter for the

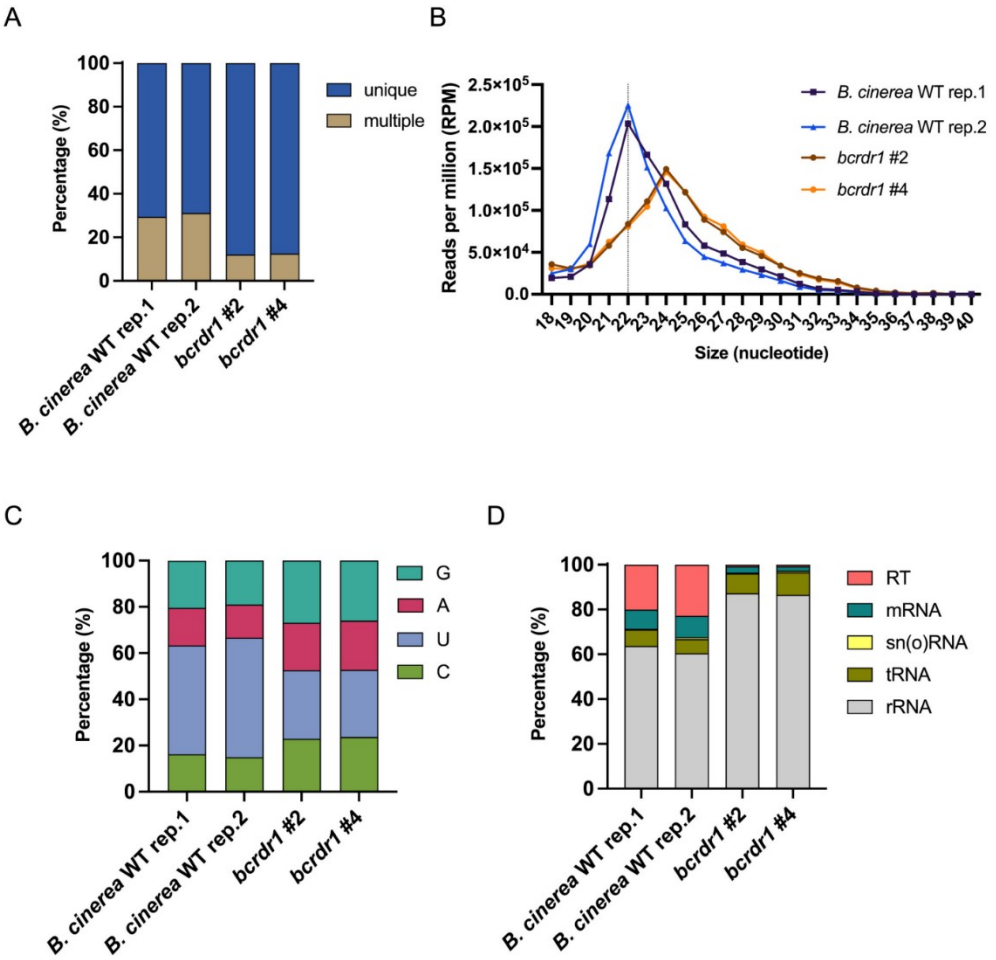

Fig 2. Small RNA sequencing analysis of *B. cinerea* WT and *bcrdr1* ko mutants. A) Fractions of Bc-sRNAs mapping unique or multiple times to a *B. cinerea* reference genome. B) Bc-sRNA size profiles (18–40 nt) of mapped Bc-sRNA reads in reads per million (RPM). C) Distribution in percentage of the four RNA nucleotides C, U, A, G at the 5'prime position of Bc-sRNAs. D) Distribution in percentage of Bc-sRNAs mapping to distinct *B. cinerea* RNA gene loci: ribosomal RNA (rRNA), transfer RNA (tRNA), small nuclear and nucleolar RNA (sn(o)RNA), messenger RNA (mRNA), and retrotransposon (RT).

https://doi.org/10.1371/journal.ppat.1011885.g002

oomycete pathogen of *A. thaliana*, *Hyaloperonospora arabidopsidis* [22]. In this adapted version, we fused the native target sites of Bc-siRNA3.1 and Bc-siR3.2 to the 5'prime or 3'ends of the *Csy4* transgene, respectively, turning *Csy4* into a target gene of these Bc-sRNAs. Csy4 constantly suppresses expression of the *GFP*, unless GFP expression is activated when Bc-sRNAs silence *Csy4*. This GFP switch-on reporter was stably expressed in transgenic *A. thaliana*

A

Bc-sRNAs	*S. lycopersicum* target genes
Bc-sRNA3.1	*SlVPS*
Bc-sRNA3.2	*SlMPKKK4*
Bc-sRNA20	*SlBhlh63*

Bc-sRNAs	*A. thaliana* target genes
Bc-sRNA3.1	*AtPRXIIF*
Bc-sRNA3.2	*AtMPK1*
Bc-sRNA5	*AtWAK*

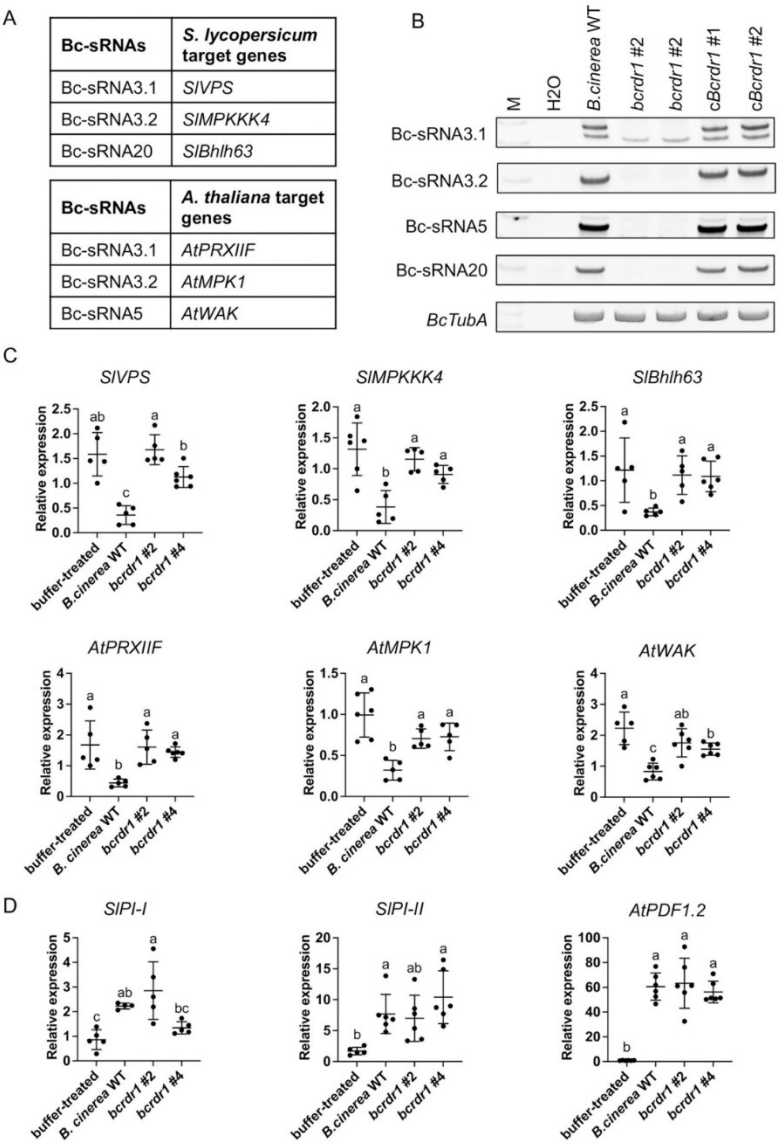

Fig 3. *B. cinerea bcrdr1* ko mutants are compromised in plant target gene suppression. A) Known *S. lycopersicum* and *A. thaliana* target genes silenced by Bc-sRNAs through cross-kingdom RNAi. B) Stem-loop reverse transcriptase PCR of Bc-sRNAs was carried out with tomato leaf samples infected with *B. cinerea* WT, *bcrdr1* ko mutants or cBcRDR1 strains at 48 hpi. Tomato leaves were inoculated with a 20 ml drop of 5 x 10^4/ml conidiospore suspension. *BcTubA* mRNA expression was used as an internal control. C) Quantitative reverse transcriptase PCR measuring mRNA levels of Bc-sRNA target genes

in *S. lycopersicum* and *A. thaliana* during infection with *B. cinerea* WT or *bcrdr1* ko mutants. D) Quantitative reverse transcriptase PCR measuring mRNA levels of immunity marker genes *SlPI-I*, *SlPI-II* and *AtPDF1.2*. In C) and D), *S. lycopersicum* leaves were inoculated with a 20 μl drop of 5 x 10^4/ml conidiospore suspension and samples were collected at 36 hpi. *A. thaliana* leaves were inoculated with a 20 μl drop of 2 x 10^5/ml conidiospore suspension and samples were collected at 60 hpi. Lines in scatter plots represent the mean and the standard deviation. Each gene was measured in at least four biological replicates. The *SlActin2* or *AtActin2* were used as reference genes. Statistical analysis was performed using ANOVA followed by a Tukey post-hoc test with *p*-value threshold $p < 0.05$.

https://doi.org/10.1371/journal.ppat.1011885.g003

plants. With these reporter plants, we were able to visualize *B. cinerea*-induced cross-kingdom RNAi in infected leaf tissue by fluorescent microscopy. Inoculating seedling leaves of reporter plants with *B. cinerea* WT conidiospore suspension led to enhanced GFP expression compared to leaves inoculated with the *bcrdr1* #2 ko mutant or treated with water (Figs 4B and S10). The non-invasive GFP switch-on reporter allowed us to quantify cross-kingdom RNAi by life-time imaging. We recorded a time lapse video of GFP activity in reporter plants either inoculated with *B. cinerea* WT or *bcrdr1* ko #2 for 45 hours (S1 Video). A clear increase in the GFP signal was apparent in *B. cinerea* WT infected leaves after 24 hpi (Figs 4C and S10). This signal was not related to plant auto-fluorescence, because no GFP signal was detected in *B. cinerea* WT-infected *A. thaliana* WT plants (S11 Fig). We verified the results obtained by fluorescence microscopy when measuring *GFP* mRNA and GFP protein levels by quantitative reverse transcriptase PCR and Western blot analysis using an anti-GFP antibody (Fig 4D and 4E). Using rosette leaves of adult *A. thaliana* plants, we confirmed among three independent infection series the activation of the GFP signal upon infection with *B. cinerea* WT, but not in leaves inoculated with the two *bcrdr1* ko #2 and #4 mutants or when infected with the previously characterized *bcdcl1/bcdcl2* double knock-out (*bcdcl1/2*) mutant strain (S12 Fig). The *bcdcl1/2* mutant is unable to produce reporter-activating Bc-sRNAs [13]. GFP activation was specific to *B. cinerea* infection, because infection with the oomycete pathogen of *A. thaliana*, *Hyaloperonospora arabidopsidis*, did not switch on the GFP reporter (Figs S13 and S14).

Referring to earlier in this study, we had observed that *bcrdr1* mutants developed less biomass during infection due to reduced virulence (Fig 1C). To rule out that reduced *B. cinerea bcrdr1* biomass could be responsible for lower GFP activity when inoculating the cross-kingdom RNAi reporter plants, we used 10x higher conidiospore suspension compared to *B. cinerea* WT inoculation and found that with increased conidiospore concentration, GFP activity was still significantly lower with *bcrdr1* ko (S15 Fig). Interestingly, GFP activity was the strongest at and beyond the infection front of *B. cinerea* (S15 and S16 Figs). This might indicate that cross-kingdom RNAi was the strongest in newly infected leaf cells and might spread into non-infected plant cell layers.

B. cinerea small RNAs translocated into plants promote infection

Several independent studies revealed that knockout or knockdown of DCLs led to loss of Bc-sRNA biogenesis and reduced pathogenicity in *B. cinerea* and other fungal pathogens [11,13,23–29]. Here, we demonstrated that knocking out the *BcRDR1* leads to loss of Bc-sRNA production, compromises cross-kingdom RNAi, and reduces pathogenicity. However, *BcRDR1* deletion might have affected other endogenous small RNA regulatory processes in the fungus that are relevant for infection [30]. Therefore, we aimed to further validate that cross-kingdom RNAi was part of *B. cinerea* pathogenicity. Transgenes producing small RNA sponges, for example RNA short tandem target mimic (STTM), can block microRNA- and siRNA-induced silencing of plant endogenous and exogenous target genes [22, 31]. We cloned a Bc-siRNA3.2/Bc-sRNA5 double STTM (Fig 5A) and transformed it into *A. thaliana* for stable expression. We could isolate three independent *A. thaliana* STTM T2 lines and infected

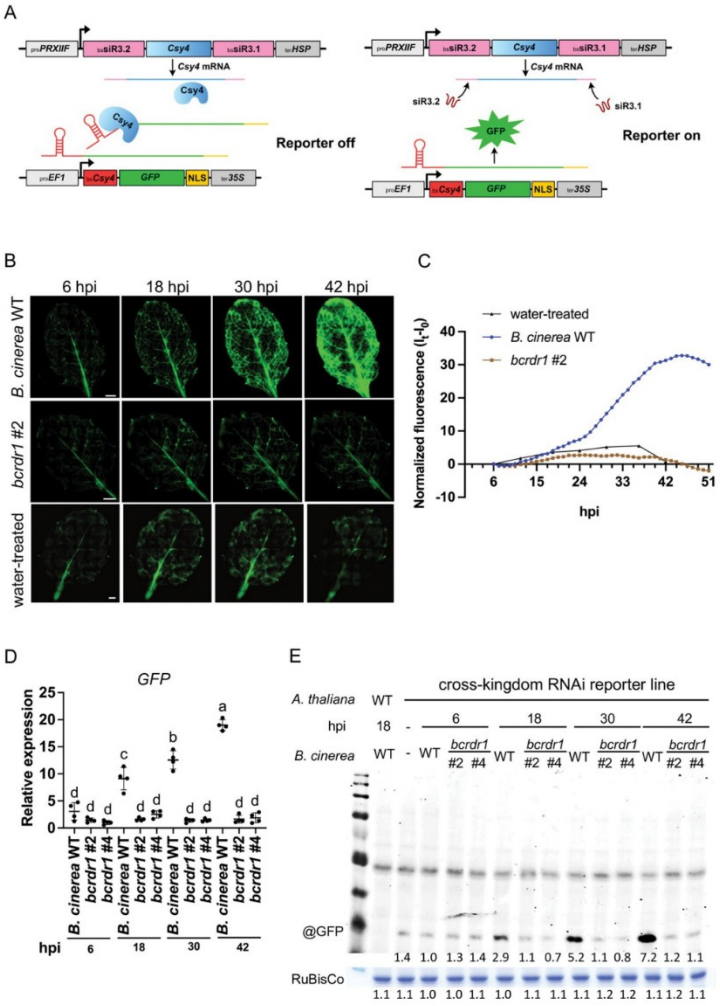

Fig 4. *B. cinerea bcrdr1* ko mutants are compromised in cross-kingdom RNAi. A) Schematic overview of a GFP-based switch-on cross-kingdom RNAi reporter suitable for *in planta* expression. B) Fluorescence microscopy images from *B. cinerea* WT, *bcrdr1* #2 or water-treated GFP reporter plant seedlings at different time points. A 5 μl drop of a 5 x 10^5/ml conidiospore suspension was placed at the center of the leaf before placing a glass covering slip on the top that dispersed the conidiospore suspension over the entire leaf surface. The scale bars represent 1 mm. C) GFP quantification in WT and *bcrdr1* ko #2-infected seedling leaves or water-treated leaves from 6–51 hpi. For normalization, GFP fluorescence signal intensity at different time points (I_t) was subtracted with the initial GFP signal intensity (I_0). D) Quantitative reverse transcriptase PCR analysis of relative *GFP* mRNA expression in cross-kingdom RNAi reporter plants during *B. cinerea* infection. *AtActin2* was used as a reference gene. Statistical analysis was performed using ANOVA followed by a Tukey post-hoc test with *p*-value threshold $p < 0.05$. The "-"symbol represents water-treated leaves. E) Western blot analysis of GFP expression in cross-kingdom RNAi reporter plants during *B. cinerea* infection using a @GFP antibody. The ribulose 1,5-bisphosphate carboxylase/oxygenase (RuBisCo) signal detected by Coomassie Brilliant Blue (CBB) staining was used as a loading control. Numbers indicate GFP and RuBisCo signal intensities estimated by the FIJI software.

https://doi.org/10.1371/journal.ppat.1011885.g004

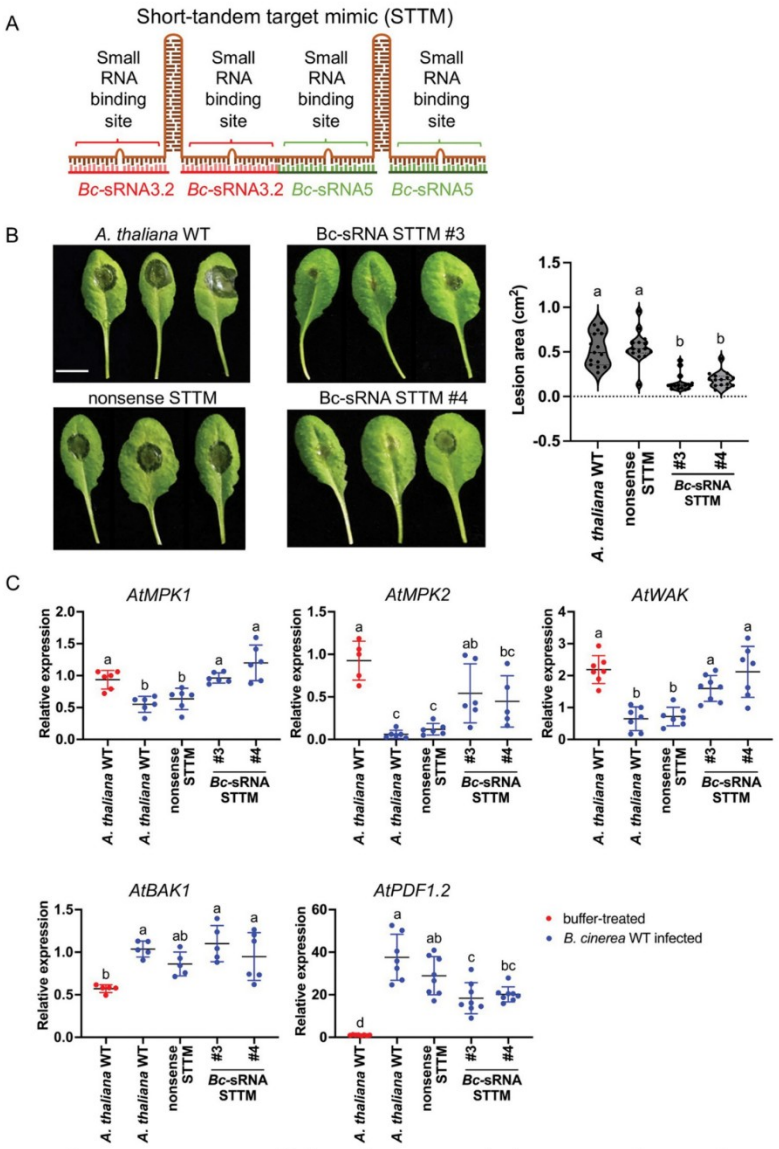

Fig 5. A plant expressing Bc-sRNA STTM blocks cross-kingdom RNAi and reduces *B. cinerea* pathogenicity. A) Schematic overview of the STTM construct to block Bc-sRNA3.2 and Bc-sRNA5 *in planta*. B) *A. thaliana* detached leaf inoculation assay using a 20 μl drop of 2 x 10^5/ml conidiospore suspension of *B. cinerea* WT, comparing three independent Bc-sRNA STTM T2 plant lines (#3, #4, #6) with *A. thaliana* WT and a nonsense STTM T2 plant line serving as negative controls. Lesion sizes were measured at 60 hpi and a minimum 15 lesions per plant line were used for statistical analysis

using ANOVA followed by a Tukey post-hoc test with p-value threshold $p < 0.05$. The scale bars represent 1 cm. C) Quantitative reverse transcriptase PCR measuring mRNA levels of Bc-sRNA target genes in *A. thaliana AtMPK1*, *AtMPK2*, and *AtWAK* comparing STTM lines and WT during *B. cinerea* infection of WT plants (red dots) or STTM-expressing plants (blue dots) at 48 hpi. Lines in scatter plots represent the mean and the standard deviation. Each gene was measured in at least five biological replicates. The *At-Actin* was used as a reference gene. *AtBAK1* and *AtPDF1.2* were measured as plant immunity marker genes induced during *B. cinerea* infection. Statistical analysis was performed using ANOVA followed by a Tukey post-hoc test with p-value threshold $p < 0.05$.

https://doi.org/10.1371/journal.ppat.1011885.g005

those lines with *B. cinerea* WT. Bc-sRNAs STTM plants exhibited reduced lesion sizes induced by *B. cinerea*, compared to *A. thaliana* WT or a transgenic *A. thaliana* line expressing a non-sense RNA-STTM (Figs 5B and S17A). In consistence, Bc-sRNA3.2 and Bc-sRNA5 target genes in *A. thaliana*, *AtMPK1*, *AtMPK2*, and *AtWAK* were suppressed in *A. thaliana* WT or *A. thaliana* expressing a nonsense RNA STTM upon *B. cinerea* infection, but suppression of those host target genes was abolished in the Bc-sRNA STTM plant lines (Figs 5C and S17B). Successful infection of all plant lines resulted in an induced host defense response due to *B. cinerea* infection, which was validated by measured up-regulation of the *A. thaliana* immunity-related genes *AtBAK1* and *AtPDF1.2*. These results confirmed that cross-kingdom RNAi is an important part of *B. cinerea* pathogenicity.

We previously found that expressing a triple STTM in *A. thaliana* that blocked small RNAs of the oomycete pathogen *Hyaloperonospora arabidopsidis* led to reduced disease levels [22]. We hypothesized that combining binding sites of different types of pathogen and parasite small RNAs that are known to induce cross-kingdom RNAi might create a multi-pathogen resistant plant genotype. We designed a "master" STTM to block the two *B. cinerea* Bc-sRNA3.2 and Bc-siRNA5, the two *H. arabidopsidis* small RNAs, Hpa-sRNA2 and Hpa-sRNA90 [22], as well as the two *Cuscuta campestris* ccm-miR12497b and ccm-miR12480 [32] and the *Phytophthora infestans* Pi-miRNA8788 [33]. *A. thaliana* master STTM plants grew and developed normally and did not show any pleiotropic defect (S18 Fig). We inoculated three independent T2 master STTM plant lines with *B. cinerea* and found that all transgenic lines exhibited reduced fungal lesion sizes (S17A and S17B Fig) and plant target gene de-repression (S17C Fig), confirming our results obtained with the Bc-sRNA STTM plants. Interestingly, a master STTM plant also revealed reduced disease levels when inoculated with the oomycete *H. arabidopsidis* (S17E Fig). Reduced infection was not due to constantly enhanced plant immunity, according to non-induced expression of *AtPR1* or *AtPFD1.2* in non-treated plants (S17D Fig). Further, inoculating Bc-sRNA- or master STTM plant lines with the bacterial pathogen *Pseudomonas syringae* DC3000 did not result in reduced bacterial colony numbers (S17F Fig). Based on these observations, we propose that STTMs might be a future application against pathogen small RNAs to design multi-pathogen resistant plants.

Discussion

In this study, we demonstrated that BcRDR1 is a pathogenicity factor that is required for cross-kingdom RNAi in the fungal plant pathogen *B. cinerea*. Previously, a *bcdcl1/2* mutant was characterized to be impaired in pathogenicity, Bc-sRNA biogenesis, and cross-kingdom RNAi [13,26]. This *dcl1dcl2* ko mutant exhibited reduced growth in axenic culture as well as on plant leaves that could be partially complemented by ectopic Bc-sRNA expression in transgenic *A. thaliana* [13]. Effective *BcDCL1*/*BcDCL2* gene knockdown via both host-induced gene silencing or RNA spray-induced gene silencing was sufficient to reduce *B. cinerea* disease symptoms on various plant species and tissues supporting a functional role of BcDCLs in pathogenicity [23,24,26]. Recently, the impact of *bcdcl1dcl2* ko generated in the *ku70* ko background was debated to not exhibit any growth defect in axenic culture and no or only mildly

reduced pathogenicity on plant leaves [34,35]. The *bcrdr1* ko mutants characterized here did not display any growth defect when grown in axenic culture, but a significant reduction in lesion size formation during plant infection and reduced *in planta* fungal biomass when infecting the two plant host species *S. lycopersicum* and *A. thaliana*. Furthermore, *bcrdr1* ko mutants were impaired in activating a Bc-sRNAs-responsive switch-on cross-kingdom RNAi reporter expressed in transgenic *A. thaliana*. Moreover, we confirmed with further evidence the importance of cross-kingdom RNAi in *B. cinerea* pathogenicity using a STTM approach. Blocking Bc-sRNAs via STTM expression in *A. thaliana* led to reduced *B. cinerea* disease symptoms. A similar approach demonstrated the relevance of cross-kingdom RNAi in the oomycete pathogen *H. arabidopsidis* infecting *A. thaliana* [22].

RDR knock out in different fungal plant pathogens resulted in pleiotropic defects on growth, development, and pathogenicity. The rice blast fungus *M. oryzae* comprises three RDRs named MoRDRP1-MoRDRP3, and the MoRDRP1 is the closest orthologue of BcRDR1. Isolated *mordrp1* ko mutants exhibited reduced growth, conidia formation, and disease symptoms on rice leaves [10]. Unlike *bcrdr1*, *mordrp1* revealed only moderate changes in small RNA production, but *mordrp2* ko was strongly impaired in retrotransposon- and intergenic-derived 21–23 nt small RNA production. Thus, the underlying MoRDRP1 mode of action in pathogenicity remained obscure. In the head blight-inducing fungal pathogen *F. graminearum* five RDRs, named FgRdRP1-FgRdRP5, were identified. In two independent studies, distinct roles of FgRdRPs in fungal development and pathogenicity were reported [11,36]. Studying *fgrdrp* ko mutants revealed neither altered scab disease symptoms when infecting flowering wheat heads or rot symptoms on tomato fruits, nor defects in vegetative development under normal or abiotic stress growth conditions [36]. On the contrary, different *fgrdrp* ko mutants displayed alterations in asexual and sexual development. Moreover, infecting wheat spikes with *fgrdrp2*, *fgrdrp3* and *fgrdrp4* ko mutants at 9 days post inoculation resulted in reduced head blight symptoms, which correlated with lower pathogen DNA content and levels of the mycotoxin Deoxynivalenol per seed dry weight [11]. The role of FgRdRPs in small RNA biogenesis has not been studied so far. The alternating numbers of RDR homologs in different fungal species and their distinct roles in small RNA biogenesis and pathogenicity indicate a rapid RDR neo-functionalization of the RNAi components in fungi. The unknown roles of BcRDR2 and BcRDR3 in *B. cinerea* need to be investigated in future studies.

Movement of small RNAs between fungi and plants has been observed multiple times [37]. Cross-kingdom RNAi has been discovered in other plant- or animal-associated fungal, oomycete, and bacterial microbes, for pathogens and symbionts [14,16]. It will be interesting to investigate whether microbial RDRs play a broader role in diverse plant-microbe interactions and in cross-kingdom RNA communication and its practical implementation by RNAi-based crop protection strategies.

Materials and methods

Fungal and plant materials and growth conditions

Botrytis cinerea (Pers.: Fr.) strain B05.10 was used for this study. Standard cultivation was carried out on HA medium (10 g/L malt extract, 4 g/L yeast extract, 4 g/L glucose, 15 g/L agar). *B. cinerea bcrdr1* ko and *bcdcl1dcl2* ko mutant strains were grown on HA medium supplemented with 70 μg/mL hygromycin B (Carl Roth GmbH). Fungal plates were incubated at room temperature in a growth chamber under long wavelength UV light (EUROLITE; 20 W to stimulate sporulation. The tomato (*Solanum lycopersicum* (L.) cultivar Heinz) used in this study was grown under the condition of 24˚C, 16 h light/8 h dark, 60% humidity in a growth cabinet. *Arabidopsis thaliana* (L.) ecotype Col-0 was grown under short day condition (10 h light/ 14 h

dark, 22˚C, 60% relative humidity) for *Botrytis* infection. For *H. arabidopsidis* infection, *Arabidopsis* Col-0 was grown under long day condition (16 h light/ 8 h dark, 22˚C, 60% relative humidity). Transgenic T1 and T2 *A. thaliana* lines were selected on 1/2 Murashige and Skoog (MS) medium supplemented with kanamycin (Carl Roth; 100 μg/mL). Independent plant transformant lines were indicated (e.g., STTM #3).

Cloning of *bcrdr* ko and cBcRDR1 complementation vectors, plant STTMs and cross-kingdom RNAi reporter

The Golden Gate cloning strategy was used for cloning fungal gene ko and gene complementation cassettes as well as plant expression vectors following the instruction, as described in Binder *et al.* [38]. The STTM sequences were designed, as described previously [31], and flanking region with BsaI recognition sites were introduced. A previously designed transgenic *A. thaliana* line that expressed a STTM with a randomized sequence of *H. arabidopsidis* small RNA target site [22] was used as a nonsense STTM control in this study.

For *A. thaliana* reporter lines, a Csy4 coding sequence was synthesized by MWG Eurofins with codon optimization for expression in plants, and the reporter cassette were assembled, as previously described [22]. The native promoter of the Bc-sRNA3.1 target gene *AtPRXIIF* was used to control the transcription level of the *Csy4* transgene in order to mimic natural Bc-sRNA target expression.

Fungal and plant transformation

B. cinerea was transformed as previously described [39] with minor modifications. Transformed fungal protoplasts were mixed with SH agar (0.6 M sucrose, 5 mM Tris-HCl (pH 6.5), 1 mM $(NH_4)H_2PO_4$, 8 g/L agar) without any antibiotics and incubated in darkness for 24 hours. A second layer of fresh SH agar containing hygromycin B (25 μg/ml) was added to the top after pre-incubation. The plates were further incubated in darkness until isolation of fungal transformants. For *A. thaliana* transformation, a previously described floral dip method was used [40].

Plant infection assay

S. lycopersicum pathogenicity assays were performed on detached leaves from 4- to 5-week-old plants. *B. cinerea* conidia were resuspended in 1% malt extract at a final concentration of 5×10^4 conidia/ml. *S. lycopersicum* leaves were inoculated with 20 μl conidia suspension and inoculated in a humidity plastic box. The detached leaves were placed on moist filter paper and then incubated in a closed plastic box. *A. thaliana* pathogenicity assays were performed on detached leaves from 5-week-old plants by inoculation with 2×10^5 conidia/ml *B. cinerea* conidia resuspended in 1% malt extract. 15 μl conidia suspension was dropped at the center of each leaf and inoculated in a humidity plastic box. Infected leaves were photographed, and lesion area was measured using the Fiji software (ImageJ version 2.1.0/1.53c).

Hyaloperonospora arabidopsidis (GÄUM.) isolate Noco2 was maintained on *A. thaliana* Col-0 WT plants. Two-week-old plants were inoculated with 2×10^4 conidia/ml suspension. Samples were harvested at 7 dpi into 10 ml of sterile water. The sporangiophore numbers were counted on detached cotyledons using a binocular microscope.

Pseudomonas syringae pv. *tomato* DC3000 was streaked out on LB agar plates with Rifampicin for 2 days at 28˚C. A single colony from the plate was inoculated with LB liquid medium with Rifampicin overnight. *Pseudomonas* cells were harvested and re-suspended in 10 mM $MgCl_2$ with 0.04% Silwet L-77 and adjusted to OD_{600} = 0.02. 5-week-old *A. thaliana* plants were sprayed with *Pseudomonas* suspension. Samples were harvested at 3 dpi and 4 leaf discs

per plant were collected then homogenized in 10 mM $MgCl_2$ for one biological replicate. A serial dilution on LB agar plates with Rifampicin was performed to count colony forming units.

Microscopic analysis of the switch-on GFP cross-kingdom RNAi reporter

For recording GFP time infection course with switch-on in cross-kingdom RNAi reporter plants, 3-week-old *A. thaliana* seedlings were cultivated on ½ MS + 1% sucrose agar plates and inoculated on plates with $2x10^5$ conidiospore/ml *B. cinerea* resuspended in 1% malt extract medium pre-incubated for 1 hours. The pre-incubated conidiospore suspension was washed twice with sterile water before 5 μl was dropped at the center of one leaf per seedling. For time course video, the Leica DMi8 Thunder Imager equipped with a Leica DFC9000 GT camera was used and whole seedlings were imaged. Imaging was set to start 6 h post conidiospore inoculation and images were taken in cycles of 22.5 mins for 45 h in total. Raw imaging data were processed using the Leica LAS X microscope software. Video editing was performed using Adobe Premiere Pro CC version13.0. GFP fluorescence intensity raw data were normalized at given time points (I_t) by subtracting the initial GFP intensity (I_0).

For the documentation of GFP signals in adult reporter plants, detached rosette leaves from 5-week-old *A. thaliana* plants were inoculated with 2×10^5 conidia/ml *B. cinerea* conidia resuspended in 1% malt extract for 1 hour. Conidiospore suspension was washed with sterile water and 20 μl was dropped on the leaf. Single leaf images of GFP signals and bright field (BF) were recorded on a Leica DM6 B upright microscope equipped with a Leica DFC9000 GT camera.

Trypan Blue staining

Leaf samples were collected and stained with Trypan Blue solution as described previously [41]. Microscopic images were taken with a DFC450 CCD-Camera (Leica) on a CTR 6000 microscope.

GUS staining

Leaf samples were vacuum-infiltrated with GUS staining solution (0.5 mg/ml X-Gluc, 100 mM phosphate buffer pH 7.0, 10 mM EDTA pH 7.0, 1 mM K3[Fe(CN)6], 1 mM K4[Fe(CN)6], 0.1% Triton X-100) and incubated over night at 37˚C. Leaves were de-stained with 70% ethanol overnight and microscopic images were taken under DFC450 CCD-Camera (Leica) on a CTR 6000 microscope.

Genotyping PCR

A CTAB method followed by chloroform extraction and isopropanol precipitation was used for DNA extraction from fungal mycelium [42]. The GoTaq G2 Polymerase (Promega) was used for genotyping PCR using PCR primers as listed in S1 Table.

Quantitative PCR

For fungal biomass quantification, genomic DNA was isolated using the CTAB method [43]. Relative fungal biomass was estimated by qPCR using the *BcTubA* primers (S1 Table). Raw data were normalized to plant genomic DNA estimation using the *AtActin2* or *SlActin2* primers (S1 Table).

For gene expression analysis, a CTAB method was used for total RNA extraction [44]. Genomic DNA was removed by DNase I (Sigma-Aldrich) treatment following the

manufacturer's instruction. 1 μg of total RNA from each sample was used for cDNA synthesis using the SuperScriptIII reverse transcriptase (ThermoFisher Scientific). Genomic DNA quantities and gene expression were measured by quantitative real-time PCR using the Primaquant low ROX qPCR master mix (Steinbrenner, Laborsysteme). Differential gene expression level was calculated using the $2^{-\Delta\Delta Ct}$ method [45]. Primers used in quantitative RT-PCR are listed in S1 Table and raw data are given in S3 Table.

Stem-loop reverse transcription PCR

Small RNA detection by stem-loop reverse transcriptase PCR was carried out following the protocol, as described [46]. 1 μg of total RNA was used for small RNA-specific RT and PCR. Reverse transcriptase PCR products were separated on a 10% non-denaturing polyacrylamide gel followed by ethidium bromide staining. Primers used in stem-loop reverse transcriptase PCR are listed in S1 Table.

Small RNA sequencing

Small RNAs were isolated from total RNA extracts using 15% polyacrylamide gel electrophoresis. Isolated small RNAs were subjected for library cloning using the Next Small RNA Prep kit (NEB) and sequenced on an Illumina NextSeq 2000 platform. The Illumina sequencing data were analyzed using the GALAXY Biostar server [47]. Raw data were de-multiplexed (Illumina Demultiplex, Galaxy Version 1.0.0) and adapter sequences were removed (Clip adaptor sequence, Galaxy Version 1.0.0). Sequence raw data are deposited at the NCBI SRA server (BioProject ID PRJNA978613). Reads were then mapped to the reference genome assembly of *B. cinerea* (ASM14353v4) using the BOWTIE2 algorithm (Galaxy Version 2.3.4.2) in end-to-end alignment mode, without setting–k or–a options. To assign Bc-sRNA to different types of RNA encoding genes, the sequence information of *B. cinerea* ribosomal RNAs, transfer RNAs, small nuclear and nucleolar RNAs, and mRNA were downloaded from the Ensembl database. Retrotransposon sequences was used as annotated in a previous study [17]. Reads were counted and normalized on total *B. cinerea* reads per million (RPM).

Small RNA coverage plots were produced from the above sRNA alignment, separating coverages by alignment strand and read length (grouping reads < 20 and > 25 nucleotides long). Coverage values represent the cumulative depth of the separate groups at every read position, normalized by aligned reads per million (RPM).

RDR homology search

Neurospora crassa QDE-1 and SAD-1 amino acid sequences (S2 Table) were used for Blastp search against the *B. cinerea* strain B05.10 (Taxon ID: 332648) protein reference database in Uniprot. RDR Active sites alignment was conducted with CLC Main Workbench (version 20.0.4).

Phylogeny

CLC Main Workbench (version 20.0.4) was used for phylogenetic analysis and composing the DNA sequence labels. Alignment was conducted with amino acid sequences of each RDR by default multiple alignment algorithms. Gap open cost was set for 15.0 and gap extension cost was set as 1.0. Phylogenetic tree was carried out by neighbor joining algorithm with 2000 replicates bootstrap. Kimura protein distance is used for protein distance measurement.

Data plotting and statistical analysis

GraphPad Prism 9 software was used for plotting and statistical analysis. For multi-samples comparison, one-way ANOVA with Tukey multiple comparisons test (p-value < 0.05) was carried out for data analysis. For *H. arabidopsidis* infection assay, unpaired t-test was carried out. Statistical significance was set for two-tailed p-value < 0.05 (*), p-value < 0.01 (**).

Data accessibility

Sequencing data have been deposited in NCBI SRA (BioProject ID PRJNA978613).

Supporting information

S1 Fig. Fungal RDR phylogenetic analysis (A) and amino acid sequence alignment of the RDR active site (B). The bar in (A) represents length of branch. Min and max refers to levels of conservation in (B). Amino acids sequences used in this analysis are given in S2 Table.
(PDF)

S2 Fig. Expression levels of the three *BcRDRs*. *BcRDRs* mRNA levels were measured in two independent replicates by qRT-PCR using the *BcTubA* as a reference gene. Lines in scatter plots represent the mean and the standard deviation. Statistical analysis was performed using ANOVA followed by a Tukey post-hoc test with p-value threshold $p < 0.05$.
(PDF)

S3 Fig. Generation of *bcrdr* ko mutants and cBcRDR1 gene complementation strains. A) Schematic overview of the *bcrdr1* ko and *cBcRDR1* complementation cloning strategies. B) Genotyping PCRs assessing *bcrdr1* gene ko and the insertion of the ko cassette into the *BcRDR1* genomic context. C) Genotyping PCRs assessing the insertion of the *cBcRDR1* cassette into the *bcrdr1* ko genomic context and RT-PCR assessing expression of *BcRDR1* in WT, *bcrdr1* ko mutant and cBcRDR1 complementation strains. D) Schematic overview of the *bcrdr2* ko cloning strategy. E) Genotyping PCR assessing *bcrdr2* gene ko.
(PDF)

S4 Fig. Replicates of infection series with *B. cinerea* WT and *bcrdr1* ko mutants on detached *S. lycopersicum* (A) and *A. thaliana* (B) leaves. A 20 μl drop of 5 x 10^4/ml condidiospores was placed on the leaves. The scale bars represent 1 cm. Lesion size induced by *B. cinerea* infection was measured at 48 hpi. Numbers given the analyzed lesions per plot. Statistical analysis was performed using ANOVA followed by a Tukey post-hoc test with p-value threshold $p < 0.05$.
(PDF)

S5 Fig. *B. cinerea* WT, *bcrdr1* ko, *bcrdr2* ko mutants and cBcRDR1 growth on 1% malt extract agar. A) Plate growth images were taken at 4 days. The scale bars represent 1 cm. B) To measure growth curves, a drop of 2 x 10^5/ml 10 μl conidiospore suspension was placed at the center of the agar plate and colony diameter was measured at 3, 4 and 5 days. Data represent 5 replicates. Statistical analysis was performed using ANOVA followed by a Tukey post-hoc test with p-value threshold $p < 0.05$.
(PDF)

S6 Fig. Expression analysis of known *B. cinerea* virulence genes in the *bcrdr1* ko mutants. mRNA levels of *BcPG1* (*Bcin14g00850*), *BcNEP1* (*Bcin06g06720*), *BcSpl1* (*Bcin03g00500*), *BcXyn11A* (*Bcin03g00480*) and *BcHIP1* (*Bcin14g01200*) was compared in *B. cinerea* WT and the *bcrdr1* ko mutants #2 and #4 grown in axenic culture in four biological replicates. The *BcTubA* was used as a reference gene. Statistical analysis was performed using ANOVA

followed by a Tukey post-hoc test with p-value threshold $p < 0.05$.
(PDF)

S7 Fig. A) Mapping results at the *BcGyspy1* and *BcGypsy3* loci obtained from *B. cinerea* WT and *bcrdr1* ko mutants small RNA sequencing data. Reads per million (RPM) values > 0 indicate sense alignment, RPM values < 0 indicates antisense alignment. Color-code indicates Bc-sRNA sizes. B) Size profiles of Bc-sRNAs mapped to the *BcGypsy1* and *BcGypsy3* loci in *B. cinerea* WT or *bcrdr*1 ko mutants #2 and #4. C) Expression levels of *BcGypsy1* and *BcGypsy3* mRNAs in *B. cinerea* WT and *bcrdr1* ko mutants when grown in axenic culture. D) Expression levels of *BcGypsy1* and *BcGypsy3* mRNAs in *B. cinerea* WT grown under axenic culture condition and during tomato infection at 48 hpi. E) Expression level comparison of *BcGypsy1* and *BcGypsy3* mRNAs in *B. cinerea* WT versus *bcrdr1* ko mutants #2 and #4 when grown under axenic culture condition or during tomato infection at 48 hpi. In C), D) and E), *BcTubA* mRNA was used as a reference gene expression. Lines in scatter plots represent the mean and the standard deviation. Statistical analysis was performed using ANOVA followed by a Tukey post-hoc test with p-value threshold $p < 0.05$.
(PDF)

S8 Fig. Stem-loop RT-PCR of Bc-sRNAs comparing *B. cinerea* WT and *bcrdr1* ko mutants. Bc-sRNAs were detected in tomato leaf samples infected with *B. cinerea* at 48 hpi. Figure represents full-scale gel images of results, as given in Fig 3B.
(PDF)

S9 Fig. Biological replicates of mRNA expression measurements of known Bc-sRNA target genes in *S. lycopersicum* (A) and *A. thaliana* (B) during infection with *B. cinerea* WT and *bcrdr1* ko mutants. Samples were taken at 36 hpi or 60 hpi for *S. lycopersicum* and *A. thaliana*, respectively. The *SlActin2* or the *AtActin2* were used as reference genes. Lines in scatter plots represent the mean and the standard deviation. Statistical analysis was performed using ANOVA followed by a Tukey post-hoc test with p-value threshold $p < 0.05$.
(PDF)

S10 Fig. Independent infection time series using GFP switch-on cross-kingdom RNAi reporter plant seedlings infected with *B. cinerea* WT, *bcrdr1* ko mutant #2 or water-treated. A) Fluorescence microscopy images at different time points of infection. A 5 μl drop of a 2 x 10^5/ml conidiospore suspension was placed at the center of the leaf before placing a glass covering slip on the top that dispersed the spore suspension and led to GFP activation over the entire leaf. The scale bars represent 1 mm. B) Normalized GFP signal quantification of whole seedling leaves over the time series of 6–42 hpi.
(PDF)

S11 Fig. Fluorescence microscopic imaging of *A. thaliana* WT seedlings infected with *B. cinerea* WT. The scale bars represent 1 mm.
(PDF)

S12 Fig. Three independent infection series and fluorescence microscopic imaging using detached rosette leaves of adult GFP switch-on cross-kingdom RNAi reporter plants. Leaves were inoculated with a 20 μl drop of 2 x 10^5/ml conidiospore suspension of *B. cinerea* WT, *bcrdr1* ko mutants, and a *bcdcl1/2* mutant. *A. thaliana* WT plants were infected with *B. cinerea* WT to assess auto-fluorescence, and water-treated GFP reporter plants were assessed for reporter auto-activity. The scale bars represent 500 μm.
(PDF)

S13 Fig. Infection of the GFP reporter seedling plants with the oomycete pathogen *Hyaloperonospora arabidopsidis*. 10 ml of a 2 x 10^4/ml conidiospore suspension was sprayed onto leaves. Trypan Blue staining visualized oomycete hyphae in the infected leaf. Outlines indicate the same leaf area in fluorescence and Trypan Blue staining images.
(PDF)

S14 Fig. Infection of a transgenic *A. thaliana* cross-kingdom RNAi reporter line with a GUS reporter. This reporter line was previously designed to demonstrate cross-kingdom RNAi triggered by small RNAs secreted by the oomycete *H. arabidopsidis* (Dunker *et al*., 2020 [22]). A) Infection of the GUS reporter line with *H. arabidopsidis* showing GUS at infecting oomycete hyphae. B) Infection of the GUS reporter line with *B. cinerea* revealed no GUS activation at infection sites (indicated by a turquoise arrows). C) Infection of a GUS reporter line carrying scrambled small RNA target sites with *H. arabidopsidis* showing no GUS activity. D) Infection of the scrambled GUS reporter line with *B. cinerea* showing no GUS activity at infection sites (indicated by a turquoise arrows). For *B. cinerea* inoculation, a 20 μl drop of 2 x 10^5 conidiospores were placed onto leaves. For *H. arabidopsidis* infection, 10 ml of a 2 x 10^4/ml conidiospore suspension were sprayed onto leaves. The scale bars represent 100 μm.
(PDF)

S15 Fig. Fluorescence microscopy imaging, mRNA and protein expression measurement with adult rosette leaves of the GFP switch-on cross-kingdom RNAi reporter plant using 10x conidiospore concentration for *bcrdr1* inoculation. A) Fluorescence microscopy images at 24 hpi indicated enhanced GFP expression in reporter plants at infection sites of *B. cinerea* WT in contrast to GFP non-expressing *A. thaliana* WT plants, water-treated GFP reporter plants or GFP reporter plants infected with *bcrdr1* ko mutants. The turquoise arrow in B) indicates the infection front of the *B. cinerea* WT inoculation. The scale bars in A) and B) represent 500 μm. C) GFP mRNA expression levels in *A. thaliana* WT plants (red dots), *A. thaliana* GFP reporter plants (blue dots) infected with *B. cinerea* WT, *bcrdr1* ko mutants or water-treated. The *AtActin2* was used as a reference gene. D) Western blot analysis of GFP expression using a @GFP antibody. RuBisCo signals were visualized by Coomassie Brilliant Blue staining. Numbers indicate GFP and RuBisCo intensities estimated by the FIJI software. E) *B. cinerea* genomic DNA in infected *A. thaliana* WT or GFP reporter plants was measured by qPCR using primers of the *BcTubA* gene. Raw data were normalized to plant DNA using *AtActin2* primers. Lines in scatter plots of qRT-PCR data in C) and qPCR of *B. cinerea* genomic DNA in E) represent the mean and the standard deviation. Statistical analysis was performed using ANOVA followed by a Tukey post-hoc test with p-value threshold $p < 0.05$.
(PDF)

S16 Fig. Fluorescence microscopy imaging of adult rosette leaves from the GFP switch-on cross-kingdom RNAi reporter plants infected with *B. cinerea* WT at 36 hpi. *B. cinerea* mycelium was visualized by Trypan Blue staining. Squares in images indicate area of magnification. The red asterisks indicate the same leaf trichome in merged BF/GFP and Trypan Blue images. The turquoise arrow indicates *B. cinerea* mycelium. The scale bars represent 500 μm.
(PDF)

S17 Fig. Infection series with *B. cinerea*, *H. arabidopsidis* and *P. syringae* DC3000 in transgenic T2 *A. thaliana* lines expressing a Bc-sRNA or master STTM. A) Leaf images of *A. thaliana* STTMs upon *B. cinerea* infection with 2 x 10^5 conidiospores/ml at 60 hpi. The scale bar in represent 1 cm. B) Lesion area induced by *B. cinerea* infection was measured at 48 hpi. C) mRNA expression levels of Bc-sRNA target genes *AtMPK1* and *AtWAK* in *A. thaliana*. The *AtActin2* was used as a reference gene. Lines in scatter plots represent the mean and the

standard deviation. Statistical analysis was performed using ANOVA followed by a Tukey post-hoc test with p-value threshold $p < 0.05$. D) Semi-quantitative RT-PCR of the *A. thaliana* immunity-associated genes *AtPR1* and *AtPDF1.2*. *B. cinerea*-infected leaves were used as an immunogenic control. E) Infection of the master STTM line #3 with the oomycete *H. arabidopsidis*. Oomycete sporangiophores were counted at 7 dpi in three replicated inoculation experiments. F) Infection of *A. thaliana* STTM lines with the bacterial pathogen *Pseudomonas syringae* DC3000. Colony-forming units (cfu) of were counted at 3 dpi. Statistical analysis in B), C), E), F) was performed using ANOVA followed by a Tukey post-hoc test with p-value threshold $p < 0.05$. Statistical analysis in E) replicate #1 and replicate #2 was carried out by unpaired t-test with two-tailed p-value < 0.05 (*), p-value < 0.01 (**).
(PDF)

S18 Fig. Plant images showing unaltered growth phenotype of *A. thaliana* STTM plants. Pictures were taken at 38 days after growing in short-day condition. The scale bar represents 1 cm.
(PDF)

S1 Video. Time course of the GFP cross-kingdom RNAi reporter activity upon *A. thaliana* leaf inoculation from 6–51 hpi with *B. cinerea* WT (left site) or *bcrdr1* ko mutant #2 (right site).
(MP4)

S1 Table. DNA oligonucleotides used in this study.
(XLSX)

S2 Table. Amino acid sequences used in phylogeny analysis.
(XLSX)

S3 Table. qPCR and qRT-PCR raw data $2^{-\Delta\Delta Ct}$ values.
(XLSX)

Acknowledgments

We thank Dr. Claude Becker for critical proofreading of this work. We want to thank the Gene Center Munich for Illumina NextSeq sequencing service. We would like to thank Dr. Martin Parniske for scientific discussions and providing access to the Golden Gate cloning system, Dr. Silke Robatzek and Dr. Eliana Mor for the access to and technical assistance with the DMi8 Thunder Imager microscope, and Dr. Dagmar Hann for sharing with us the *Pst* DC3000 strain. We thank Annika Lübbe for supporting the GUS staining. We thank Verena Klingl for technical support to isolate *Botrytis bcrdr1* ko transformants and Ignacio Mohr for helping with the *H. arabidopsidis* inoculation. We thank Franz Oberkofler for video editing.

Author Contributions

Conceptualization: Arne Weiberg.

Data curation: An-Po Cheng, Nathan R. Johnson.

Formal analysis: An-Po Cheng, Bernhard Lederer, Lorenz Oberkofler, Nathan R. Johnson, Fabian Platten.

Funding acquisition: Arne Weiberg.

Investigation: An-Po Cheng, Lihong Huang.

Methodology: An-Po Cheng, Bernhard Lederer, Lorenz Oberkofler, Florian Dunker, Constance Tisserant.

Project administration: Arne Weiberg.

Supervision: Arne Weiberg.

Writing – original draft: An-Po Cheng, Arne Weiberg.

Writing – review & editing: An-Po Cheng, Bernhard Lederer, Lorenz Oberkofler, Lihong Huang, Nathan R. Johnson, Fabian Platten, Florian Dunker, Constance Tisserant, Arne Weiberg.

References

1. Machitani M, Yasukawa M, Nakashima J, Furuichi Y, Masutomi K. RNA-dependent RNA polymerase, RdRP, a promising therapeutic target for cancer and potentially COVID-19. Cancer Sci. 2020; 111 (11):3976–3984. https://doi.org/10.1111/cas.14618 PMID: 32805774
2. Chang SS, Zhang Z, Liu Y. RNA interference pathways in fungi: mechanisms and functions. Annu Rev Microbiol. 2012; 66:305–323. https://doi.org/10.1146/annurev-micro-092611-150138 PMID: 22746336
3. Mello CC, Conte D Jr. Revealing the world of RNA interference. Nature. 2004; 431(7006):338–342. https://doi.org/10.1038/nature02872 PMID: 15372040
4. Matzke MA, Mosher RA. RNA-directed DNA methylation: an epigenetic pathway of increasing complexity. Nat Rev Genet. 2014; 15(6):394–408. https://doi.org/10.1038/nrg3683 PMID: 24805120
5. Boccara M, Sarazin A, Thiebeauld O, Jay F, Voinnet O, Navarro L, et al. The Arabidopsis miR472-RDR6 silencing pathway modulates PAMP-and effector-triggered immunity through the post-transcriptional control of disease resistance genes. Plos Pathogens. 2014; 10(1). https://doi.org/10.1371/journal.ppat.1003883 PMID: 24453975
6. Garcia-Ruiz H, Takeda A, Chapman EJ, Sullivan CM, Fahlgren N, Brempelis KJ, et al. Arabidopsis RNA-dependent RNA polymerases and Dicer-like proteins in antiviral defense and small interfering RNA biogenesis during Turnip Mosaic Virus infection. Plant Cell. 2010; 22(2):481–496. https://doi.org/10.1105/tpc.109.073056 PMID: 20190077
7. Torres-Martinez S, Ruiz-Vazquez RM. The RNAi Universe in fungi: a varied landscape of small RNAs and biological functions. Annu Rev Microbiol. 2017; 71:371–391. https://doi.org/10.1146/annurev-micro-090816-093352 PMID: 28657888
8. Calo S, Nicolas FE, Vila A, Torres-Martinez S, Ruiz-Vazquez RM. Two distinct RNA-dependent RNA polymerases are required for initiation and amplification of RNA silencing in the basal fungus *Mucor circinelloides*. Mol Microbiol. 2012; 83(2):379–394.
9. Zhang DX, Spiering MJ, Nuss DL. Characterizing the roles of *Cryphonectria parasitica* RNA-dependent RNA polymerase-like genes in antiviral defense, viral recombination and transposon transcript accumulation. PLoS One. 2014; 9(9). https://doi.org/10.1371/journal.pone.0108653 PMID: 25268858
10. Raman V, Simon SA, Demirci F, Nakano M, Meyers BC, Donofrio NM. Small RNA functions are required for growth and development of *Magnaporthe oryzae*. Mol Plant Microbe Interact. 2017; 30 (7):517–530.
11. Gaffar FY, Imani J, Karlovsky P, Koch A, Kogel KH. Different components of the RNA interference machinery are required for conidiation, ascosporogenesis, virulence, Deoxynivalenol production, and fungal inhibition by exogenous double-stranded RNA in the Head Blight pathogen *Fusarium graminearum*. Front Microbiol. 2019; 10:1662. https://doi.org/10.3389/fmicb.2019.01662 PMID: 31616385
12. Wang M, Weiberg A, Dellota E Jr, Yamane D, Jin H. *Botrytis* small RNA Bc-siR37 suppresses plant defense genes by cross-kingdom RNAi. RNA Biol. 2017; 14(4):421–428.
13. Weiberg A, Wang M, Lin FM, Zhao H, Zhang Z, Kaloshian I, et al. Fungal small RNAs suppress plant immunity by hijacking host RNA interference pathways. Science. 2013; 342(6154):118–123. https://doi.org/10.1126/science.1239705 PMID: 24092744
14. Weiberg A, Bellinger M, Jin H. Conversations between kingdoms: small RNAs. Curr Opin Biotechnol. 2015; 32:207–215. https://doi.org/10.1016/j.copbio.2014.12.025 PMID: 25622136
15. Weiberg A, Wang M, Bellinger M, Jin H. Small RNAs: a new paradigm in plant-microbe interactions. Annu Rev Phytopathol. 2014; 52:495–516. https://doi.org/10.1146/annurev-phyto-102313-045933 PMID: 25090478

16. Cai Q, He B, Weiberg A, Buck AH, Jin H. Small RNAs and extracellular vesicles: New mechanisms of cross-species communication and innovative tools for disease control. PLoS Pathog. 2019; 15(12): e1008090. https://doi.org/10.1371/journal.ppat.1008090 PMID: 31887135

17. Porquier A, Tisserant C, Salinas F, Glassl C, Wange L, Enard W, et al. Retrotransposons as pathogenicity factors of the plant pathogenic fungus *Botrytis cinerea*. Genome Biol. 2021; 22(1):225. https://doi.org/10.1186/s13059-021-02446-4 PMID: 34399815

18. Shiu PK, Raju NB, Zickler D, Metzenberg RL. Meiotic silencing by unpaired DNA. Cell. 2001; 107 (7):905–916. https://doi.org/10.1016/s0092-8674(01)00609-2 PMID: 11779466

19. Cogoni C, Macino G. Isolation of *quelling-defective* (*qde*) mutants impaired in posttranscriptional transgene-induced gene silencing in *Neurospora crassa*. Proc Natl Acad Sci U S A. 1997; 94(19):10233–10238.

20. Leisen T, Werner J, Pattar P, Safari N, Ymeri E, Sommer F, et al. Multiple knockout mutants reveal a high redundancy of phytotoxic compounds contributing to necrotrophic pathogenesis of *Botrytis cinerea*. PLoS Pathog. 2022; 18(3):e1010367. https://doi.org/10.1371/journal.ppat.1010367 PMID: 35239739

21. Haurwitz RE, Jinek M, Wiedenheft B, Zhou K, Doudna JA. Sequence- and structure-specific RNA processing by a CRISPR endonuclease. Science. 2010; 329(5997):1355–1358. https://doi.org/10.1126/science.1192272 PMID: 20829488

22. Dunker F, Trutzenberg A, Rothenpieler JS, Kuhn S, Prols R, Schreiber T, et al. Oomycete small RNAs bind to the plant RNA-induced silencing complex for virulence. Elife. 2020; 9:e56096. https://doi.org/10.7554/eLife.56096 PMID: 32441255

23. Qiao L, Lan C, Capriotti L, Ah-Fong A, Nino Sanchez J, Hamby R, et al. Spray-induced gene silencing for disease control is dependent on the efficiency of pathogen RNA uptake. Plant Biotechnol J. 2021. https://doi.org/10.1111/pbi.13589 PMID: 33774895

24. Qiao L, Nino-Sanchez J, Hamby R, Capriotti L, Chen A, Mezzetti B, et al. Artificial nanovesicles for dsRNA delivery in spray-induced gene silencing for crop protection. Plant Biotechnol J. 2023; 21 (4):854–865. https://doi.org/10.1111/pbi.14001 PMID: 36601704

25. Wang M, Jin H. Spray-induced gene silencing: a powerful innovative strategy for crop protection. Trends Microbiol. 2017; 25(1):4–6. https://doi.org/10.1016/j.tim.2016.11.011 PMID: 27923542

26. Wang M, Weiberg A, Lin FM, Thomma BP, Huang HD, Jin H. Bidirectional cross-kingdom RNAi and fungal uptake of external RNAs confer plant protection. Nat Plants. 2016; 2:16151. https://doi.org/10.1038/nplants.2016.151 PMID: 27643635

27. Werner BT, Gaffar FY, Schuemann J, Biedenkopf D, Koch AM. RNA-spray-mediated silencing of *Fusarium graminearum AGO* and *DCL* genes improve barley disease resistance. Front Plant Sci. 2020; 11:476. https://doi.org/10.3389/fpls.2020.00476 PMID: 32411160

28. Werner BT, Koch A, Secic E, Engelhardt J, Jelonek L, Steinbrenner J, et al. *Fusarium graminearum* DICER-like-dependent sRNAs are required for the suppression of host immune genes and full virulence. PLoS One. 2021; 16(8):e0252365. https://doi.org/10.1371/journal.pone.0252365 PMID: 34351929

29. Zanini S, Secic E, Busche T, Galli M, Zheng Y, Kalinowski J, et al. Comparative analysis of transcriptome and sRNAs expression patterns in the *Brachypodium distachyon- Magnaporthe oryzae* pathosystems. Int J Mol Sci. 2021; 22(2). https://doi.org/10.3390/ijms22020650 PMID: 33440747

30. Goehre V, Weiberg A. RNA dialogues in fungal-plant relationships. The Mycota—Plant Relationships. 2023; 5:31–51.

31. Tang G, Yan J, Gu Y, Qiao M, Fan R, Mao Y, et al. Construction of short tandem target mimic (STTM) to block the functions of plant and animal microRNAs. Methods. 2012; 58(2):118–125. https://doi.org/10.1016/j.ymeth.2012.10.006 PMID: 23098881

32. Shahid S, Kim G, Johnson NR, Wafula E, Wang F, Coruh C, et al. MicroRNAs from the parasitic plant *Cuscuta campestris* target host messenger RNAs. Nature. 2018; 553(7686):82–85.

33. Hu X, Persson Hoden K, Liao Z, Asman A, Dixelius C. *Phytophthora infestans* Ago1-associated miRNA promotes potato late blight disease. New Phytol. 2022; 233(1):443–457.

34. He B, Cai Q, Weiberg A, Cheng AP, Ouyang SQ, Borkovich KA, et al. *Botrytis cinerea* small RNAs are associated with tomato AGO1 and silence tomato target genes supporting cross-kingdom RNAi between the fungal pathogen *B. cinerea* and its tomato host. BioRxiv. 2023. https://doi.org/10.1101/2022.12.30.522274

35. Qin S, Veloso J, Baak M, Boogmans B, Bosman T, Puccetti G, et al. Molecular characterization reveals no functional evidence for naturally occurring cross-kingdom RNA interference in the early stages of *Botrytis cinerea*-tomato interaction. Mol Plant Pathol. 2023; 24(1):3–15.

36. Chen Y, Gao Q, Huang M, Liu Y, Liu Z, Liu X, et al. Characterization of RNA silencing components in the plant pathogenic fungus *Fusarium graminearum*. Sci Rep. 2015; 5:12500. https://doi.org/10.1038/srep12500 PMID: 26212591

37. Wang MY, Dean RA. Movement of small RNAs in and between plants and fungi. Molecular Plant Pathology. 2020; 21(4):589–601. https://doi.org/10.1111/mpp.12911 PMID: 32027079

38. Binder A, Lambert J, Morbitzer R, Popp C, Ott T, Lahaye T, et al. A modular plasmid assembly kit for multigene expression, gene silencing and silencing rescue in plants. PLoS One. 2014; 9(2):e88218. https://doi.org/10.1371/journal.pone.0088218 PMID: 24551083

39. Muller N, Leroch M, Schumacher J, Zimmer D, Konnel A, Klug K, et al. Investigations on VELVET regulatory mutants confirm the role of host tissue acidification and secretion of proteins in the pathogenesis of *Botrytis cinerea*. New Phytol. 2018; 219(3):1062–1074.

40. Clough SJ, Bent AF. Floral dip: a simplified method for *Agrobacterium*-mediated transformation of *Arabidopsis thaliana*. Plant J. 1998; 16(6):735–743.

41. Koch E, Slusarenko A. Arabidopsis is susceptible to infection by a downy mildew fungus. Plant Cell. 1990; 2(5):437–445. https://doi.org/10.1105/tpc.2.5.437 PMID: 2152169

42. Chen DH, Ronald PC. A rapid DNA minipreparation method suitable for AFLP and other PCR applications. Plant Molecular Biology Reporter. 1999; 17(1):53–57.

43. Calderon-Cortes N, Quesada M, Cano-Camacho H, Zavala-Paramo G. A simple and rapid method for DNA isolation from xylophagous insects. Int J Mol Sci. 2010; 11(12):5056–5064. https://doi.org/10.3390/ijms11125056 PMID: 21614191

44. Bemm F, Becker D, Larisch C, Kreuzer I, Escalante-Perez M, Schulze WX, et al. Venus flytrap carnivorous lifestyle builds on herbivore defense strategies. Genome Res. 2016; 26(6):812–825. https://doi.org/10.1101/gr.202200.115 PMID: 27197216

45. Livak KJ, Schmittgen TD. Analysis of relative gene expression data using real-time quantitative PCR and the 2(T)(-Delta Delta C) method. Methods. 2001; 25(4):402–408.

46. Varkonyi-Gasic E, Wu R, Wood M, Walton EF, Hellens RP. Protocol: a highly sensitive RT-PCR method for detection and quantification of microRNAs. Plant Methods. 2007; 3:12. https://doi.org/10.1186/1746-4811-3-12 PMID: 17931426

47. Giardine B, Riemer C, Hardison RC, Burhans R, Elnitski L, Shah P, et al. Galaxy: a platform for interactive large-scale genome analysis. Genome Res. 2005; 15(10):1451–1455. https://doi.org/10.1101/gr.4086505 PMID: 16169926

S1 Fig.

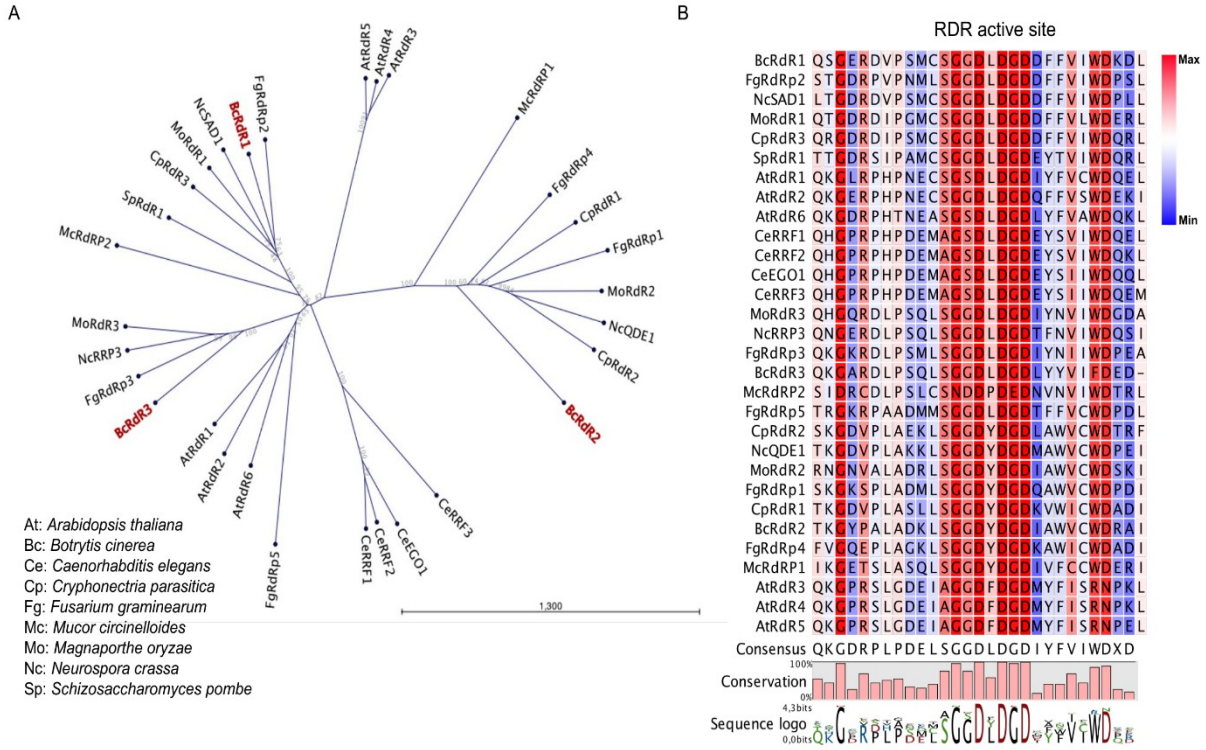
A
B
RDR active site
Max
Min
AtRdR5
AtRdR4
AtRdR3
McRdRP1
FgRdRp4
CpRdR1
FgRdRp1
MoRdR2
NcQDE1
CpRdR2
BcRdR2
CeRRF3
CeEGO1
CeRRF2
CeRRF1
FgRdRp5
AtRdR6
AtRdR2
AtRdR1
BcRdR3
FgRdRp3
NcRRP3
MoRdR3
McRdRP2
SpRdR1
CpRdR3
MoRdR1
NcSAD1
BcRdR1
FgRdRp2
1,300
At: Arabidopsis thaliana
Bc: Botrytis cinerea
Ce: Caenorhabditis elegans
Cp: Cryphonectria parasitica
Fg: Fusarium graminearum
Mc: Mucor circinelloides
Mo: Magnaporthe oryzae
Nc: Neurospora crassa
Sp: Schizosaccharomyces pombe
BcRdR1 QSGERDVPSMCSGGDLDGDDFFVIWDKDL
FgRdRp2 STGDRPVPNMLSGGDLDGDDFFVIWDPSL
NcSAD1 LTGDRDVPSMCSGGDLDGDDFFVIWDPLL
MoRdR1 QTGDRDIPGMCSGGDLDGDDFFVLWDERL
CpRdR3 QRGDRDIPSMCSGGDLDGDDFFVIWDQRL
SpRdR1 TTGDRSIPAMCSGGDLDGDEYTVIWDQRL
AtRdR1 QKGLRPHPNECSGSDLDGDIYFVCWDQEL
AtRdR2 QKGERPHPNECSGGDLDGDQFFVSWDEKI
AtRdR6 QKGDRPHTNEASGSDLDGDLYFVAWDQKL
CeRRF1 QHGPRPHPDEMAGSDLDGDEYSVIWDQEL
CeRRF2 QHGPRPHPDEMAGSDLDGDEYSVIWDQKL
CeEGO1 QHGPRPHPDEMAGSDLDGDEYSIIWDQQL
CeRRF3 QHGPRPHPDEMAGSDLDGDEYSIIWDQEM
MoRdR3 QHGQRDLPSQLSGGDLDGDIYNVIWDGDA
NcRRP3 QNGERDLPSQLSGGDLDGDTFNVIWDQSI
FgRdRp3 QKGKRDLPSMLSGGDLDGDIYNIIWDPEA
BcRdR3 QKGARDLPSQLSGGDLDGDLYYVIFDED-
McRdRP2 SIDRCDLPSLCSNDDPDEDNVNVIWDTRL
FgRdRp5 TRGKRPAADMMSGGDLDGDTFFVCWDPDL
CpRdR2 SKGDVPLAEKLSGGDYDGDLAWVCWDTRF
NcQDE1 TKGDVPLAKKLSGGDYDGDMAWVCWDPEI
MoRdR2 RNGNVALADRLSGGDYDGDIAWVCWDSKI
FgRdRp1 SKGKSPLADMLSGGDYDGDQAWVCWDPDI
CpRdR1 TKGDVPLASLLSGGDYDGDKVWICWDADI
BcRdR2 TKGYPALADKLSGGDYDGDIAWVCWDRAI
FgRdRp4 FVGQEPLAGKLSGGDYDGDKAWICWDADI
McRdRP1 IKGETSLASQLSGGDYDGDIVFCCWDERI
AtRdR3 QKGPRSLGDEIAGGDFDGDMYFISRNPKL
AtRdR4 QKGPRSLGDEIAGGDFDGDMYFISRNPKL
AtRdR5 QKGPRSLGDEIAGGDFDGDMYFISRNPEL
Consensus QKGDRPLPDELSGGDLDGDIYFVIWDXD
Conservation
Sequence logo

S2 Fig.

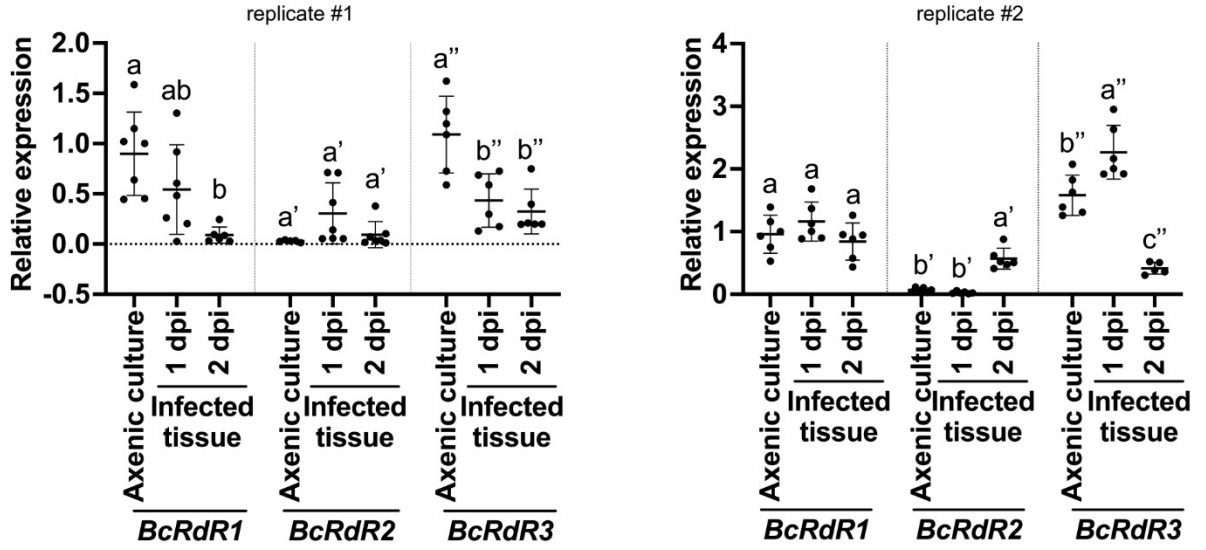
replicate #1
replicate #2
Relative expression
Axenic culture
1 dpi
2 dpi
Infected tissue
BcRdR1
BcRdR2
BcRdR3
a
ab
b
a'
a'
a'
a"
b"
b"
b'
b'
a'
b"
a"
c"

S3 Fig.

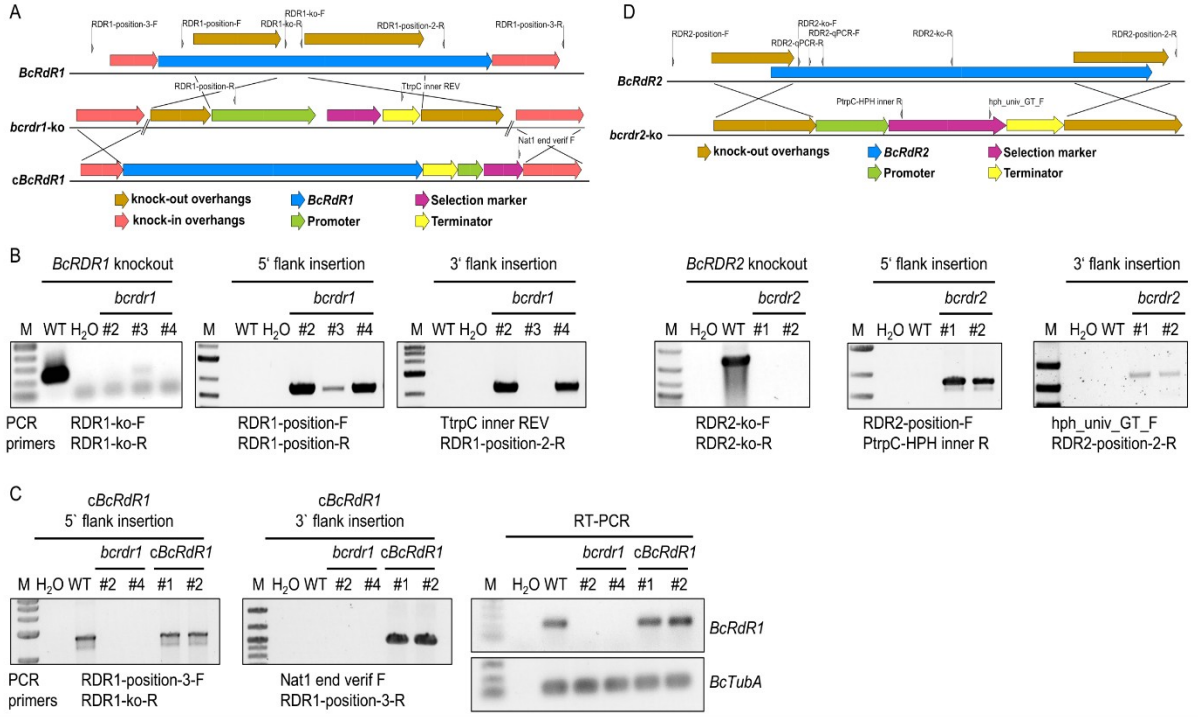
A
RDR1-position-3-F
RDR1-position-F
RDR1-ko-F
RDR1-ko-R
RDR1-position-2-R
RDR1-position-3-R
BcRdR1
RDR1-position-R
TtrpC inner REV
bcrdr1-ko
Nat1 end verif F
cBcRdR1
knock-out overhangs
knock-in overhangs
BcRdR1
Promoter
Selection marker
Terminator
D
RDR2-position-F
RDR2-ko-F
RDR2-qPCR-F
RDR2-qPCR-R
RDR2-ko-R
RDR2-position-2-R
BcRdR2
PtrpC-HPH inner R
hph_univ_GT_F
bcrdr2-ko
knock-out overhangs
BcRdR2
Promoter
Selection marker
Terminator
B
BcRDR1 knockout
bcrdr1
5' flank insertion
3' flank insertion
M WT H2O #2 #3 #4
PCR primers
RDR1-ko-F
RDR1-ko-R
RDR1-position-F
RDR1-position-R
TtrpC inner REV
RDR1-position-2-R
BcRDR2 knockout
bcrdr2
M H2O WT #1 #2
RDR2-ko-F
RDR2-ko-R
RDR2-position-F
PtrpC-HPH inner R
hph_univ_GT_F
RDR2-position-2-R
C
cBcRdR1
5` flank insertion
3` flank insertion
RT-PCR
bcrdr1 cBcRdR1
M H2O WT #2 #4 #1 #2
PCR primers
RDR1-position-3-F
RDR1-ko-R
Nat1 end verif F
RDR1-position-3-R
BcRdR1
BcTubA

S4 Fig.

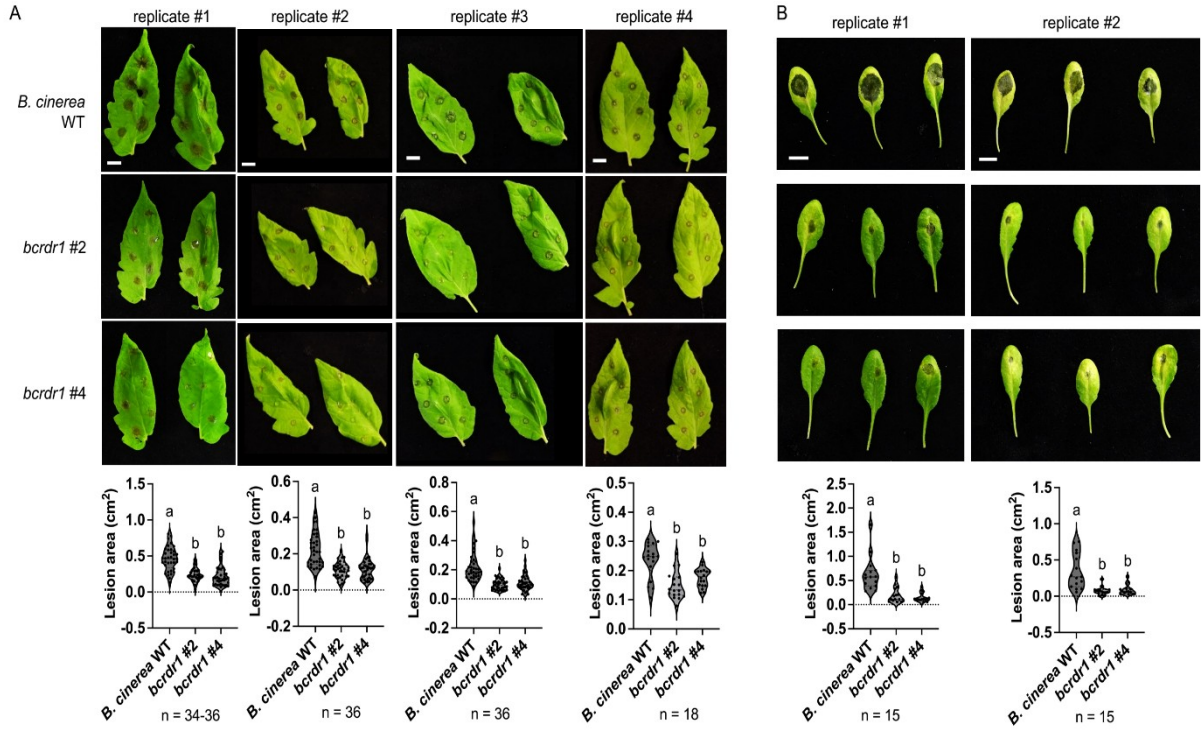
A
replicate #1
replicate #2
replicate #3
replicate #4
B. cinerea WT
bcrdr1 #2
bcrdr1 #4
Lesion area (cm²)
B. cinerea WT
bcrdr1 #2
bcrdr1 #4
n = 34-36
n = 36
n = 36
n = 18
B
replicate #1
replicate #2
n = 15
n = 15

S5 Fig.

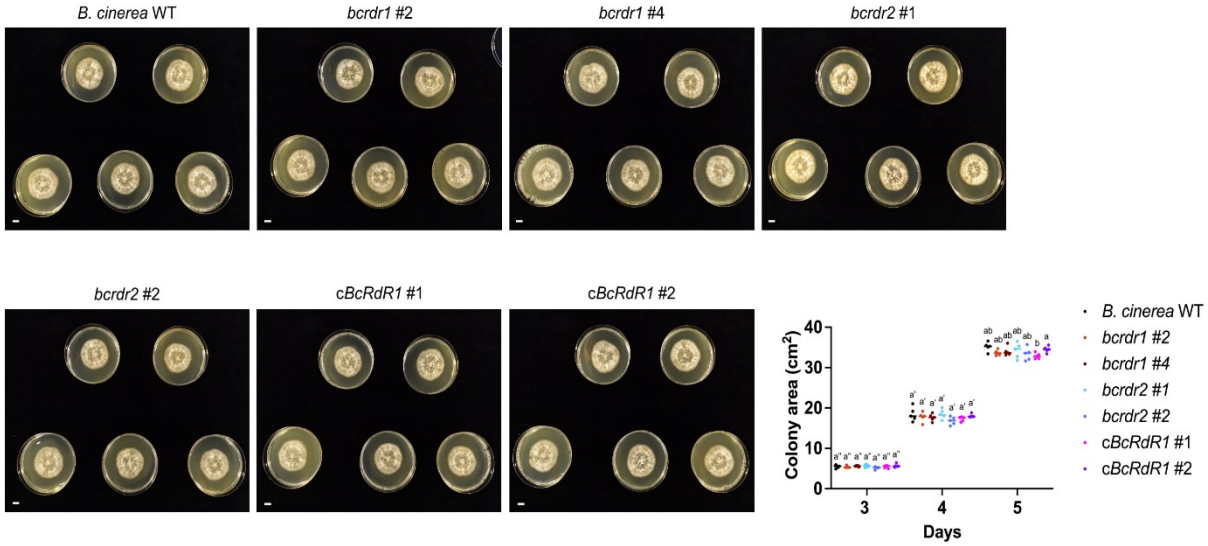

S6 Fig.

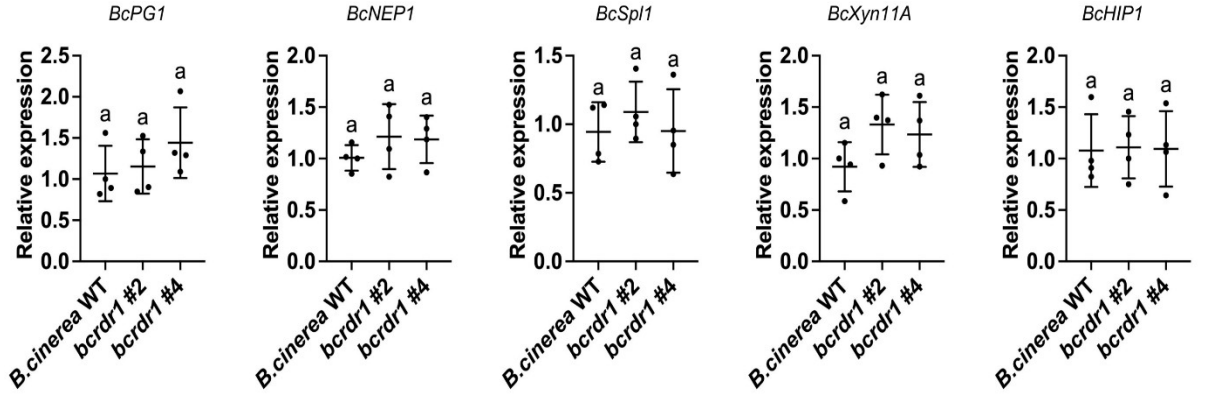

S7 Fig.

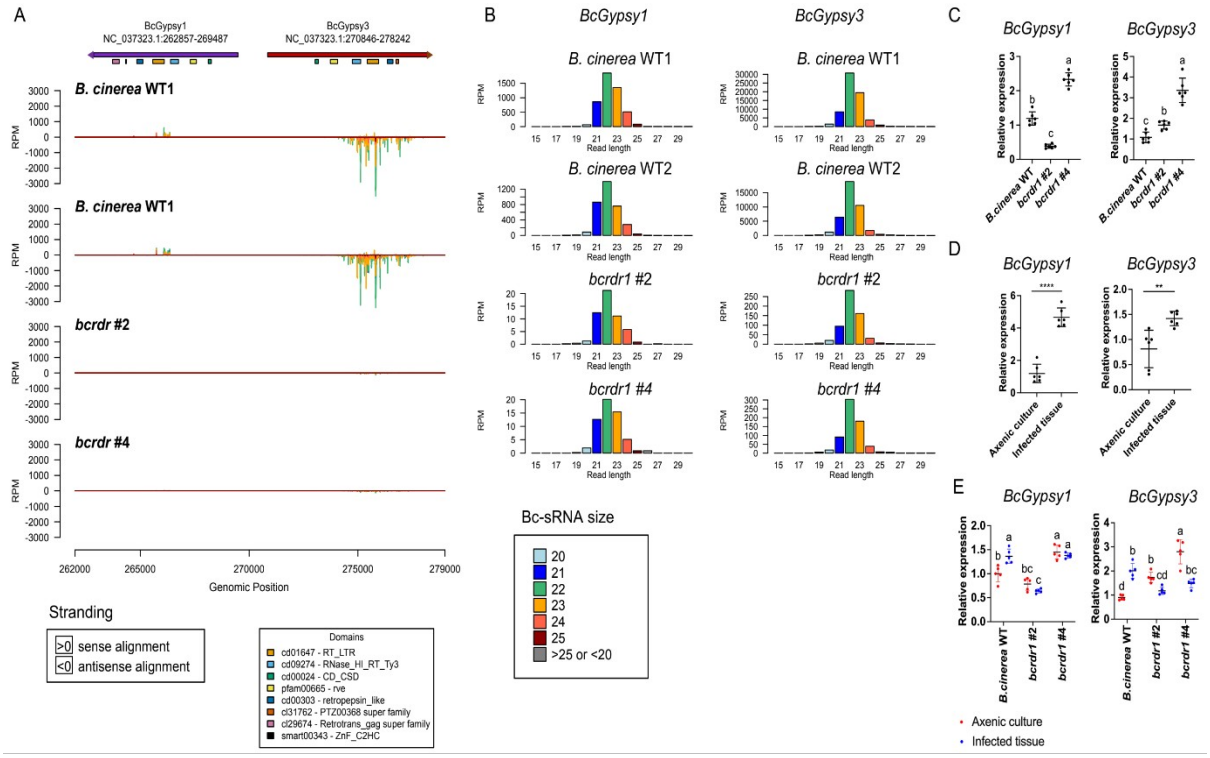
A
BcGypsy1
NC_037323.1:262857-269487
BcGypsy3
NC_037323.1:270846-278242
B. cinerea WT1
B. cinerea WT1
bcrdr #2
bcrdr #4
RPM
Genomic Position
Stranding
>0 sense alignment
<0 antisense alignment
Domains
cd01647 - RT_LTR
cd09274 - RNase_HI_RT_Ty3
cd00024 - CD_CSD
pfam00665 - rve
cd00303 - retropepsin_like
cd31762 - PTZD0368 super family
cl29674 - Retrotrans_gag super family
smart00343 - ZnF_C2HC
B
BcGypsy1
BcGypsy3
B. cinerea WT1
B. cinerea WT2
bcrdr1 #2
bcrdr1 #4
Read length
Bc-sRNA size
20
21
22
23
24
25
>25 or <20
C
BcGypsy1
BcGypsy3
Relative expression
B.cinerea WT
bcrdr1 #2
bcrdr1 #4
D
BcGypsy1
BcGypsy3
Relative expression
Axenic culture
Infected tissue
E
BcGypsy1
BcGypsy3
Relative expression
B.cinerea WT
bcrdr1 #2
bcrdr1 #4
Axenic culture
Infected tissue

S8 Fig.

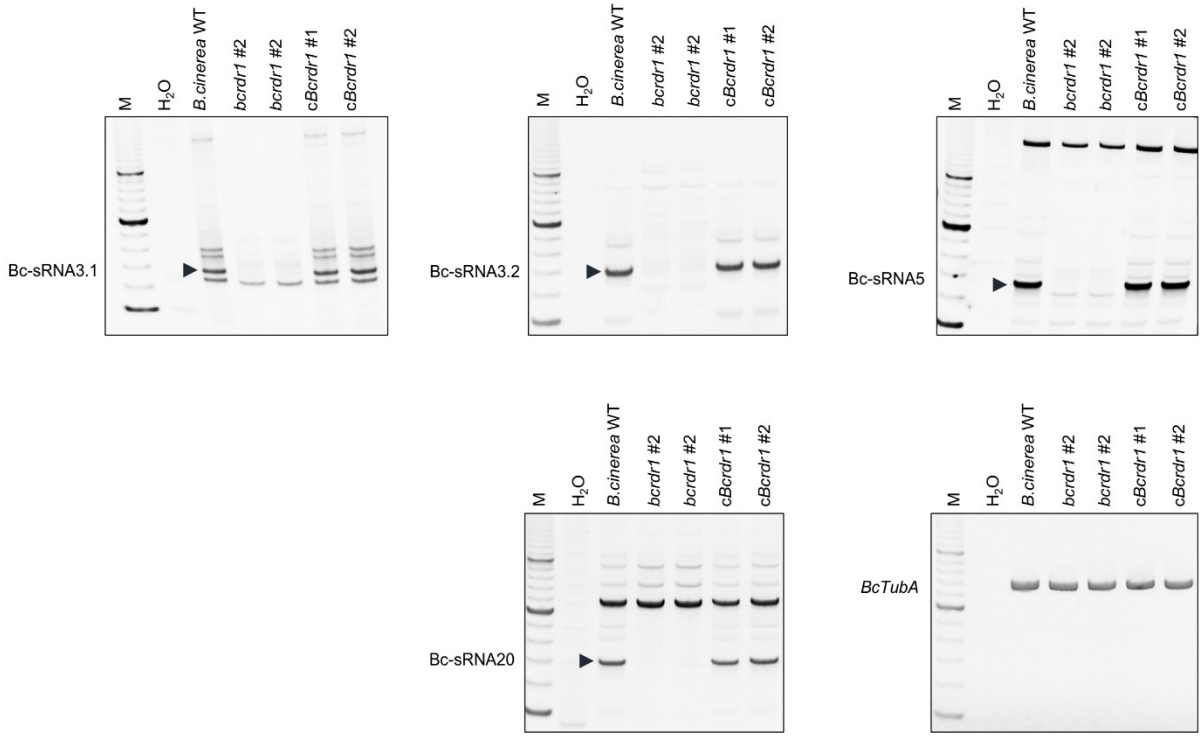
M
H2O
B.cinerea WT
bcrdr1 #2
bcrdr1 #2
cBcrdr1 #1
cBcrdr1 #2
Bc-sRNA3.1
Bc-sRNA3.2
Bc-sRNA5
Bc-sRNA20
BcTubA

S9 Fig.

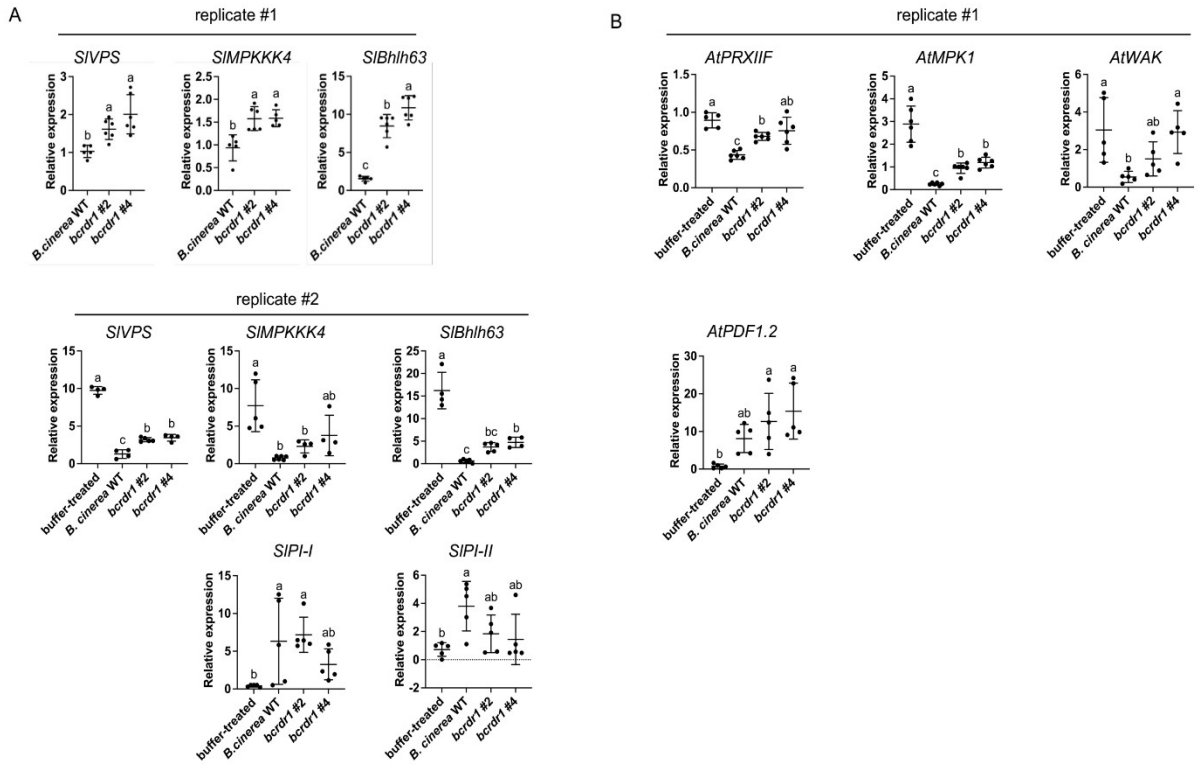
A
replicate #1
SlVPS
SlMPKKK4
SlBhlh63
Relative expression
B.cinerea WT
bcrdr1 #2
bcrdr1 #4
replicate #2
SlPI-I
SlPI-II
B
AtPRXIIF
AtMPK1
AtWAK
AtPDF1.2
buffer-treated
B. cinerea WT

S10 Fig.

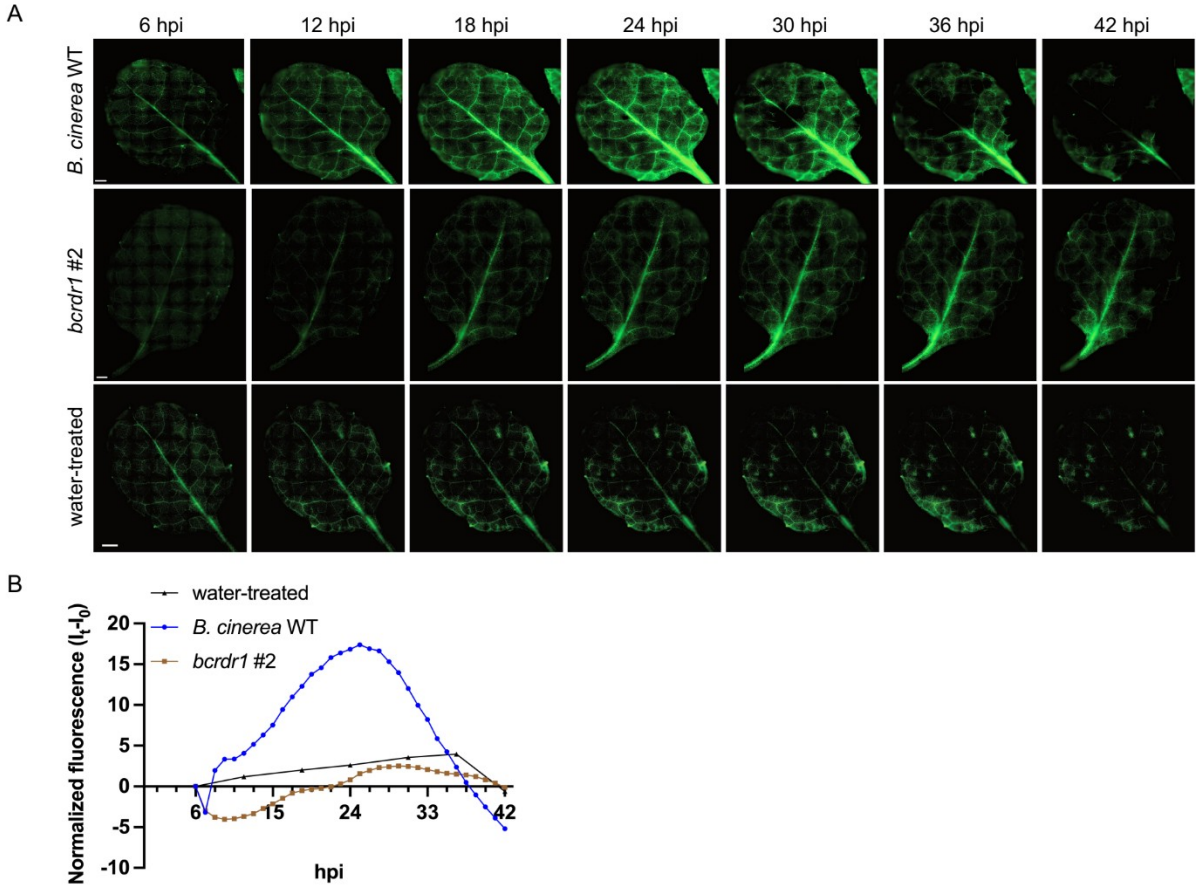

S11 Fig.

A. thaliana WT infected with *B. cinerea* WT

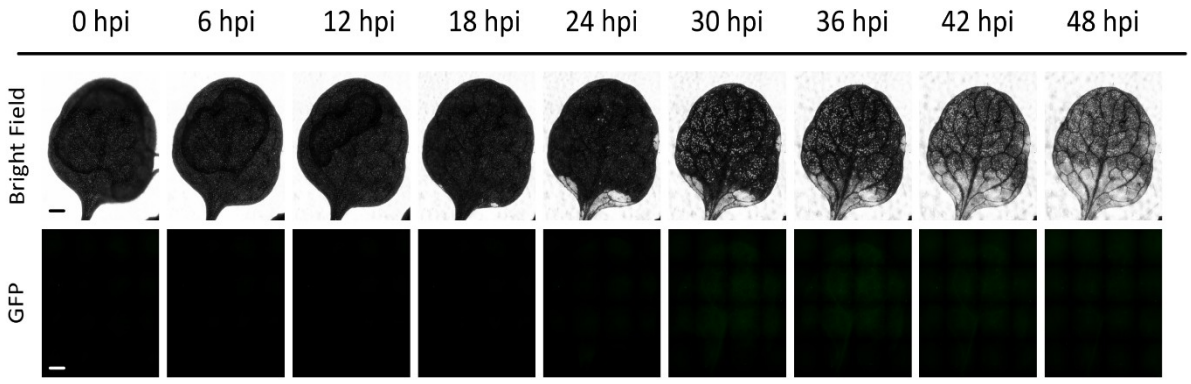

S12 Fig.

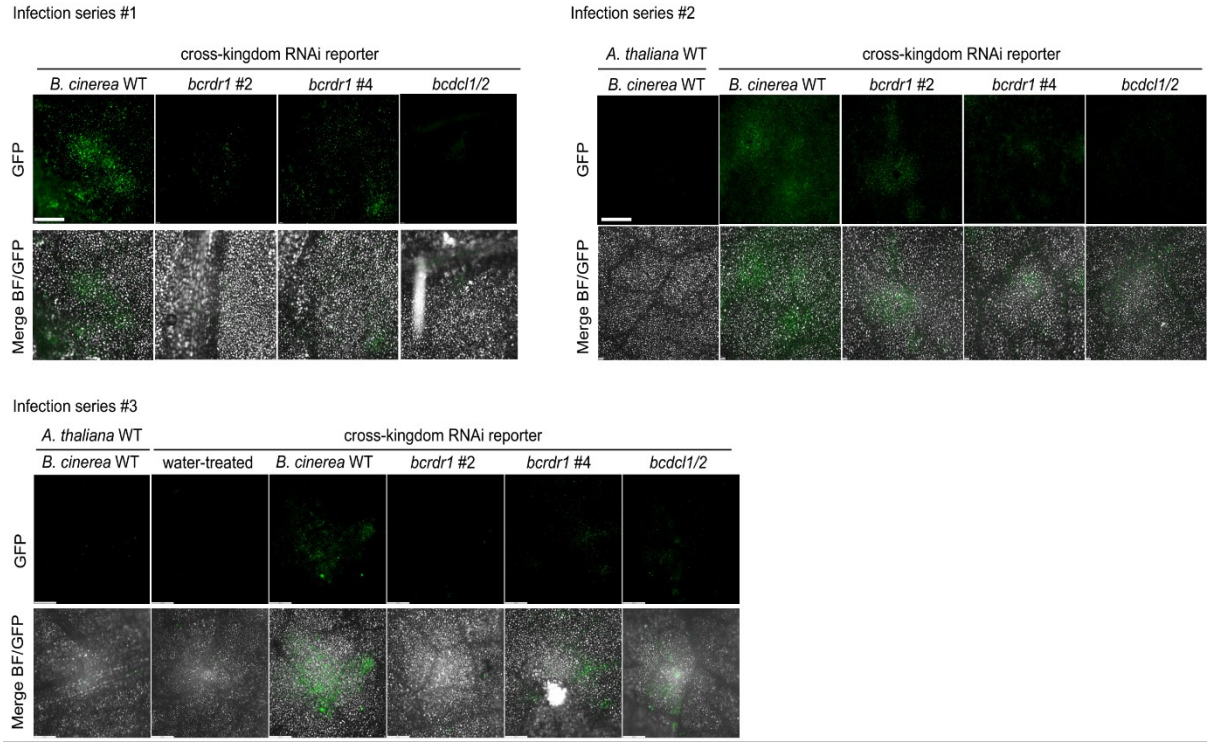
Infection series #1
cross-kingdom RNAi reporter
B. cinerea WT
bcrdr1 #2
bcrdr1 #4
bcdcl1/2
GFP
Merge BF/GFP
Infection series #2
A. thaliana WT
cross-kingdom RNAi reporter
B. cinerea WT
B. cinerea WT
bcrdr1 #2
bcrdr1 #4
bcdcl1/2
GFP
Merge BF/GFP
Infection series #3
A. thaliana WT
cross-kingdom RNAi reporter
B. cinerea WT
water-treated
B. cinerea WT
bcrdr1 #2
bcrdr1 #4
bcdcl1/2
GFP
Merge BF/GFP

S13 Fig.

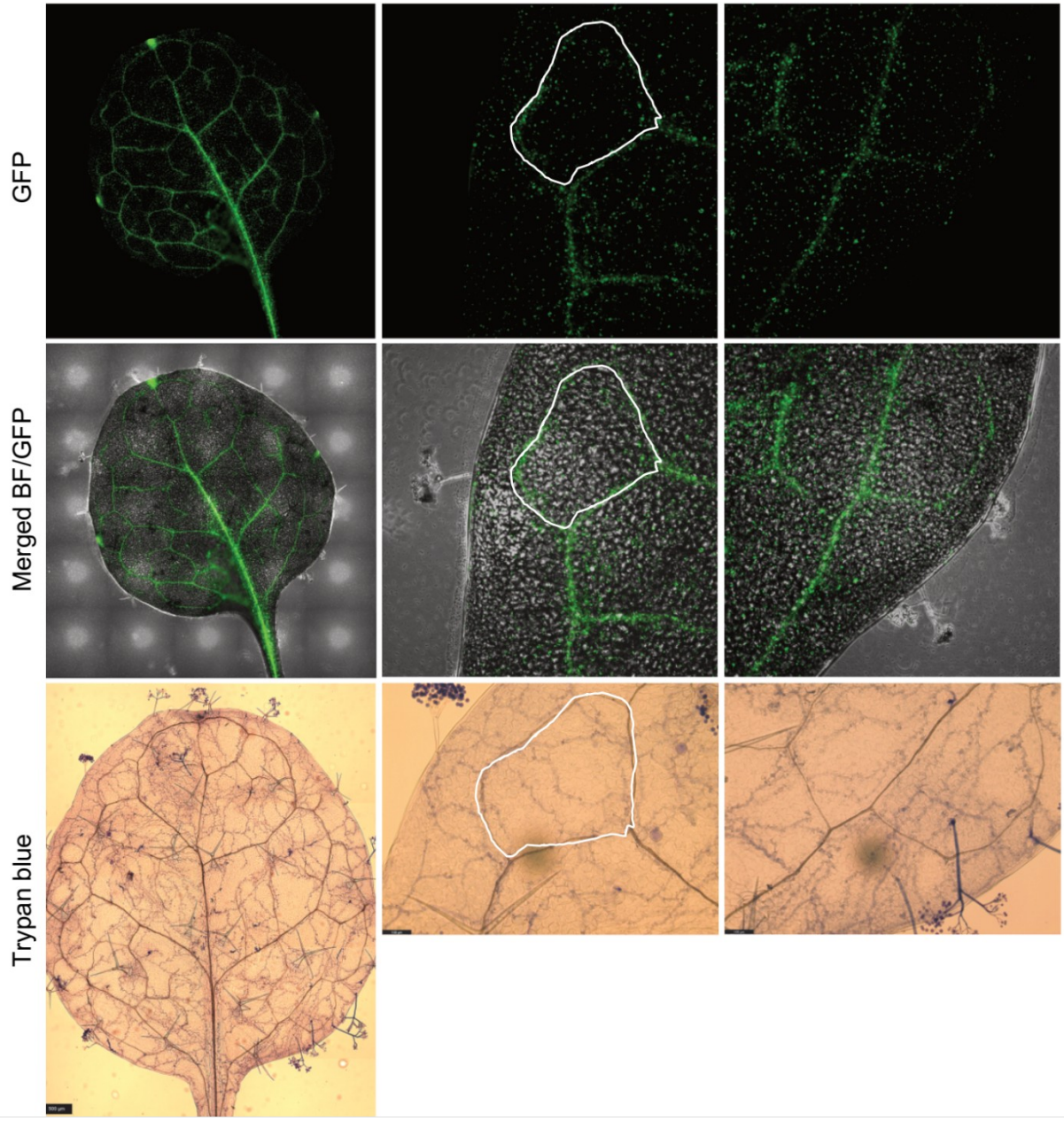

S14 Fig.

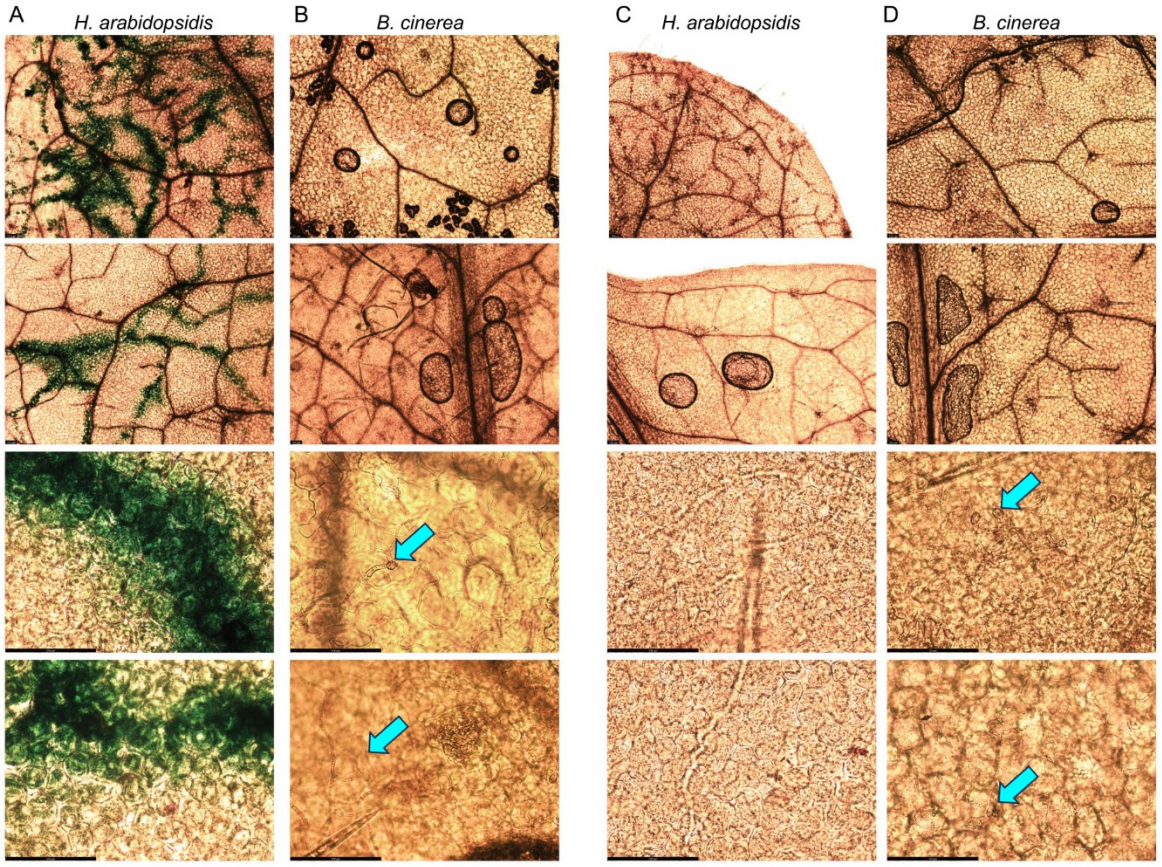

S15 Fig.

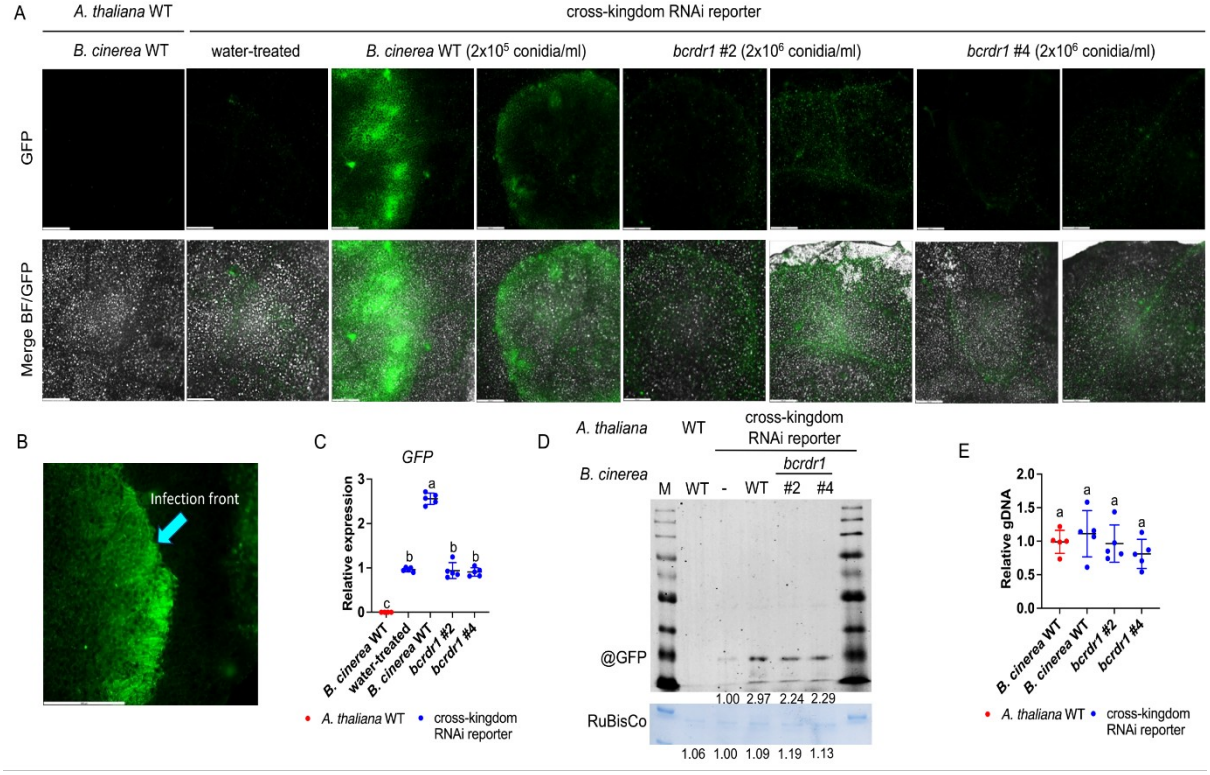

S16 Fig.

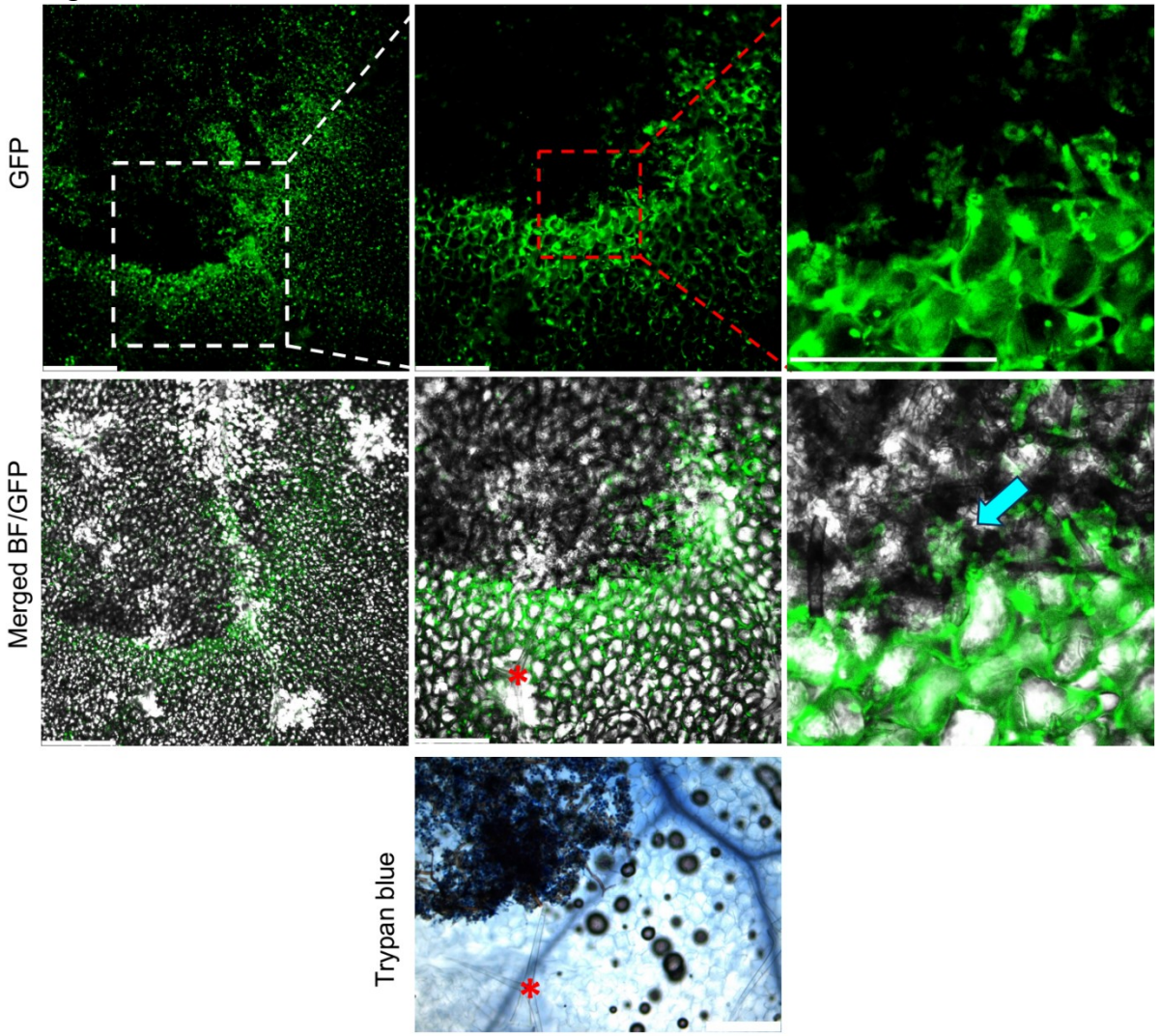

S17 Fig.

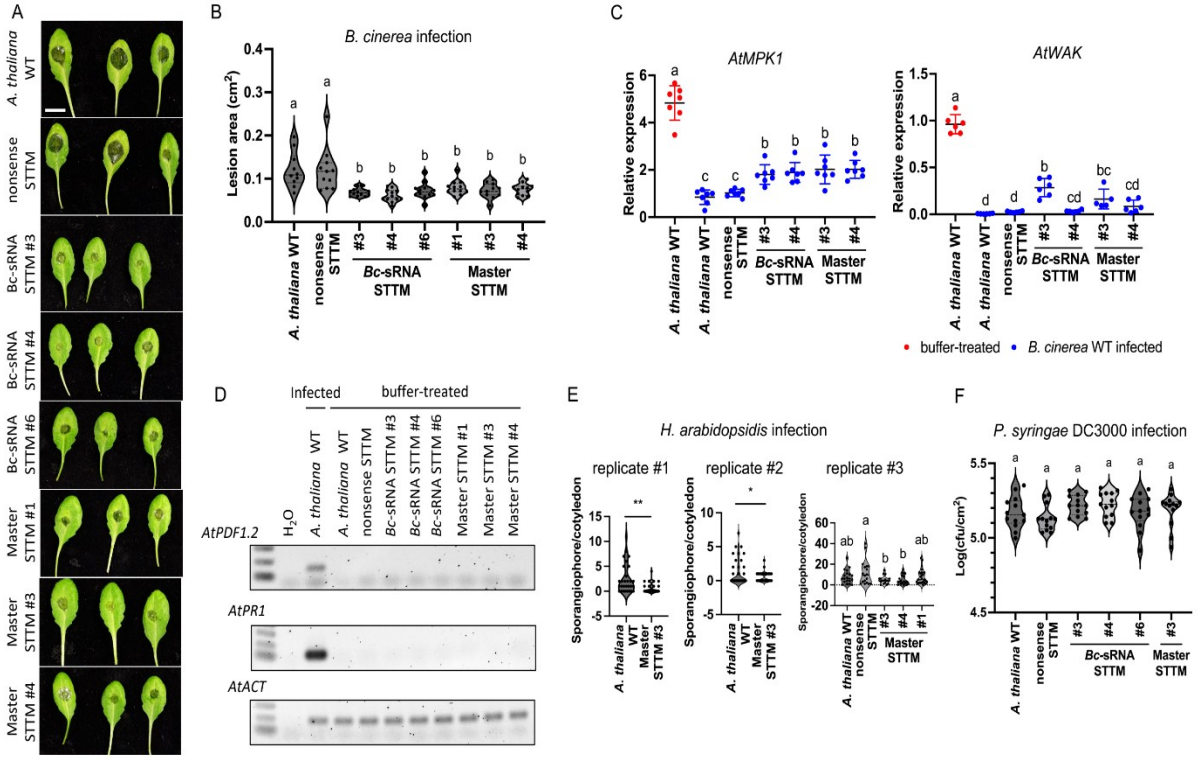

S18 Fig.

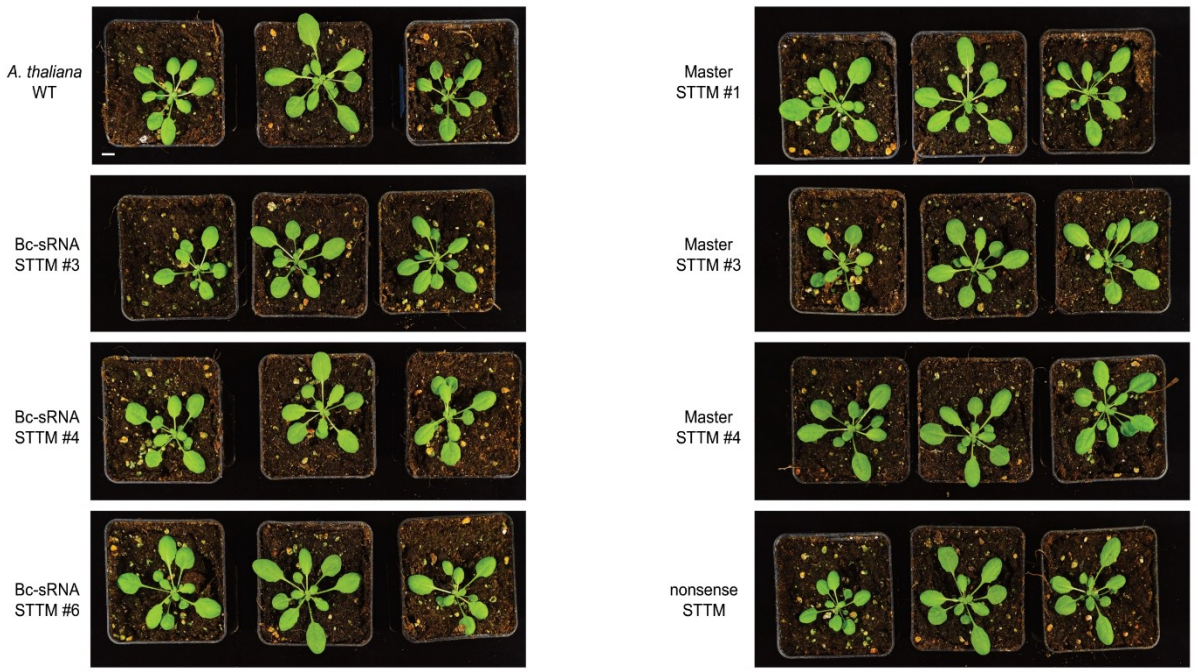

II. A fungal RNA-dependent RNA polymerase is a novel player in plant infection and cross-kingdom RNA interference

PNAS RESEARCH ARTICLE | PLANT BIOLOGY

Fungal Argonaute proteins act in bidirectional cross-kingdom RNA interference during plant infection

An-Po Cheng[a], Lihong Huang[a,1], Lorenz Oberkofler[a], Nathan R. Johnson[b,c], Adrian-Stefan Glodeanu[a], Kyra Stillman[a], and Arne Weiberg[a,d,2]

Affiliations are included on p. 11.

Edited by R. Poethig, University of Pennsylvania, Philadelphia, PA; received November 2, 2024; accepted March 11, 2025

Argonaute (AGO) proteins bind to small RNAs to induce RNA interference (RNAi), a conserved gene regulatory mechanism in animal, plant, and fungal kingdoms. Small RNAs of the fungal plant pathogen *Botrytis cinerea* were previously shown to translocate into plant cells and to bind to the host AGO, which induced cross-kingdom RNAi to promote infection. However, the role of pathogen AGOs during host infection stayed elusive. In this study, we revealed that members of fungal plant pathogen *B. cinerea* BcAGO family contribute to plant infection. BcAGO1 binds to both fungal and plant small RNAs during infection and acts in bidirectional cross-kingdom RNAi, from fungus to plant and vice versa. BcAGO2 also binds fungal and plant small RNAs but acts independent from BcAGO1 by regulating distinct genes. Nevertheless, BcAGO2 is important for infection, as it is required for effective pathogen small RNA delivery into host cells and fungal induced cross-kingdom RNAi. Providing these mechanistic insights of pathogen AGOs promises to improve RNAi-based crop protection strategies.

Argonaute | cross-kingdom RNA interference | small RNA | plant–fungal interaction

Significance

Cross-kingdom RNA interference (RNAi) is an emerging field in plant-microbe research, but the underlying biological processes are barely understood. Argonaute (AGO) proteins are small RNA binding proteins that are key factors in RNAi by inducing gene silencing. The functional role of AGOs in RNA silencing is highly conserved from fungi to plants and humans. In this study, we demonstrate that different members of the AGO family in the fungal plant pathogen *Botrytis cinerea* act in bidirectional cross-kingdom RNAi during infection of host plants, such as tomato. Uncovering the critical role of fungal AGOs during plant infection and their underlying molecular mechanisms open new avenues to develop novel RNA-based strategies to control pathogens in agricultural relevant crops.

Argonautes (AGOs) belong to a conserved protein family and are key compounds of the RNA interference (RNAi) pathway, directing (post-) transcriptional gene silencing in animals, plants, and fungi. AGOs comprise a modular structure of PAZ, MID, and PIWI protein domains that are functional and crucial in RNA binding and gene silencing (1). In plants, different AGO proteins bind to distinct classes of regulatory small RNAs, small-interfering (si)RNAs and micro(mi)RNAs, to form a ribonucleoprotein complex, known as the RNA-induced silencing complex (RISC). Previous studies revealed key biological functions of AGO proteins for the posttranscriptional regulation of RNAs and the remodeling of heterochromatin at the DNA level to fine-tune gene expression, as well as for the silencing of transposons and viruses (2).

In fungi, AGOs have been well characterized in different species. The *Neurospora crassa* AGO named QDE2 is required for RNAi in the quelling process (3, 4). Another *N. crassa* AGO, named SMS-2, mediates meiotic silencing of unpaired DNA (MSUD) during sexual reproduction (5). In the basidiomycete *Cryptococcus neoformans*, sex-induced silencing (SIS) is another RNAi mechanism that depends on the fungal AGO1 (6). RNAi-related heterochromatic silencing of centromere regions is dependent on AGO1 in the fission yeast *Schizosaccharomyces pombe* (7). Fungal AGO proteins contribute to transposon and transgene silencing, defense against mycovirus, endogenous gene regulation, and DNA repair (8–11). Studies with *ago* loss-of-function mutants in diverse fungal species revealed AGO involvement in regulating metabolic processes as well as affecting fungal growth, differentiation, development, and pathogenicity (12–14).

Botrytis cinerea is a destructive fungal plant pathogen that infects more than 1,400 different plant species and causes the gray mold disease in many economically important crops (15, 16). *B. cinerea* secretes small RNAs (BcsRNAs) into plant cells that bind to the plant's own AGO1 to manipulate host immunity genes (17, 18); a virulence mechanism called cross-kingdom RNAi (19). The biogenesis of cross-kingdom BcsRNAs requires the RNA-dependent RNA polymerase (RDR)1 and two Dicer-like (DCL) proteins (20, 21), while *B. cinerea* Δ*bcdcl1dcl2* and Δ*bcdrr1* knockout mutants exhibited reduced infectivity (18, 20, 21).

Cross-kingdom and transspecies RNAi have been reported in distinct pathogenic and mutualistic host-interacting organisms, including fungi, oomycetes, bacteria, parasitic plants, and nematodes (18, 22–28). Moreover, cross-kingdom RNAi is bidirectional, because plants send small RNAs into interacting species to defend themselves against fungal pathogens (20, 29, 30).

In this study, we identified and characterized the *B. cinerea* AGO protein family during infection of the host plant *Solanum lycopersicum* (tomato). Intriguingly, Δ*bcago1* knockout

Author contributions: A.W. designed research; A.-P.C., L.H., L.O., A.-S.G., and K.S. performed research; A.-P.C. and N.R.J. analyzed data; and A.-P.C. and A.W. wrote the paper.

The authors declare no competing interest.

This article is a PNAS Direct Submission.

[1]Present address: Joint School of Life Sciences, The Guangdong-Hong Kong-Macau Joint Laboratory for Cell Fate Regulation and Diseases, Guangzhou Medical University, Guangzhou 511436, China.

[2]To whom correspondence may be addressed. Email: arne.weiberg@uni-hamburg.de.

This article contains supporting information online at https://www.pnas.org/lookup/suppl/doi:10.1073/pnas.2422756122/-/DCSupplemental.

Published April 23, 2025.

mutants failed to induce cross-kingdom RNAi similar to Δ*bcdcl1dcl2* and Δ*bcrdr1* mutants (21); however, Δ*bcago1* was not impaired in virulence. Our data show that BcAGO1 mediates bidirectional cross-kingdom RNAi, from fungus to plants and vice versa. BcAGO2 is also involved in fungal-induced cross-kingdom RNAi and is a crucial pathogenicity factor. Our study reveals diversified regulatory functions of different fungal AGOs that contributes to our understanding of the molecular mechanisms of plant infection by this economically important pathogen.

Results

AGOs in the Fungal Plant Pathogen *B. cinerea*. In this study, we aimed to investigate the role(s) of *B. cinerea* BcAGOs during tomato infection. We performed a BLASTp search using the full-length protein sequence of the well-characterized *N. crassa* QDE2 as a query in the genome sequence of the *B. cinerea* strain B05.10 (31) to identify BcAGOs. Four BcAGO proteins that we termed BcAGO1, BcAGO2, BcAGO3, and BcAGO4 were predicted to comprise conserved PAZ and PIWI domains (*SI Appendix*, Fig. S1*A*). The MID domain and an AGO-conserved N-terminal domains were also found in the BcAGO1 and BcAGO2 using InterPro (32). The PIWI domain of all four putative BcAGOs contained a conserved aspartic acid (D)/glutamic acid (E)/D/histidine (H) catalytic tetrad (*SI Appendix*, Fig. S2), suggesting that BcAGOs could function as slicer proteins (1, 33).

We classified the four BcAGOs regarding functional homology by performing phylogenetic analysis including AGO amino acid sequences of different ascomycete species and the well-characterized *Arabidopsis thaliana* AtAGO1 and *Homo sapiens* HsAGO2 (*SI Appendix*, Fig. S1*B* and Table S1). The phylogenetic tree positioned BcAGO1 into the fungal quelling clade and the BcAGO2 into the fungal MSUD clade. BcAGO3 and BcAGO4 laid outside these two clades and were of unknown homologous function.

The coding gene sequence of *BcAGO4* for the *B. cinerea* strain B05.10 (ASM83294v1) included a predicted premature stop codon in the third exon (*SI Appendix*, Fig. S3*A*), which suggested that *BcAGO4* is a pseudogene. The stop codon likely resulted in the automated annotation of the N- and the C-terminal part of *BcAGO4* into two separate genes, *Bcin15g05050* and *Bc15g05060*, as deposited in the Ensembl database. This point mutation was not found in genome sequences of two other released *B. cinerea* genome sequences of the strains T4 (GCA_000227075) and BcDW1 (GCA_000349525), respectively (*SI Appendix*, Fig. S3*B*). To exclude the possibility that this mutation was an error introduced during whole genome sequencing, we cloned *BcAGO4* from the B05.10 strain and confirmed this mutation being present by Sanger sequencing (*SI Appendix*, Fig. S3*C*). This shows that there is within-species genetic variation at the *BcAGO4* locus among *B. cinerea* strains. In the following experiments of this study, we used the strain B05.10.

Accumulation of Fungal Cross-Kingdom Small RNAs Depends on BcAGO1. We first explored the possibility that BcAGOs might control BcsRNA accumulation. For this, we generated Δ*bcago* ko mutants and isolated two individual knockout (ko) mutant strains for each BcAGO, referred to as Δ*bcago1*, Δ*bcago2*, Δ*bcago3*, Δ*bcago4* (*SI Appendix*, Fig. S4*A*). We performed stem-loop reverse transcription (RT)-PCR of BcsRNAs, collecting samples of *B. cinerea* grown in axenic culture and from infected tomato leaves (Sl-infected). We chose the BcsRNA3.1, BcsRNA3.2, BcsRNA20, because these were previously found to induce cross-kingdom RNAi of tomato genes during *B. cinerea* infection (18, 21, 34). We determined that Δ*bcago1* ko mutants and a Δ*bcago1ago2* double-ko lost the accumulation of BcsRNA3.1, BcsRNA3.2, and BcsRNA20 (Fig. 1*A* and *SI Appendix*, Fig. S5). BcsRNA accumulation was reconstituted in a 3xHA-tagged BcAGO1 complementation strain (*SI Appendix*, Figs. S4*B* and S6). In the case of BcsRNA3.1, we obtained a lower PCR band instead of the expected size. We cloned and sequenced several clones which revealed the lower band represented a PCR artifact (*SI Appendix*, Fig. S7) but was not a shorter version of BcsRNA3.1.

We next performed comparative small RNA deep sequencing analysis to profile global changes of BcsRNA accumulation. Two independent strains of each Δ*bcago* ko mutant and *B. cinerea* wild type (WT) were grown in axenic culture for small RNA extraction and Illumina library preparation. Upon raw read processing, we mapped reads to the *B. cinerea* reference genome allowing a maximum of one mismatch. These BcsRNAs mapped either one or multiple times, when we chose a single "best" map-location with multiple-mappers (35) (*SI Appendix*, Fig. S8*A*). BcsRNA reads mapped to various annotated genomic regions (*SI Appendix*, Fig. S8*B*) and showed an overall size enrichment for 21 to 22 nt reads (Fig. 1*B*). An exception was Δ*bcago1*, which lost most of the 21 to 22 nucleotides (nt) BcsRNAs that were mainly derived from retrotransposons (RT) (*SI Appendix*, Fig. S8*B*).

To measure quantitative differences in BcsRNA accumulation, we annotated *BcsRNA* producing genomic loci in *B. cinerea*, using one of the *B. cinerea* WT small RNA-seq datasets. We defined *BcsRNA* loci as regions with coverage above the chromosomal average, defined by a Poisson probability $P < 10^{-4}$. Nearby regions (<150 bases apart), given a 10-nucleotide buffer on both sides (Fig. 1*C* and *SI Appendix*, Fig. S8*C*). With these criteria, we identified in total 4,397 *BcsRNA* loci (*SI Appendix*, Table S2), covering 96.3% of the mapped BcsRNAs (*SI Appendix*, Fig. S8*D*). Annotated loci included many which were not size-specific and were likely derived from but not limited to mRNA degradation (*SI Appendix*, Fig. S8*E*). Most of the 21 to 22 nt size-specific *BcsRNA* loci were found in nonannotated genomic regions, nearby genes, and within gene bodies of exonic and intronic regions. More than 50% of these 21 to 22 nt size-specific *BcsRNA* loci overlapped with RT (Fig. 1*D*). As non-size-specific BcsRNAs derived from mRNAs were likely degradation products and not BcAGO-associated, these served as controls for normalization of size-specific BcsRNAs (*SI Appendix*, Fig. S9 *A* and *B*). All differentially expressed *BcsRNA* loci identified by pairwise comparison between Δ*bcago* ko mutants and *B. cinerea* WT are listed in *SI Appendix*, Table S3. Normalized read counts of *BcsRNA* loci confirmed that Δ*bcago1* ko mutants showed the strongest change in BcsRNA expression, with mostly decreased 21 to 22 nt size-specific *BcsRNA* loci expression (Fig. 1*E* and *SI Appendix*, Fig. S9*C*). Mutants for Δ*bcago1* clustered distinctly from the other genotypes, while the rest clustered together in an unordered manner. The short branches in the dendrogram indicated that these were very similar in profile, highlighting the lack of BcsRNA profile changes in Δ*bcago2*, Δ*bcago3* and Δ*bcago4* compared to *B. cinerea* WT. Therefore, Δ*bcago1* exhibited reduced small RNA accumulation, similar to Δ*bcrdr1* and Δ*bcdcl1dcl2* double-ko mutants, as reported in previous studies (20, 21).

BcAGO1 and BcAGO2 are Required for Fungal-Induced Cross-Kingdom RNAi. Since Δ*bcago1* ko mutants lost accumulation of 21 to 22 nt BcsRNAs, we anticipated that Δ*bcago1* ko mutant might be compromised in cross-kingdom RNAi during plant infection. We recently developed a Green Fluorescent Protein (GFP) "switch on" cross-kingdom RNAi reporter system carrying the BcsRNA3.1 and BcsRNA3.2 target sites of *A. thaliana* genes.

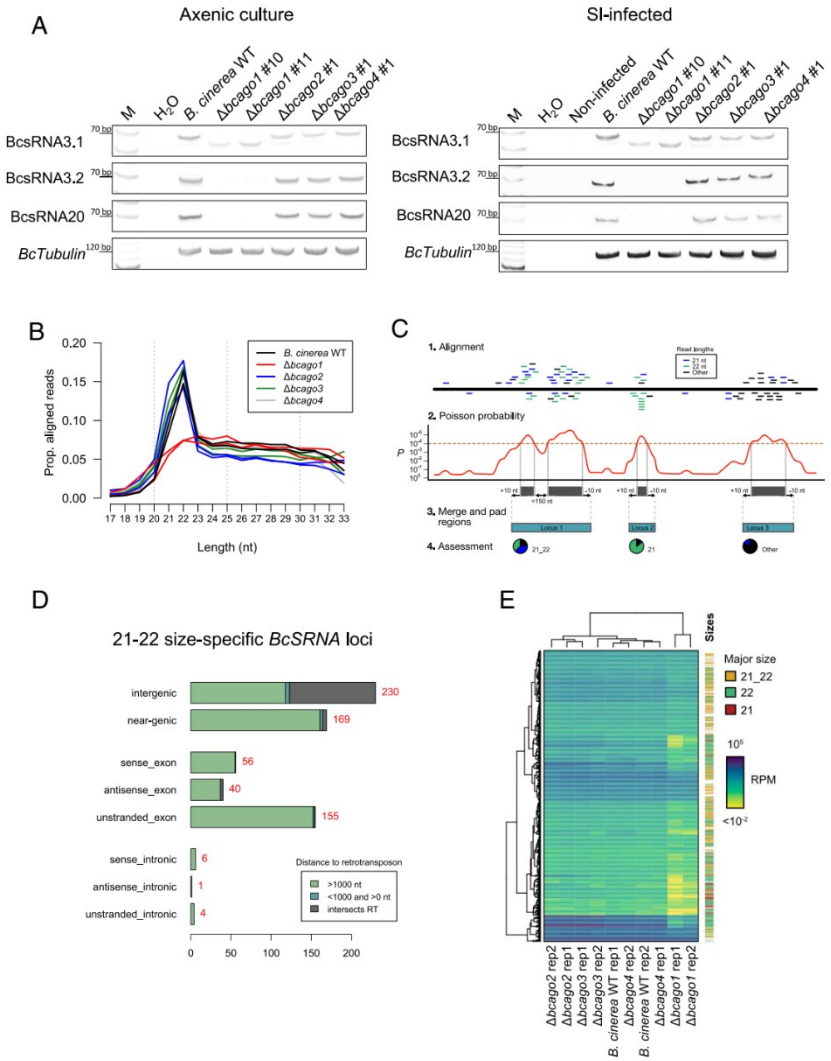

Fig. 1. Small RNA profiling of *Botrytis cinerea* Δ*bcago* ko mutants. (*A*) Stem-loop RT-PCR of BcsRNAs known to induce cross-kingdom RNAi in plants. Samples were from *B. cinerea* strains grown in axenic culture or infected tomato (SI-infected) condition. *BcTubulin* mRNA was used as an internal control. M: 1 kb DNA ladder. (*B*) Size profiles of total BcsRNA reads detected in *B. cinerea* WT and Δ*bcago* ko mutants in two biological replicates by Illumina deep sequencing. (*C*) Schematic representation of the definition for *BcsRNA* loci, using a *B. cinerea* WT small RNA sequencing dataset. (*D*) Absolute numbers of 21 to 22 nt size-specific *BcsRNA* loci overlapping with different annotated regions in the *B. cinerea* genome in the context of retrotransposons (RT). (*E*) Heat map and cluster analysis of differentially expressed *BcsRNA* loci comparing *B. cinerea* WT and Δ*bcago* ko mutants.

When infecting transgenic *A. thaliana* reporter plants with *B. cinerea*, GFP expression is turned on within 24 to 48 h post inoculation (hpi) (21). We used this *A. thaliana* reporter line to further inspect cross-kingdom RNAi with the Δ*bcago* ko mutants. We infected seedlings with *B. cinerea* WT and Δ*bcago* ko mutants and recorded GFP signal expression in infected leaves in a time course by fluorescence microscopy (Fig. 2*A* and *SI Appendix*, Figs. S10*A* and S11*A*). This analysis indicated some background fluorescence intensity (I_0) in the reporter plants. Therefore, we calculated relative increase of GFP fluorescence intensity (I_t-I_0) at different time points of infection (I_t), following a previously reported analysis (21). Inoculation with Δ*bcago1* ko strain did not induce GFP signal at any measured time point, while Δ*bcago2* caused an increase in GFP signal intensity, but to a lesser extent than *B. cinerea* WT (Fig. 2*B* and *SI Appendix*, Fig. S10*B*). These observations were corroborated in an immunoblot analysis of GFP levels of infected leaves (Fig. 2*C* and *SI Appendix*, Fig. S10*C*). We repeated inoculation of the GFP reporter plants with the Δ*bcago3* or Δ*bcago4* and similar GFP induction was observed as with *B. cinerea* WT (*SI Appendix*, Fig. S11). Hence, BcAGO3 and BcAGO4 were dispensable for inducing cross-kingdom RNAi. We measured *B. cinerea* genomic DNA levels in the *A. thaliana*

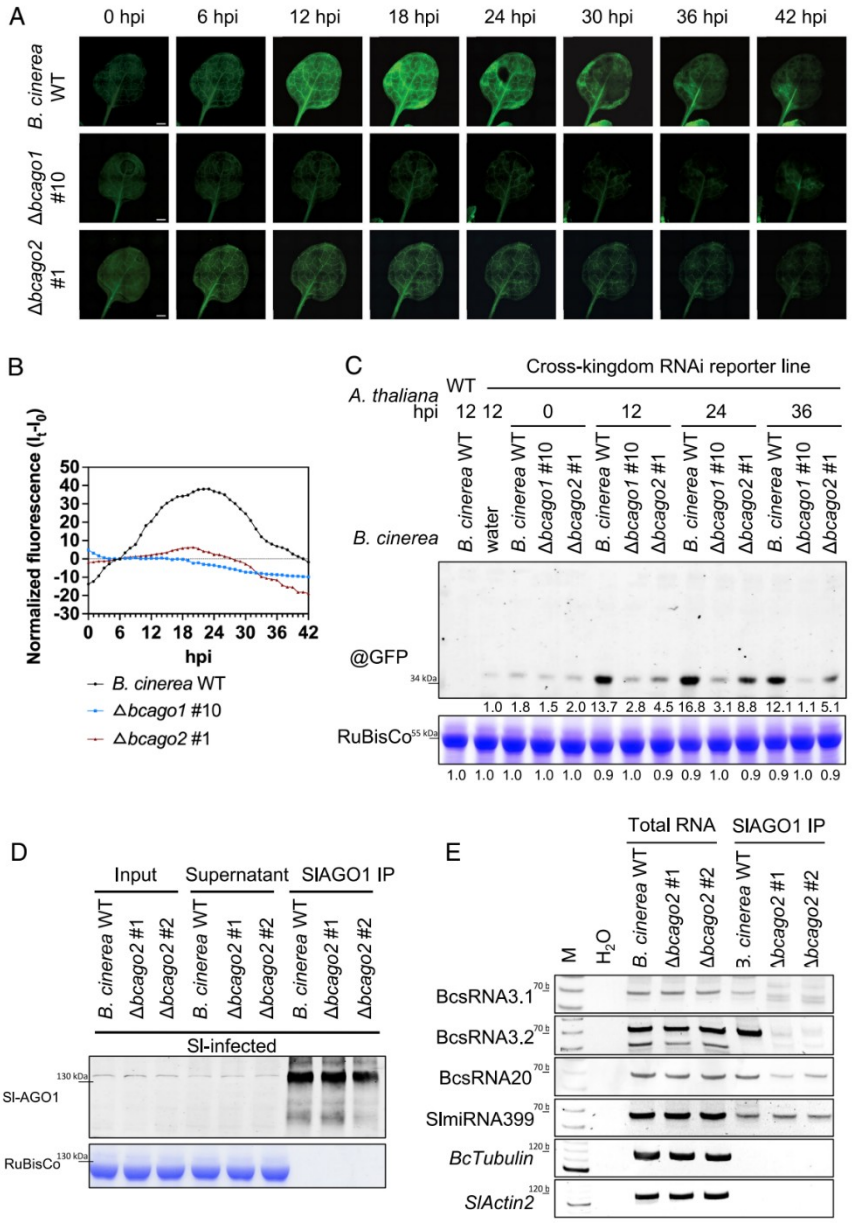

Fig. 2. BcAGO1 and BcAGO2 are required for fungal-induced cross-kingdom RNAi. (*A*) Fluorescence microscopy images from GFP reporter plant seedlings at different time points. A 5 µl drop of a 5 × 10^5/ml conidiospore suspension was placed at the center of the leaf before placing a glass covering slip on the top that dispersed the conidiospore suspension over the entire leaf surface. (Scale bar, 1 mm.) (*B*) GFP quantification in infected seedling leaves from 0 to 42 hpi. For normalization, GFP fluorescence signal intensity at different time points (I_t) was subtracted with the initial GFP signal intensity (I_0). (*C*) Immunoblot analysis of GFP expression in cross-kingdom RNAi reporter plants at four time points upon *B. cinerea* infection using a @GFP antibody. The ribulose 1,5-bisphosphate carboxylase/oxygenase (RuBisCo) signal detected by Coomassie Brilliant Blue (CBB) staining was used as a protein loading control. Numbers indicate GFP and RuBisCo signal intensities estimated by the FIJI software. (*D*) Immunoblot analysis of SlAGO1 IP from leaf tissue infected with *B. cinerea* WT or Δ*bcago2* ko mutants using an anti-AGO1 antibody. RuBisCo signal detected by CBB staining was used as a protein loading control. (*E*) Stem-loop RT-PCR of BcsRNA3.1, BcsRNA3.2, and BcsRNA20 using SlAGO1 IP samples. Total RNA samples were used as a control for BcsRNA accumulation in *B. cinerea* WT and Δ*bcago2* ko mutant samples. The SlmiR399 was used as a control for the successful small RNA isolation from the SlAGO1 IP fraction, and *BcTubulin* and *SlActin2* mRNA were used as a control indicating no unspecific RNA-binding. M: 10 bp DNA ladder.

reporter plants at the same time point as the GFP measurements and observed no difference between WT, Δ*bcago1*, or Δ*bcago2* inoculations (*SI Appendix*, Fig. S10*D*). This suggested that the observed lower GFP activation was not due to a diminished *B. cinerea* colonization.

Ineffective cross-kingdom RNAi during infection with the Δ*bcago2* ko strain, which accumulated BcsRNAs (Fig. 1*A*), suggested that BcsRNA translocation into plant cells might be disturbed. To test this possibility, we performed tomato AGO1 coimmunopurification (SlAGO1 IP) followed by BcsRNA stem-loop RT PCR. Immunoblot analysis confirmed successful SlAGO1 isolation from leaf tissue infected with *B. cinerea* WT or individual Δ*bcago2* ko mutants (Fig. 2*D*). The BcsRNA3.1, BcsRNA3.2, and BcsRNA20 were all detected in the SlAGO1 IP fraction when infecting with *B. cinerea* WT. In the cases with Δ*bcago2* ko mutants, no BcsRNA3.1 PCR band was detected, and the BcsRNA3.2 and BcsRNA20 band intensities were reduced. The tomato SlmiR399 binding to SlAGO1 was used as an internal control. Hence, the Δ*bcago2* ko lost the capability to effectively deliver BcsRNAs into plant AGO1 during infection (Fig. 2*E*).

We next measured mRNA levels of the known tomato target genes of BcsRNA3.1, BcsRNA3.2, and BcsRNA20, namely *SlVPS, SlMPKKK4*, and *SlBhlh63* by quantitative RT-PCR (qRT-PCR) (21, 34). *SlMPKKK4* and *SlBhlh63* were no longer suppressed upon infection with Δ*bcago1* ko strains (*SI Appendix*, Fig. S12*A*), agreeing with the loss of BcsRNA3.2 and BcsRNA20 accumulation. Similarly, previous findings showed that the Δ*bcrdr1* also lost BcsRNA accumulation and was no longer able to suppress these target genes upon infection (21). Target gene suppression was reconstituted upon infection with a 3xHA-BcAGO1 complementation strain. MPKKK4 is part of a conserved plant immune signaling cassette that involves the downstream targets MPK3/MPK6 and WRKY33 (*SI Appendix*, Fig. S13*A*) (36). When infecting tomato with Δ*bcago1* ko mutants, *SlMPK3* and *SlWRKY33* were higher expressed compared to infection with *B. cinerea* WT or Δ*bcago2* (*SI Appendix*, Fig. S13*B*). This result supported that Δ*bcago1* ko strains lost suppression of this plant immune signaling pathway.

SlMPKKK4 and *SlBhlh63* showed similar expression levels upon infection comparing Δ*bcago2* and *B. cinerea* WT. *SlVPS* expression was suppressed upon infection with Δ*bcago1* at similar levels as with *B. cinerea* WT, but *SlVPS* gene expression was induced upon Δ*bcago2* infection. In consistence, the BcsRNA3.1 targeting *SlVPS* was not delivered into SlAGO1 upon infection when infecting with the Δ*bcago2* ko compared to *B. cinerea* WT (Fig. 2*E*). All three tomato target genes were no longer suppressed upon infection with a Δ*bcago1ago2* double-ko (*SI Appendix*, Fig. S12*A*). The tomato immunity marker gene *Sl-Proteinase Inhibitor* (*PI*)-*II* was used as a nontarget gene control. *SlPI-II* was more strongly induced when infecting with Δ*bcago2* ko mutants compared to *B. cinerea* WT or Δ*bcago1* ko (*SI Appendix*, Fig. S12*B*).

These results confirmed that BcAGO1 and BcAGO2 contributed to host gene silencing and immunity suppression during tomato infection. We concluded that both BcAGO1 and BcAGO2 contributed to fungal-induced cross-kingdom RNAi by regulating distinct tomato target genes.

***B. cinerea* BcAGO2 Is a Fungal Pathogenicity Factor.** To gain further information on the functional role of BcAGOs during tomato infection, we measured *BcAGO* mRNA levels in axenic culture and in Sl-infected sample conditions by qRT-PCR (Fig. 3*A*). *BcAGO1* was stronger expressed under both conditions compared to *BcAGO2*, *BcAGO3*, and *BcAGO4*. The *BcAGO2* and *BcAGO3* displayed upregulation at 1 d post inoculation (dpi). *BcAGO4* showed low expression in both conditions.

We next compared disease severity induced by Δ*bcago* ko mutants using a tomato leaf infection assay. Following conidiospore drop (Fig. 3*C*) or agar plug inoculation methods (*SI Appendix*, Fig. S14*B*), we observed that Δ*bcago2* ko mutants induced smaller lesion areas compared to WT. The Δ*bcago1ago2* double-ko showed reduced virulence, similar to Δ*bcago2* single ko. Conversely, reduced pathogenicity of Δ*bcago2* was reverted in 3xHA-BcAGO2 strains (Fig. 3*C* and *SI Appendix*, Fig. S14*A*). Accordingly, we measured significantly less *B. cinerea* genomic DNA, a proxy for pathogen biomass, in leaf tissue infected with the Δ*bcago2* (Fig. 3*D*). Notably, Δ*bcago2* induced only marginal smaller lesions when infecting *A. thaliana* compared to *B. cinerea* WT (*SI Appendix*, Fig. S14*C*). When growing Δ*bcago* ko mutants on agar plates, we observed normal fungal growth and development in all strains (Fig. 3*C* and *SI Appendix*, Fig. S15).

Based on these results, we concluded that BcAGO2 is a pathogenicity factor in *B. cinerea* and impeded cross-kingdom RNAi in the Δ*bcago2 ko* mutants could explain the reduced pathogenicity. Surprisingly, Δ*bcago1* ko mutants did not display any noticeable change in tomato or *A. thaliana* infection, although we demonstrated in this study that Δ*bcago1* was no longer inducing fungal cross-kingdom RNAi and it was hampered in suppressing tomato immunity.

Hence, we observed distinct phenotypes in Δ*bcago1* and Δ*bcago2* ko mutants, suggesting the presence of two distinct RNAi pathways in *B. cinerea*. When measuring gene expression of *BcAGO2* in the Δ*bcago1* ko mutant background or vice versa, we revealed compensatory expression when grown in axenic culture (*SI Appendix*, Fig. S16) indicating regulatory crosstalk between both BcAGO RNAi pathways. This effect was less obvious when measuring BcAGO expression during tomato infection, but this crosstalk might have influenced the infection phenotypes observed with the Δ*bcago1* and Δ*bcago2* ko mutants.

BcAGO1 Facilitates Tomato-Induced Cross-Kingdom RNAi. In a previous study, *A. thaliana* was reported to send small RNA into *B. cinerea* to induce cross-kingdom RNAi in the fungus (29). These plant-derived cross-kingdom small RNAs are produced by the *A. thaliana* AtDCL2/DCL3/DCL4, and an *A. thaliana atdcl2dcl3dcl4* triple mutant showed higher susceptibility to *B. cinerea* infection. We speculated that enhanced susceptibility of the *atdcl2dcl3dcl4* mutant would be obsolete, when infecting with the Δ*bcago1*, because neither the plant nor *B. cinerea* could induce cross-kingdom RNAi (*SI Appendix*, Fig. S17*A*). Indeed, infection of *atdcl2dcl3dcl4* plants with Δ*bcago1* indicated plant infection levels similar to *A. thaliana* WT plants infected with *B. cinerea* WT or Δ*bcago1* (*SI Appendix*, Fig. S17*B*). Thus, we anticipated that BcAGO1 could have a second function during plant infection, and this could be to bind plant-derived small RNAs that could trigger silencing of fungal genes as a defense response.

To test this hypothesis, we performed BcAGO coimmunopurification (BcAGO IP) coupled to small RNA deep sequencing to identify tomato small RNAs that bind to BcAGOs during infection. For this experiment, we used transgenic *B. cinerea* strains expressing 3xHA-tagged BcAGO1 or 3xHA-BcAGO2 in the Δ*bcago1* or Δ*bcago2* ko mutant background, respectively. As observed previously in this study, the transgenic 3xHA-BcAGO1 strains could revert the loss of BcsRNA accumulation in the Δ*bcago1* and 3xHA-BcAGO2 reverted the reduced disease phenotype of the Δ*bcago2* ko strains, confirming that both 3xHA-BcAGO constructs were functional. Upon immunoblot confirmation of successful BcAGO IP (*SI Appendix*, Fig. S18), we

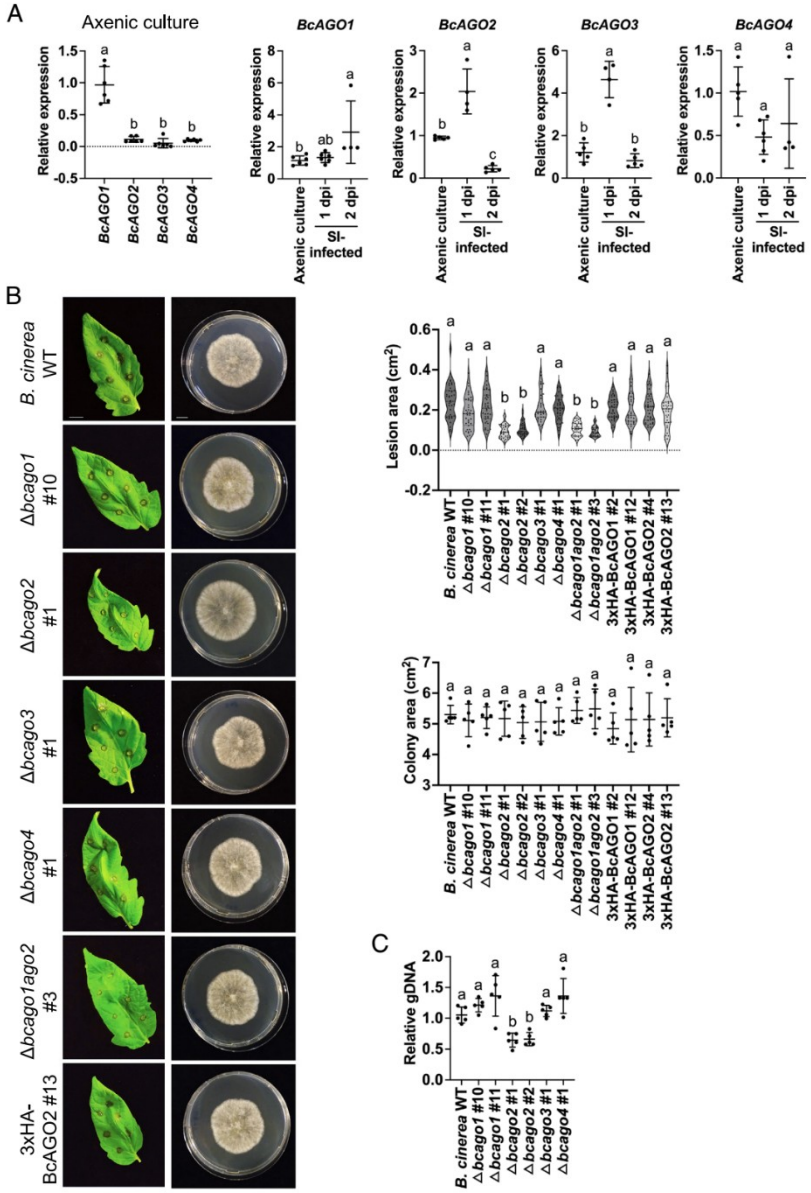

Fig. 3. BcAGO2 is a pathogenicity factor in *B. cinerea*. (*A*) Relative mRNA expression of *BcAGO*s in axenic culture or in SI-infected samples at 48 hpi measured by qRT-PCR. *B. cinerea BcTubulin* was used as a housekeeping gene. (*B*) Tomato leaf infection and agar plate growth assays with *B. cinerea* WT and different Δ*bcago* mutant strains. Leaf images were taken at 48 hpi to measure lesion area. Colony size on agar plates was measured in four independent cultures per strain at 3 d post cultivation start. (*C*) Relative *B. cinerea* genomic DNA (gDNA) was quantified in SI-infected samples at 48 hpi by qRT-PCR, measuring tomato gDNA as a reference. In all plots, data points represent biological replicates and error bars indicate the SD. The letters indicate significant difference using one-way ANOVA and Tukey test with $P < 0.05$.

isolated small RNAs for cloning and Illumina-based sequencing. We sequenced two biological replicates from axenic culture and three biological replicates for SI-infected samples (*SI Appendix*, Fig. S19*A*). Small RNA sequencing analysis revealed a shift of size enrichment from 24 nt reads in axenic culture to 21 to 22 nt reads in SI-infected samples for both BcAGO1 and BcAGO2 IPs (Fig. 4*A*). When mapping reads to the *B. cinerea* or the tomato reference genomes, we identified sequences that exclusively mapped to one or the other species with at least one mismatch to the opposite reference genome, accordingly. For BcsRNAs, 21 to

22 nt long retrotransposon-derived reads were enriched in SI-infected samples (Fig. 4*B*). The cross-kingdom BcsRNA3.1, BcsRNA3.2, BcsRNA5, and BcsRNA20, which are all derived from RT (18), indicated higher read numbers in SI-infected samples compared to axenic culture (Fig. 4*C*). This result was consistent with a previous finding that retrotransposon-derived 21 to 22 nt BcsRNAs are induced upon plant infection (34). Likewise, when mapping reads to our defined *BcsRNA* loci, we observed overlapping BcsRNA accumulation between BcAGO1 and BcAGO2 (*SI Appendix*, Fig. S19 *B–D*) and a size preference of 21 to 22 nt long reads in size-specific loci (Fig. 4*D*).

Among BcAGO-bound tomato small RNAs (SlsRNAs), 21 nt long reads were enriched in the BcAGO1 and BcAGO2 IPs (Fig. 5*A*). Remarkably, SlsRNAs reached up to 50% of mapped read counts in the BcAGO1 IP samples (*SI Appendix*, Fig. S20*A*), indicating massive invasion of tomato small RNAs into BcAGO1 during infection. The SlsRNA reads mapped to different annotated genetic loci, with the majority of them being associated with DNA repeats, mRNAs, tRNAs, and rRNAs (*SI Appendix*, Fig. S20*B*). Similar to the BcAGO-bound BcsRNA fraction, the SlsRNAs largely overlapped in binding to BcAGO1 and BcAGO2 during infection. Among most abundant SlsRNAs, higher read numbers

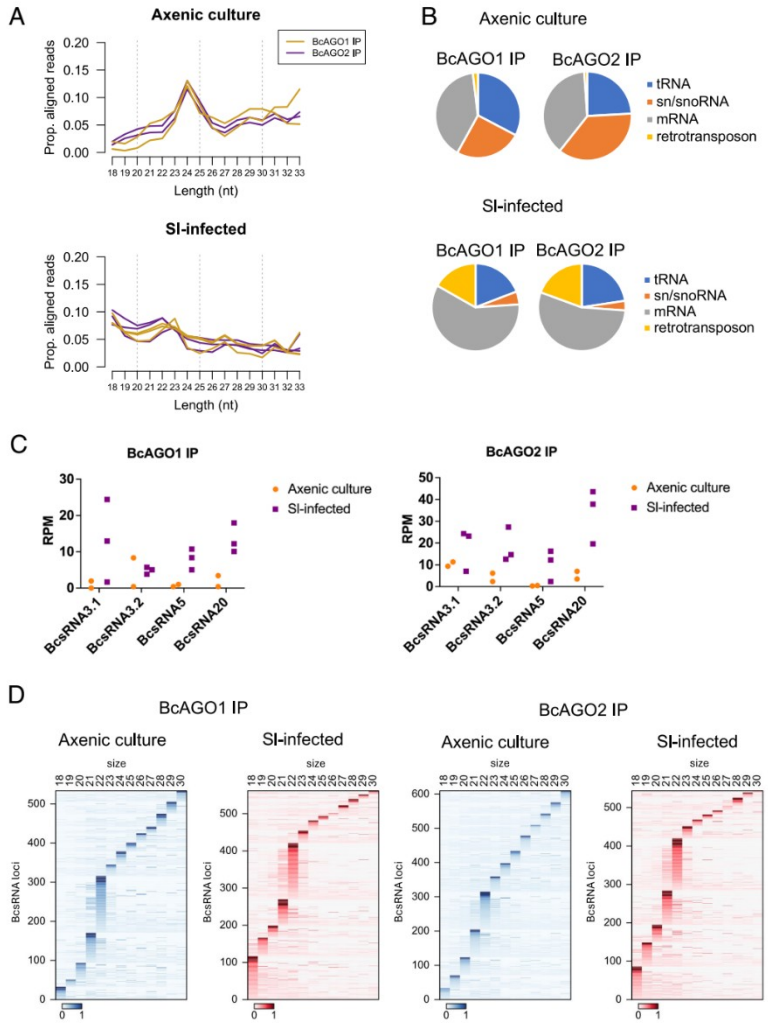

Fig. 4. Small RNA binding profiles of BcAGO1 and BcAGO2 change during tomato infection. (*A*) Size distribution of total small RNA reads binding to BcAGOs in axenic culture with two biological replicates or in SI-infected samples with three biological replicates at 48 hpi, as revealed by BcAGO IP and small RNA-seq. (*B*) Relative fractions of BcAGO-bound total BcsRNA reads mapping to different annotated genetic loci in the *B. cinerea* genome, including transfer RNA (tRNA), small nuclear and small nucleolar (sn/snoRNA), messenger RNA (mRNA), RT. (*C*) Normalized read counts per million (RPM) of different BcsRNAs binding to BcAGOs in axenic culture or SI-infected samples. (*D*) Heatmaps of the size profile for BcAGO-bound BcsRNAs mapping to defined *BcsRNA* loci. Color scales indicate locus normalized expression, showing expression as a proportion of the highest-expressed size. Axenic culture and SI-infected samples are shown on blue- and red-color scales, respectively.

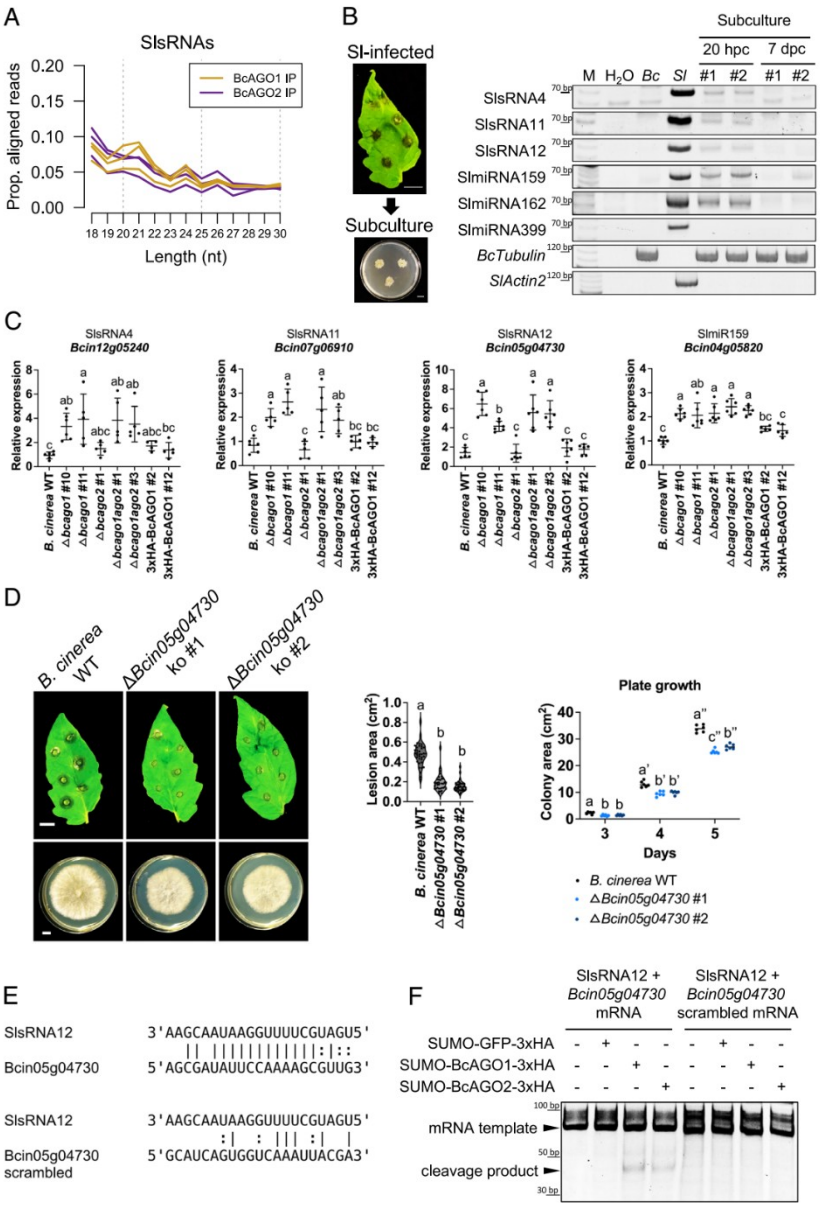

Fig. 5. Tomato small RNAs bind to BcAGOs during infection and induce cross-kingdom RNAi of *B. cinerea* genes. (*A*) Size distribution of SlsRNAs binding to BcAGO1 or BcAGO2 in Sl-infected samples, as revealed by BcAGO IP and small RNA-seq. (*B*) *Left*, *B. cinerea* was reisolated from Sl-infected material and grown in subculture on agar plates. Subculture samples were collected from the colony edge. Right, stem-loop RT-PCR of selected SlsRNAs detected in two biological replicates (#) of reisolated *B. cinerea* samples collected at 20 h or 7 d post cultivation start. Noninfected tomato leaves (*Sl*) were used as a positive control, and *B. cinerea* that was not reisolated from infected tomato as well as water were used as negative controls. The SlmiR399 was used as another negative control representing a highly expressed SlsRNA which was never detected in the BcAGO IP datasets. (*C*) Relative mRNA expression of predicted *B. cinerea* genes targeted by SlsRNAs was measured in Sl-infected samples at 48 hpi. *B. cinerea BcActin* was used as a housekeeping gene. (*D*) Tomato leaf infection and agar plate growth assays with *B. cinerea* WT and two independent target gene Δ*Bcin05g04730* ko strains (#). Leaf images were taken at 48 hpi to measure lesion area. Colony size on agar plates was measured in six independent cultures per strain at 3 to 5 d post cultivation start. In all plots, data points represent biological replicates. Error bars indicate the SD and numbers indicate significant difference using one-way ANOVA and the Tukey test with $P < 0.05$. (*E*) Alignments of the native *Bcin05g04730* target site of SlsRNA12 or a target site scrambled version. (*F*) RNA in vitro cleavage assay using recombinant BcAGO that was preincubated with the SlsRNA12 and mixed with the native or scrambled *Bcin05g04730* target RNA, as template. GFP was used as a nonspecific protein control. Template RNA was in the size of 94 bases and the expected cleavage products of 59 and 35 bases.

were counted in BcAGO1 IP samples compared to BcAGO2 IP (*SI Appendix*, Fig. S21*A*).

We next investigated the possibility that SlsRNA candidates silence *B. cinerea* genes during infection. We considered 21 to 22 nt SlsRNA reads with an average of >100 RPM in the BcAGO1 or BcAGO2 IP small RNA-seq datasets. We filtered out all SlsRNA reads mapping to ribosomal RNA (rRNA), small nuclear or nucleolar RNA (snRNA/snoRNA), or protein coding transcripts (in sense orientation), as these did not likely represent regulatory RNAs but RNA degradation products. In total, we predicted 74 *B. cinerea* target genes of 21 SlsRNA candidates using the TAPIR tool with stringent parameter setting (*SI Appendix*, Table S4). These SlsRNA candidates were detected in all BcAGO IP datasets (*SI Appendix*, Fig. S21*A*). We repeated BcAGO1 IP coupled to stem-loop RT-PCR (*SI Appendix*, Fig. S21*B*) that validated candidate small RNAs truly bound to BcAGO1 during tomato infection, as identified by deep sequencing.

We chose a subset of 10 SlsRNAs to confirm that these invaded into *B. cinerea* during tomato infection. For this, we reisolated *B. cinerea* from Sl-infected leaf tissue to subculture on agar plates (Fig. 5*B*). *B. cinerea* subculture samples were taken from the colony edge after 20 h or 7 d for SlsRNA analysis. The SlmiRNA159, SlmiR162, SlsRNA4, SlsRNA11, and SlsRNA12 were detected in independent *B. cinerea* reisolation samples by stem-loop RT-PCR (Fig. 5*B* and *SI Appendix*, Fig. S21*C*). PCR signals were stronger at 20 h compared to 7d indicating that SlsRNA were degraded over time in *B. cinerea* cells. These SlsRNAs were not detected in *B. cinerea* mycelium that was not reisolated from infected tomato. All tested SlsRNAs were present in tomato leaf samples. SlsRNAs were also detected in reisolated Δ*bcago1*, Δ*bcago2* and Δ*bcago1ago2* ko mutant strains, as well as in a Δ*bcrdr1* ko mutant strain that was recently characterized to be required for BcsRNA accumulation and cross-kingdom RNAi (21) (*SI Appendix*, Fig. S21*D*). In this RT-PCR assay, the SlmiR399 served as a negative control SlsRNA, because it was not detected in the BcAGO IP small RNA datasets of this work.

To further analyze whether SlsRNAs could suppress *B. cinerea* target genes through BcAGOs during infection, we measured mRNA expression of predicted target genes in Sl-infected samples, comparing *B. cinerea* WT with Δ*bcago1*, Δ*bcago2*, and Δ*bcago1ago2* ko strains. Among 14 tested *B. cinerea* candidate genes, *Bcin12g05240*, *Bcin05g04730*, *Bcin07g06910,* and *Bcin04g05820* displayed higher expression in Δ*bcago1* and Δ*bcago1ago2* ko mutants (Fig. 5*C* and *SI Appendix*, Fig. S22*A*). Failed mRNA suppression was not due to Δ*bcago1* loss-of-function per se, because elevated mRNA expression was not evident when comparing *B. cinerea* WT and Δ*bcago1* ko strains grown in axenic culture (*SI Appendix*, Fig. S22*B*). Moreover, *Bcin05g04730* was transcriptionally upregulated in Sl-infected samples upon *B. cinerea* WT infection, indicating that this gene might be relevant for fungal infection (*SI Appendix*, Fig. S22*C*). The *Bcin05g04730* encodes for a putative Serine/Threonine Protein kinase. Hence, we chose *Bcin05g04730* for targeted gene ko to assess its potential role in tomato infection. Two independent ko strains (*SI Appendix*, Fig. S23) displayed reduced lesion induction when infecting tomato. However, the mutant strains grew slightly slower on agar plates compared to *B. cinerea* (Fig. 5*D*), which could have contributed to the reduced disease phenotype.

To confirm that SlsRNA12 can direct *Bcin05g04730* mRNA slicing through BcAGO1, we performed an in vitro RNA cleavage assay. Recombinant BcAGO1, BcAGO2, or GFP protein was expressed in and isolated from an *Escherichia coli* expression system (*SI Appendix*, Fig. S24*A*). Successful mRNA cleavage was detected with both BcAGO1 and BcAGO2 (Fig. 5*E* and *SI Appendix*, Fig. S24*B*). Scrambling of the SlsRNA12 target site avoided any mRNA cleavage. This result indicated that both BcAGO1 and BcAGO2 are in principle capable to cleave *B. cinerea* mRNAs guided by SlsRNAs. Nevertheless, *Bcin05g04730* mRNA was not derepressed in Δ*bcago2,* compared to Δ*bcago1* upon tomato infection (Fig. 5*C*). This might be attributed to a lower expression level of BcAGO2 compared to BcAGO1 (Fig. 3*A*). To test this possibility, we repeated tomato infection using *B. cinerea* WT, Δ*bcago2* complemented with native promoter $BcAGO2_{pro}$-3xHA-BcAGO2 strains or Δ*bcago2* complemented with overexpressing promoter $OliC_{pro}$-3xHA-BcAGO2 strains. Overexpression of BcAGO2 was approved on mRNA and protein levels (*SI Appendix*, Fig. S25 *A* and *B*). *Bcin05g04730* mRNA level was reduced upon infection with the BcAGO2 overexpressing strains (*SI Appendix*, Fig. S25*C*) supporting the idea that the BcAGO2 level in the *B. cinerea* WT was too low to allow SlsRNA-induced cross-kingdom RNAi during infection.

Collectively, in this study, we found that BcAGOs act in bidirectional cross-kingdom RNAi during plant infection with opposite effects on the disease outcome.

Discussion

Cross-kingdom RNAi is an emerging field in host–pathogen interaction research and bidirectional cross-kingdom RNAi has been described in fungal–plant interaction. In one direction, *B. cinerea* secretes BcsRNAs into its host plants tomato and *A. thaliana* that bind to the plants' own AGO1 to silence host immunity genes (17, 18, 34). In the counterdirection, *A. thaliana* secretes small RNAs that can trigger gene suppression in *B. cinerea* (29). The role of pathogen AGOs in cross-kingdom RNAi had not been explored. We herewith provide mechanistic insights of the diversified regulatory functions of different BcAGO family members in bidirectional cross-kingdom RNAi and in plant infection.

Profiling the small RNA transcriptome revealed that BcAGO1 is required for the accumulation of cross-kingdom BcsRNAs. Reduction but not complete loss of small RNA has been reported in *ago* loss-of-function mutants before (37, 38). It is argued that small RNAs bound to AGO could experience transient protection against rapid nuclease degradation. The BcAGO1 ortholog in the fungus *N. crassa*, QDE-2 is also required for small RNA biogenesis (39). QDE-2 binds to precursor RNA and recruits another exonuclease, QIP, that makes the final step in mature small RNA biogenesis. Since *B. cinerea* possesses a QIP-like RNA nuclease (Bcin10g05730), a similar small RNA biogenesis mechanism could exist in *B. cinerea*. Alternatively, BcAGO1 might regulate BcsRNA biogenesis. For instance, the fungal *Magnaporthe oryzae* MoAGO2 interferes with RNAi triggered by hairpin and retrotransposon-derived small RNAs through the MoAGO1 and MoAGO3 (40). A similar BcAGO1-mediated RNAi feedback loop might also exist in *B. cinerea*.

When using a GFP switch-on reporter assay *in planta*, which allowed us to measure fungal-induced cross-kingdom RNAi in plants over a time course of infection, the Δ*bcago1* ko mutant failed in reporter activation. This is in agreement with a previous finding that *B. cinerea* Δ*bcrdr1* and Δ*bcdcl1dcl2* ko strains, which were impaired in cross-kingdom BcsRNA production (18, 20) also failed to induce cross-kingdom RNAi in the same reporter plant (21). Using this assay, we also observed that the Δ*bcago2* ko mutant was compromised in cross-kingdom RNAi. However, BcsRNA accumulation was largely unaltered in the Δ*bcago2*, implying another role of BcAGO2 in cross-kingdom RNAi, compared to BcAGO1, BcDCLs, and BcRDR1. For instance, *A. thaliana* AGO1 participates in packaging small RNA into extracellular

vesicles (EVs) for secretion (41). EVs are also produced by *B. cinerea* that contain BcsRNAs and are taken up into *A. thaliana* cells via clathrin-mediated endocytosis (42). Therefore, BcAGO2 might play a role in BcsRNA delivery into plant cells, which could explain compromised cross-kingdom RNAi when infecting reporter plants with Δ*bcago2* ko. The role of BcAGO1 and BcAGO2 in fungal-induced cross-kingdom RNAi was further supported by the loss of tomato target gene suppression upon infection with Δ*bcago1 and* Δ*bcago2* ko mutants. Interestingly, suppression of the tomato genes *SlMPKKK4* and *SlBhlh63* relied on BcAGO1, while *SlVPS* suppression was dependent on BcAGO2. Hence, we propose that BcAGO1 and BcAGO2 pathways are independent and act in a complementary manner in cross-kingdom RNAi.

Using Δ*bcago* ko mutants in a tomato leaf infection assay, we observed reduced pathogenicity in the Δ*bcago2* mutant. Likewise, single *ago* gene ko in the apple canker fungus *Valsa mali* reduced virulence (43). An *ago* ko in the wheat-infecting fungus *Zymoseptoria tritici* led to stop the production of asexual propagules *in planta* (13). A possible reason for the reduced pathogenicity in Δ*bcago2* could be the limited capability to induce cross-kingdom RNAi. However, infecting *A. thaliana* with the Δ*bcago1* and Δ*bcago2* mutant revealed no or only marginal effect on disease severity, respectively. *A. thaliana* siRNAs were previously reported to induce cross-kingdom RNAi in *B. cinerea* for defense (29). These *A. thaliana* defense-related siRNAs might function through BcAGO1 and BcAGO2 balancing the effect of fungal-induced cross-kingdom RNAi.

Strikingly, Δ*bcago1* did not show reduced virulence neither in tomato nor in *A. thaliana* although the loss of fungal-induced cross-kingdom RNAi. A reason could be that BcAGO1 is required for plant-induced cross-kingdom RNAi and effective silencing of fungal virulence genes, balancing its functional roles in opposite directions of cross-kingdom RNAi. This likely led to unchanged infection strength. In consistence, *A. thaliana atdcl2dcl3dcl4* triple mutants, which are blocked in the plant-induced cross-kingdom RNAi but not in the opposite direction, exhibited enhanced infection upon inoculation with Δ*bcago1* ko mutant compared to *B. cinerea* WT.

Cross-kingdom RNAi was reported in both directions during *B. cinerea*–plant interaction (20). We here found evidence that BcAGO1 was exploited for tomato-induced cross-kingdom RNAi. By profiling the BcAGO-bound small RNA repertoire during tomato infection, we identified at least 21 tomato SlsRNAs that were predicted to target 74 *B. cinerea* mRNAs. We demonstrated that four *B. cinerea* genes were suppressed during infection in a BcAGO1-dependent manner and proofed that one target gene, a serine/threonine protein kinase, was part of *B. cinerea* pathogenicity. Therefore, studying pathogen AGO-associated host small RNAs during infection, not only deciphered tomato small RNAs that were capable to induce cross-kingdom RNAi but also promise to reveal novel *B. cinerea* pathogenicity factors. Interestingly, protein kinases were also previously identified as cross-kingdom RNAi targets of *B. cinerea* (18) and the oomycete *Hyaloperonospora arabidopsidis* small RNAs (22) in *A. thaliana* and tomato host plant species, revealing that manipulating this class of enzymes has evolved in diverse biotic interactions.

In summary, we uncovered diversified functions of BcAGOs during plant infection in bidirectional cross-kingdom RNAi. This led to mechanistic insights into the complex regulatory roles of pathogen AGOs during plant infection. Translating such knowledge into innovative siRNA tools promise to improve RNAi-based crop protection strategies in future.

Materials and Methods

Fungal and Plant Materials. *B. cinerea* Pers. Fr. [*Botryotinia fuckeliana* (de Bary) Whetzel] strain B05.10 (44) was used in the study and was cultured in complete HA media (45), if not otherwise notified. *S. lycopersicum* (tomato, cultivar Heintz 1706) was grown in a climate chamber under controlled condition (16 h light/8 h dark, 24 °C, 60% relative humidity). *A. thaliana* ecotype Columbia (Col)-0 and *atdcl2dcl3dcl4* mutant were grown under short-day conditions (8 h light/16 h dark, 22 °C, 60% relative humidity).

Fungal Transformation. *B. cinerea* transformation was performed as previously described (46) with minor modifications, as described in detail in *SI Appendix*.

Infection Assays. For infection assay with spores, conidia were eluted from sporulated *B. cinerea* with 1% malt extract (45) suspension buffer, as described in details in *SI Appendix*.

DNA and RNA Extraction. Genomic DNA of *B. cinerea* pure mycelium or sporulated mycelium was isolated from at least 30 transformants for each construct using CTAB according to the previous method (47); see *SI Appendix* for more details.

RT-PCR. DNA-free total RNA was used for first-strand cDNA synthesis with an oligo dT primer and SuperScript III reverse transcriptase (Invitrogen, Thermo Fisher Scientific) according to the manufacturer's instructions. Relative transcript levels were calculated by $2^{-\Delta\Delta Ct}$ based on the previous method (48) using qPCR cycler (Quantstudio5, Thermo Fisher Scientific). Primer sequences used are listed in *SI Appendix*, Table S5.

Immunoblot Analysis. Imunoblot blot analysis of GFP was performed, as described for BcAGO IP, using primary GFP Rabbit Polyclonal Antibody (600-401-215, Rockland) and an α-rabbit IRdye800 secondary antibody (LI-COR, 1:3,000 dilution). Protein signals were detected using Odyssey imaging system (LI-COR).

AGO Immunoprecipitation for Small RNA Analysis. AGO IP for small RNA isolation and analysis was performed following a protocol as described before (REF). Details for SlAGO1 IP and BcAGO IP can be found in *SI Appendix*.

Small RNA Sequencing Analysis. Small RNA libraries were cloned following the manufacturer's instructions (NEBNext Multiplex Small RNA Library Prep for Illumina) and sequenced on an Illumina HiSeq1500 platform. For details, please see *SI Appendix*. Raw sequencing data are deposited at the NCBI-SRA database (49).

BcsRNA Loci Annotation. *BcsRNA* loci were defined using a custom pipeline based on genome-wide assessment of depth, as outlined in Fig. 1*C*. Alignments for wildtype libraries (n = 2) were used to generate a coverage profile, normalized to RPM. A Poisson distribution was fitted to assess probability that a genomic position has expression higher than background. For this, lambda was calculated for each chromosome separately, based on 40 nucleotide windows with total depth calculated from intergenic regions, using the following formula:

$$\text{lambda} = \text{window\_read\_count} / \text{intergenic\_length} * \text{intergenic\_read\_count}.$$

Intergenic regions are defined as positions not as featuretype = mRNA in the NCBI gene annotation. Regions are then defined as positions with a Poisson probability of 10^{-4} or less and merged if they are <150 nucleotides apart. Merged regions are trimmed to exclude edges which are <5% of their maximum depth. Finally, regions are padded by 10 nucleotides on either edge, resulting in *BcsRNA* loci.

Loci are assessed in terms of their basic dimensions (length, distance to prior loci) and BcsRNA profile (abundance, RPM, most common BcsRNA sequence and depth, strand preference, and complexity). Size specificity is also assessed, showing the abundance of the most common consecutive sizes for the locus. This is summarized in the field "sizecall", which is the smallest number of consecutive sizes that are > 50% of the locus abundance, with "N" indicating loci that are not specific and likely derived from degradation.

Phylogenetic Analysis. *B. cinerea* AGO proteins were identified by searching the protein databases for homologies of *N. crassa* QDE2 and SMS2 using BLAST search (50). The rooted phylogenetic tree was constructed with amino acid sequences of representative filamentous fungal AGO proteins in phyla of Ascomycota by the

RAXML method with the JTT model. Fungal species and their accession number are listed in *SI Appendix*, Table S1. The alignment was performed by MAFFT and bootstrap was calculated based on 1,000 replicates. The phylogenetic tree was built at CIPRES Science Gateway.

RNA In Vitro Cleavage Assay. RNA in vitro cleavage was performed following the procedure as previous described (51). For details, please see *SI Appendix*.

Data Plotting and Statistical Analysis. GraphPad Prism 10 software was used for plotting and statistical analysis. One-way ANOVA with the Tukey multiple comparisons test ($P < 0.05$) was performed for multisamples comparison. For two samples comparison, unpaired *t* test was performed. Statistical analysis was set for two-tailed $*P < 0.05$, $**P < 0.01$.

Data, Materials, and Software Availability. Small RNA sequencing data have been deposited in Fungal Argonaute proteins act in bidirectional cross-kingdom RNA interference during plant infection [NCBI SRA (BioProject ID PRJNA1092616) (49)]. All study data are included in the article and/or supporting information.

ACKNOWLEDGMENTS. We thank Michael Feldbrügge and Claude Becker for critical proofreading. We thank the Gene Center Munich for Illumina NextSeq sequencing service. We also would like to thank Martin Parniske for scientific discussions and providing access to the Golden Gate cloning system, Silke Robatzek and Eliana Mor for access to and technical assistance with the DMi8 Thunder Imager microscope. We thank Verena Klingl and Adriana Hörmann for technical support. AW is supported by the German Research Foundation (DFG), project ID 433194101 in the frame of the research unit RU5116. NRJ is supported by ANID-fondecyt (Chile) #11220727. LH was supported by the China Scholarship Council (CSC).

Author affiliations: [a]Faculty of Biology, Chair of Genetics, Faculty of Biology, Ludwig Maximilians University of Munich, Martinsried 82152, Germany; [b]Centro de Genómica y Bioinformática, Facultad de Ciencias, Ingeniería y Tecnología, Universidad Mayor, Santiago 5750, Chile; [c]Millennium Science Initiative—Millennium Institute for Integrative Biology, Santiago, Chile; and [d]Department of Biology, Institute of Plant Science and Microbiology, University of Hamburg, Hamburg 22607, Germany

1. G. Meister, Argonaute proteins: Functional insights and emerging roles. *Nat. Rev. Genet* **14**, 447–459 (2013).
2. G. J. Hannon, RNA interference. *Nature* **418**, 244–251 (2002).
3. S. S. Chang, Z. Zhang, Y. Liu, RNA interference pathways in fungi: Mechanisms and functions. *Annu. Rev. Microbiol.* **66**, 305–323 (2012).
4. V. Fulci, G. Macino, Quelling: Post-transcriptional gene silencing guided by small RNAs in *Neurospora crassa*. *Curr. Opin. Microbiol.* **10**, 199–203 (2007).
5. T. M. Hammond, Sixteen years of meiotic silencing by unpaired DNA. *Adv. Genet* **97**, 1–42 (2017).
6. X. Wang *et al.*, Sex-induced silencing defends the genome of *Cryptococcus neoformans* via RNAi. *Genes Dev.* **24**, 2566–2582 (2010).
7. R. A. Martienssen, M. Zaratiegui, D. B. Goto, RNA interference and heterochromatin in the fission yeast *Schizosaccharomyces pombe*. *Trends Genet* **21**, 450–456 (2005).
8. H. C. Lee *et al.*, qiRNA is a new type of small interfering RNA induced by DNA damage. *Nature* **459**, 274–U163 (2009).
9. S. Campo, K. B. Gilbert, J. C. Carrington, Small RNA-based antiviral defense in the phytopathogenic fungus *Colletotrichum higginsianum*. *PLoS Pathog* **12**, e1005640 (2016).
10. Q. Sun, G. H. Choi, D. L. Nuss, A single Argonaute gene is required for induction of RNA silencing antiviral defense and promotes viral RNA recombination. *Proc. Natl. Acad. Sci. U.S.A.* **106**, 17927–17932 (2009).
11. S. Torres-Martinez, R. M. Ruiz-Vazquez, The RNAi Universe in Fungi: A varied landscape of small RNAs and biological functions. *Annu. Rev. Microbiol.* **71**, 371–391 (2017).
12. F. Y. Gaffar, J. Imani, P. Karlovsky, A. Koch, K. H. Kogel, Different components of the RNA interference machinery are required for conidiation, ascosporogenesis, virulence, deoxynivalenol production, and fungal inhibition by exogenous double-stranded RNA in the head blight pathogen Fusarium graminearum. *Front. Microbiol.* **10**, 1662 (2019).
13. M. Habig, K. Schotanus, K. Hufnagel, P. Happel, E. H. Stukenbrock, Ago1 affects the virulence of the fungal plant pathogen *Zymoseptoria tritici*. *Genes (Basel)* **12**, 1011 (2021).
14. S. M. Jo, Y. Ayukawa, S. H. Yun, K. Komatsu, T. Arie, A putative RNA silencing component protein FoQde-2 is involved in virulence of the tomato wilt fungus *Fusarium oxysporum f. sp lycopersici*. *J. General Plant Pathol.* **84**, 395–398 (2018).
15. Y. Elad, M. Vivier, S. Fillinger, "Botrytis, the good, the bad and the ugly" in *Botrytis–The Fungus, the Pathogen and its Management in Agricultural Systems*, S. Fillinger, Y. Elad, Eds. (2016)
16. J. A. van Kan, Licensed to kill: The lifestyle of a necrotrophic plant pathogen. *Trends Plant Sci.* **11**, 247–253 (2006).
17. M. Wang, A. Weiberg, E. Dellota Jr., D. Yamane, H. Jin, Botrytis small RNA Bc-siR37 suppresses plant defense genes by cross-kingdom RNAi. *RNA Biol.* **14**, 421–428 (2017).
18. A. Weiberg *et al.*, Fungal small RNAs suppress plant immunity by hijacking host RNA interference pathways. *Science* **342**, 118–123 (2013).
19. A. Weiberg, M. Wang, M. Bellinger, H. Jin, Small RNAs: A new paradigm in plant-microbe interactions. *Annu. Rev. Phytopathol.* **52**, 495–516 (2014).
20. M. Wang *et al.*, Bidirectional cross-kingdom RNAi and fungal uptake of external RNAs confer plant protection. *Nat. Plants* **2**, 16151 (2016).
21. A. P. Cheng *et al.*, A fungal RNA-dependent RNA polymerase is a novel player in plant infection and cross-kingdom RNA interference. *PLoS Pathog* **19**, e1011885 (2023).
22. F. Dunker *et al.*, Oomycete small RNAs bind to the plant RNA-induced silencing complex for virulence. *eLife* **9**, e56096 (2020).
23. B. Ren, X. Wang, J. Duan, J. Ma, Rhizobial tRNA-derived small RNAs are signal molecules regulating plant nodulation. *Science* **365**, 919–922 (2019).
24. H. M. Ji *et al.*, Fol-miIR1, a pathogenicity factor of *Fusarium oxysporum*, confers tomato wilt disease resistance by impairing host immune responses. *New Phytol.* **232**, 705–718 (2021).
25. A. H. Buck *et al.*, Exosomes secreted by nematode parasites transfer small RNAs to mammalian cells and modulate innate immunity. *Nat. Commun.* **5**, 5488 (2014).
26. S. Shahid *et al.*, MicroRNAs from the parasitic plant *Cuscuta campestris* target host messenger RNAs. *Nature* **553**, 82–85 (2018).
27. J. Wong-Bajracharya *et al.*, The ectomycorrhizal fungus *Pisolithus microcarpus* encodes a microRNA involved in cross-kingdom gene silencing during symbiosis. *Proc. Natl. Acad. Sci. U.S.A.* **119**, e2103527119 (2022).
28. C. Cui *et al.*, A fungal pathogen deploys a small silencing RNA that attenuates mosquito immunity and facilitates infection. *Nat. Commun.* **10**, 4298 (2019).
29. Q. Cai *et al.*, Plants send small RNAs in extracellular vesicles to fungal pathogen to silence virulence genes. *Science* **360**, 1126–1129 (2018).
30. T. Zhang *et al.*, Cotton plants export microRNAs to inhibit virulence gene expression in a fungal pathogen. *Nat. Plants* **2**, 16153 (2016).
31. J. A. Van Kan *et al.*, A gapless genome sequence of the fungus *Botrytis cinerea*. *Mol. Plant Pathol.* **18**, 75–89 (2017).
32. T. Paysan-Lafosse *et al.*, InterPro in 2022. *Nucleic Acids Res.* **51**, D418–D427 (2023).
33. K. Nakanishi, D. E. Weinberg, D. P. Bartel, D. J. Patel, Structure of yeast Argonaute with guide RNA. *Nature* **486**, 368–374 (2012).
34. A. Porquier *et al.*, Retrotransposons as pathogenicity factors of the plant pathogenic fungus *Botrytis cinerea*. *Genome Biol.* **22**, 225 (2021).
35. N. R. Johnson, J. M. Yeoh, C. Coruh, M. J. Axtell, Improved placement of multi-mapping small RNAs. *G3 (Bethesda)* **6**, 2103–2111 (2016).
36. G. Wu, W. Wang, Recent advances in understanding the role of two mitogen-activated protein kinase cascades in plant immunity. *J. Exp. Bot.* **75**, 2256–2265 (2024), 10.1093/jxb/erae020.
37. S. Diederichs, D. A. Haber, Dual role for Argonautes in microRNA processing and posttranscriptional regulation of microRNA expression. *Cell* **131**, 1097–1108 (2007).
38. K. Okamura, A. Ishizuka, H. Siomi, M. C. Siomi, Distinct roles for Argonaute proteins in small RNA-directed RNA cleavage pathways. *Genes Dev.* **18**, 1655–1666 (2004).
39. H. C. Lee *et al.*, Diverse pathways generate microRNA-like RNAs and Dicer-independent small interfering RNAs in fungi. *Mol. Cell* **38**, 803–814 (2010).
40. Q. Nguyen *et al.*, A fungal Argonaute interferes with RNA interference. *Nucleic Acids Res.* **46**, 2495–2508 (2018).
41. B. He *et al.*, RNA-binding proteins contribute to small RNA loading in plant extracellular vesicles. *Nat. Plants* **7**, 342–352 (2021).
42. B. He *et al.*, Fungal small RNAs ride in extracellular vesicles to enter plant cells through clathrin-mediated endocytosis. *Nat. Commun.* **14**, 4383 (2023).
43. H. Feng *et al.*, The distinct roles of Argonaute protein 2 in the growth, stress responses and pathogenicity of the apple tree canker pathogen. *Forest. Pathol.* **47**, e12354 (2016).
44. P. Buttner *et al.*, Variations in ploidy among isolates of *Botrytis cinerea*: Implications for genetic and molecular analyses. *Curr. Genet.* **25**, 445–450 (1994).
45. G. Doehlemann, P. Berndt, M. Hahn, Different signalling pathways involving a Galpha protein, cAMP and a MAP kinase control germination of *Botrytis cinerea* conidia. *Mol. Microbiol.* **59**, 821–835 (2006).
46. N. Muller *et al.*, Investigations on VELVET regulatory mutants confirm the role of host tissue acidification and secretion of proteins in the pathogenesis of *Botrytis cinerea*. *New Phytol.* **219**, 1062–1074 (2018).
47. M. G. Murray, W. F. Thompson, Rapid isolation of high molecular weight plant DNA. *Nucleic Acids Res.* **8**, 4321–4325 (1980).
48. K. J. Livak, T. D. Schmittgen, Analysis of relative gene expression data using real-time quantitative PCR and the 2(T)(-Delta Delta C) method. *Methods* **25**, 402–408 (2001).
49. A. Weiberg, Fungal Argonaute proteins act in bidirectional cross-kingdom RNA interference during plant infection, BioProject NCBI. https://www.ncbi.nlm.nih.gov/bioproject/?term=PRJNA1092616. Deposited 27 March 2024.
50. S. F. Altschul, W. Gish, W. Miller, E. W. Myers, D. J. Lipman, Basic local alignment search tool. *J. Mol. Biol.* **215**, 403–410 (1990).
51. K. Miyoshi, H. Uejima, T. Nagami-Okada, H. Siomi, M. C. Siomi, In vitro RNA cleavage assay for Argonaute-family proteins. *Methods Mol. Biol.* **442**, 29–43 (2008).

PNAS

Supporting Information for
Paste manuscript title here.

An-Po Cheng, Lihong Huang, Lorenz Oberkofler, Nathan R Johnson, Adrian-Stefan Glodeanu, Kyra Stillman, Arne Weiberg

Corresponding author: Arne Weiberg
Email: arne.weiberg@uni-hamburg.de

This PDF file includes:

suspension were inoculated on detached leaves of six weeks old tomato plants. For *A. thaliana* infection assay, a droplet of 20 µl ($2x10^5$ spores/ml) conidial suspension were inoculated on detached leaves of five weeks old plants. Inoculation assay with mycelial plugs (Ø=0.4 cm) was performed according to the previous method (3). Mycelia on agar plates of *B. cinerea* were inoculated on detached leaves of four weeks old tomato plants. The lesion area was measured using Fiji software (ImageJ version 2.1.0/1.53c). For quantifying mycelial growth of *B. cinerea*, leaf discs three infected leaves were collected for genomic DNA extraction and qRT-PCR by using SYBR Green (Thermo Scientific) with qPCR cycler (CFX96, Bio-Rad).

DNA and RNA extraction

Genomic DNA of pure mycelium or sporulated mycelium was isolated from at least 30 transformants for each construct using CTAB according to the previous method (4) prior to chloroform/isoamyl alcohol extraction and isopropanol precipitation (5) with minor modifications (6). Mycelia growing on HA media dishes were harvested after cultivation for five to seven days in constant light or overlayed with cellophane for three days under constant dark condition. Six pairs of primers were used for genotyping transgenic transformants for each genotype of *B. cinerea*. GoTaq G2 DNA Polymerase (Promega) was used for genotyping with cycler. Primer oligos used for genotyping were listed in Table S5.

RT-PCR

Six-week-old tomatoes were treated with conidial suspension ($2x10^5$ spores/ml) of *B. cinerea* WT or ko mutant strains using a versatile sprayer (Roth Labware ®). Tomato or *A. thaliana* leaf discs were collected after 24, 48, 72 hours of treatment for *BcAGO* gene expression analysis. Four leaf discs (Ø=0.4 cm) were collected as one biological replicate. *B. cinerea* WT and genetically modified strains were cultivated on HA plates overlayed with cellophane for three days in the dark or grown on HA media for seven days under constant light for sporulation. Mycelia from the same plate were collected as a biological replicate. DNA-free total RNAs were used for first-strand cDNA synthesis with oligo $d_{20}T$ and SuperScript III reverse transcriptase (Invitrogen, Thermo Fischer Scientific) according to the manufacturer's instructions. RT reactions were diluted 10 folds with ddH_2O prior to performing qRT-PCR using SYBR Green (Invitrogen, Thermo Fischer Scientific). *B. cinerea Tubulin* (*Bcin01g08040*) was used

as reference genes to normalize mRNA. Relative transcripts were calculated by $2^{-\Delta\Delta Ct}$ based on the previous method (7) using qPCR cycler (Quantstudio5, Thermo Fisher Scientific). Primer sequences were listed in Table S5.

1µg of DNA-free total RNAs were used for a first-strand cDNA synthesis reaction with specific stem-loop RT primer and reverse transcription was carried out as described previously (8) with minor modifications. The resultant cDNA was directly used for amplification using GoTaq DNA Polymerase (Promega) on a thermo cycler initiated with 95°C for 2 min, then 32 cycles of denaturation at 95°C for 30 sec, annealing at 60°C for 30 sec and extension at 72°C for 20-180 sec (1 kb/min), followed by 5 min extension at 72°C. PCR products were visualized with 10% non-denaturing PAGE gel. Oligonucleotides were provided in Table S5.

SlAGO1 IP

Six weeks old tomato plants were inoculated for 24 hours with *B. cinerea*. For SlAGO1 IP, 5 g of infected leaf tissue were homogenized by mortar and pestle in liquid nitrogen. SlAGO1 IP was performed as previously described (22, 53). 30 ml extraction buffer (20 mM Tris-HCl pH7.5, 300 mM NaCl, 5 mM EDTA, 0.5% (v/v) NP-40, 5 mM DTT, 1 tablet cOmplete® protease inhibitor cocktail (Roche)/50 ml, 5 µl RNase inhibitor (40 U)/50 ml) was added to extract the protein. 5 mg plant α-AGO1 antibody (Agrisera) and 200 µl Protein A agarose beads (Roche) were incubated with the lysate on a wheel at 4°C for 2 hr. The beads were washed five times with washing buffer (20 mM Tris-HCl pH7.5, 300 mM NaCl, 5 mM EDTA, 0.5% (v/v) Triton X-100, 5 mM DTT, 1 tablet cOmplete® protease inhibitor cocktail (Roche)/50 ml, 5 µl RNase inhibitor (40 U)/50 ml). Imunoblot blot analysis was performed using α-AGO1 antibody (Agrisera) in 1:4000 dilution and α-rabbit IRdye800 secondary antibody (LI-COR, 1:3000 dilution). Protein signals were detected using Odyssey imaging system (LI-COR).

For small RNA isolation, 150 µl small RNA recovery buffer (100 mM Tris-HCl pH 7.5, 10 mM EDTA, 300 mM NaCl, 2% SDS, 1 µg/µl) was added to 450 µl wash buffer with beads and incubated at 65°C for 15 min. The mixture was then incubated with 450 µl water-saturated phenol for 2 min. Phenol was separated by centrifugation at 13,000 g. Once phenol/chloroform/isoamylalcohol and twice chloroform/isoamylalcohol steps were followed to remove the phenol. Small RNAs were recovered in 0.1x volume 3 M sodium acetate, 2.5x volume 96% ethanol, and 20 µg Glycogen (RNA grade) at -20°C overnight.

BcAGO IP

B. cinerea strains expressing 3xHA-BcAGO were grown in liquid HA media overnight. 5 g of fresh mycelia were homogenized by mortar and pestle and suspended in 20 ml extraction buffer according to the previous method (20 mM Tris-HCl pH7.5, 300 mM NaCl, 5 mM EDTA, 0.5% (v/v) NP-40, 5 mM DTT, 1 tablet cOmplete® protease inhibitor cocktail (Roche)/50 ml, 5 µl RNase inhibitor (40 U)/50 ml) (9). For infected tissue, 30 ml conidial suspension ($2x10^5$ spores/ml) in 1% malt extract was sprayed on 10 g detached leaves of six weeks old tomato plants using versatile sprayer. Infected leaf samples were collected at 2 days post inoculation and homogenized by mortar and pestle then suspended in 100 ml extraction buffer. The lysate was incubated on a vertical wheel and centrifuged for 40 min at 4°C. Mycelia debris was excluded by spinning down and filtered through Miracloth. EZview™ Red Anti-HA Affinity Gel (Merck) was used for BcAGO IP. Samples were incubated at 4°C for 1 h. Beads were pelleted down in a pre-cooled centrifuge at 200 × g and washed five times with Wash buffer (20 mM Tris-HCl pH7.5, 300 mM NaCl, 5 mM EDTA, 0.5% (v/v) Triton X-100, 5 mM DTT, 1 tablet cOmplete® protease inhibitor cocktail/50 ml, 5 µl RNase inhibitor (40 U)/50 ml). For immunoblot analysis, proteins were separated with 8% SDS-polyacrylamide gel at 80 volts for 30 min and 140 volts for 2 h and transferred to PVDF membrane (Immobilon-FL) overnight at 4°C. Transferred membranes were blocked with 10 ml of 5% (v/v) skim fat milk in 1× PBS at 4°C for 1 h on a rolling shaker. Membranes were then incubated overnight with primary α-HA antibody (3F10, Roche). The membranes were incubated with secondary antibody α-rat IRdye800 (LI-COR) 1 h. Protein signals were detected under Odyssey imaging system (LI-COR).

Small RNA sequencing analysis

Small RNA libraries were cloned following manufacturer's instructions (NEBNext Multiplex Small RNA Library Prep for Illumina) and sequenced on an Illumina HiSeq1500 platform.

From 20 µg total RNA extractions, small RNAs were size selected on a 15% polyacrylamide gel electrophoresis, as described previously (10). From BcAGO IP samples, RNA fractions were directly used for small RNA library cloning. Sequencing raw reads were demultiplexed, adapter-trimmed and quality-filtered (q=20). Small RNA

reads in the size range of 18-30 nt were considered for further analysis. Reads were mapped to the reference genome assemblies of *B. cinerea* strain B05.10 (Ensembl, ASM83294v1) or *S. lycopersicum* (accession Heintz SolGenomics Network, version SL4.0). This was performed using ShortStack3 (11) with unique weighting, which uses BOWTIE with zero mismatch (-v 1) as its alignment engine. Reference sequences of rRNA, tRNA, sn/snoRNA, mRNA, repeat RNA for tomato were downloaded from the SolGenomics Network FTP site, and for *B. cinerea* from the Ensembl FTP site. *B. cinerea* retrotransposon RNA reference sequences were used, as previously annotated (12). Small RNA read mapping against different RNA reference sequences was performed using BOWTIE2 (13). Raw read numbers were normalized to reads per million (RPM) to total read numbers mapped to the respective reference genome. Small RNA cross-kingdom target prediction was conducted with the TAPIR tool (14) using free energy ratio cut-off 0.7 and score cut-off 5.5. Furthermore, no gap, no three mismatches in a row and no two mismatches in a row in the seed region (2-12 nt) was permitted in the target alignment. Prediction of endogenous mRNA alignments for BcsRNAs was performed using GSTAr (https://github.com/MikeAxtell/GSTAr), which is based on RNAplex (15). These were filtered to include only targets which are 1) from an BcsRNA that is highly expressed (> 40 locus RPM), 2) to an mRNA which is induced in a specific Δ*bcago* mutant (p-value <= 0.1, L2FC > 0.58), and 3) from a BcsRNA that is either reduced in a specific Δ*bcago* mutant (p-value <= 0.1, L2FC < -0.58) or is frequently bound to an BcAGO via IP (> 30 RPM).

RNA in vitro cleavage assay

RNA *in vitro* cleavage was performed following the procedure as previous described (16). Recombinant BcAGO and GFP protein was generated using the Rosetta *Escherichia coli* strain and proteins were purified using the Ni Sepharose™ Excel system (Cytiva). Synthetic phosphorylated SlsRNA were purchased (Merck). mRNA target fragments were generated using the T7 RiboMAX^{TM} Express RNAi System (Promega). 100 nM recombinant AGO or GFP protein together with 100 nM SlsRNA and 40 U RiboLock RNase Inhibitor (Thermo Fisher Scientific) were incubated at 26°C for 90 min. Upon pre-incubation, 6 µg of target mRNA and 0.5 µg of yeast RNA were added to the reaction. The reaction was incubated at 26°C and stopped after 60 min.

References

1. N. Muller *et al.*, Investigations on VELVET regulatory mutants confirm the role of host tissue acidification and secretion of proteins in the pathogenesis of *Botrytis cinerea*. *New Phytol* **219**, 1062-1074 (2018).
2. G. Doehlemann, P. Berndt, M. Hahn, Different signalling pathways involving a Galpha protein, cAMP and a MAP kinase control germination of *Botrytis cinerea* conidia. *Mol Microbiol* **59**, 821-835 (2006).
3. U. Stein, Standardization of inoculation and incubation in testing new grapevine varieties for *Botrytis* resistance. *Applied Botany* **59**, 1-9 (1985).
4. M. G. Murray, W. F. Thompson, Rapid isolation of high molecular weight plant DNA. *Nucleic Acids Res* **8**, 4321-4325 (1980).
5. D. H. Chen, P. C. Ronald, A rapid DNA minipreparation method suitable for AFLP and other PCR applications. *Plant Molecular Biology Reporter* **17**, 53-57 (1999).
6. G. C. Allen, M. A. Flores-Vergara, S. Krasynanski, S. Kumar, W. F. Thompson, A modified protocol for rapid DNA isolation from plant tissues using cetyltrimethylammonium bromide. *Nat Protoc* **1**, 2320-2325 (2006).
7. K. J. Livak, T. D. Schmittgen, Analysis of relative gene expression data using real-time quantitative PCR and the 2(T)(-Delta Delta C) method. *Methods* **25**, 402-408 (2001).
8. E. Varkonyi-Gasic, R. Wu, M. Wood, E. F. Walton, R. P. Hellens, Protocol: a highly sensitive RT-PCR method for detection and quantification of microRNAs. *Plant Methods* **3**, 12 (2007).
9. F. Dunker, B. Lederer, A. Weiberg, Plant ARGONAUTE Protein Immunopurification for Pathogen Cross Kingdom Small RNA Analysis. *Bio Protoc* **11**, e3911 (2021).
10. A. Weiberg *et al.*, Fungal small RNAs suppress plant immunity by hijacking host RNA interference pathways. *Science* **342**, 118-123 (2013).
11. N. R. Johnson, J. M. Yeoh, C. Coruh, M. J. Axtell, Improved Placement of Multi-mapping Small RNAs. *G3 (Bethesda)* **6**, 2103-2111 (2016).
12. A. Porquier *et al.*, Retrotransposons as pathogenicity factors of the plant pathogenic fungus Botrytis cinerea. *Genome Biol* **22**, 225 (2021).
13. B. Langmead, S. L. Salzberg, Fast gapped-read alignment with Bowtie 2. *Nat Methods* **9**, 357-359 (2012).
14. E. Bonnet, Y. He, K. Billiau, Y. Van de Peer, TAPIR, a web server for the prediction of plant microRNA targets, including target mimics. *Bioinformatics* **26**, 1566-1568 (2010).
15. R. Lorenz *et al.*, ViennaRNA Package 2.0. *Algorithms Mol Biol* **6**, 26 (2011).
16. K. Miyoshi, H. Uejima, T. Nagami-Okada, H. Siomi, M. C. Siomi, In vitro RNA cleavage assay for Argonaute-family proteins. *Methods Mol Biol* **442**, 29-43 (2008).

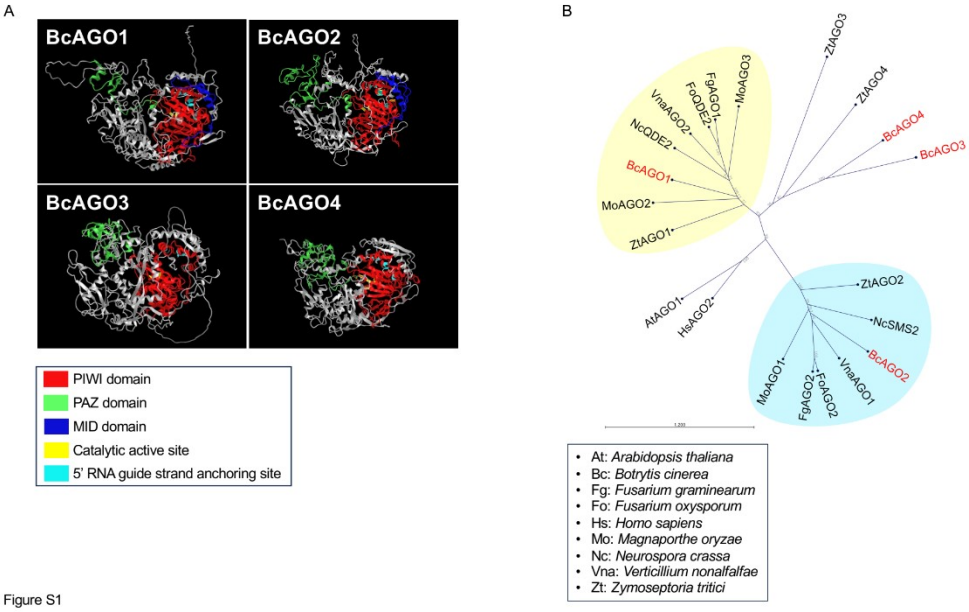

Figure S1

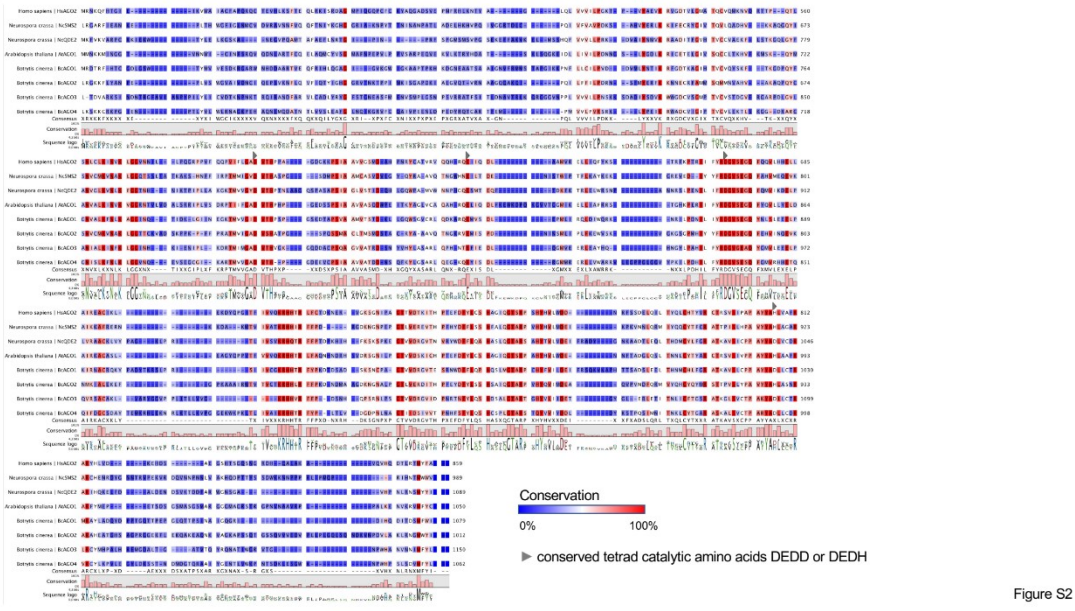

Figure S2

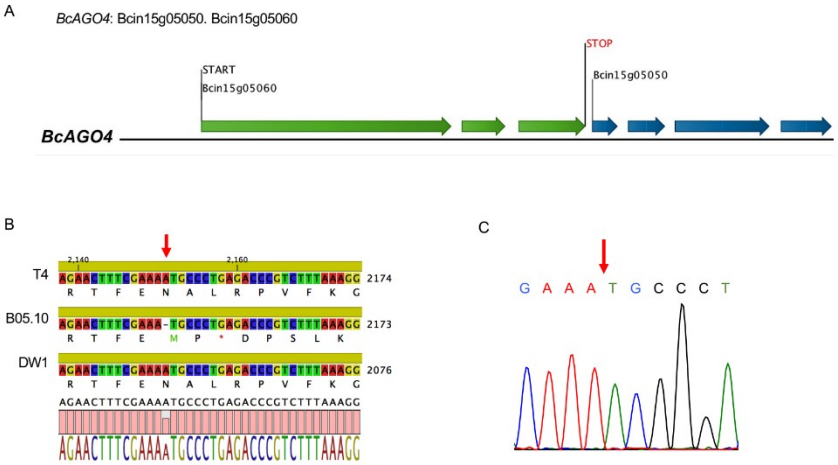

Figure S3

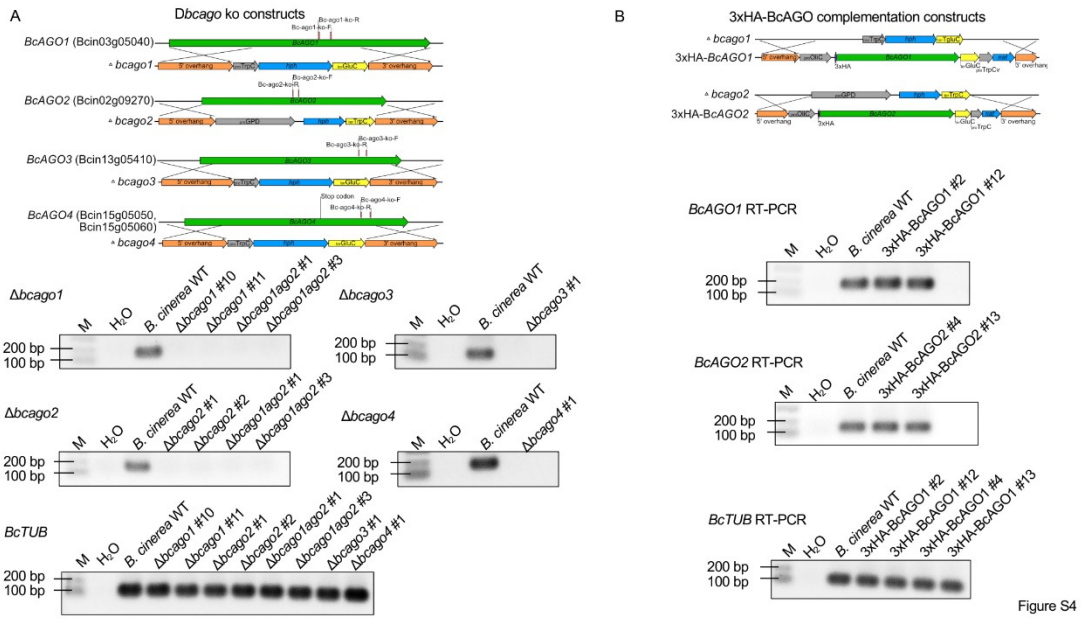

Figure S4

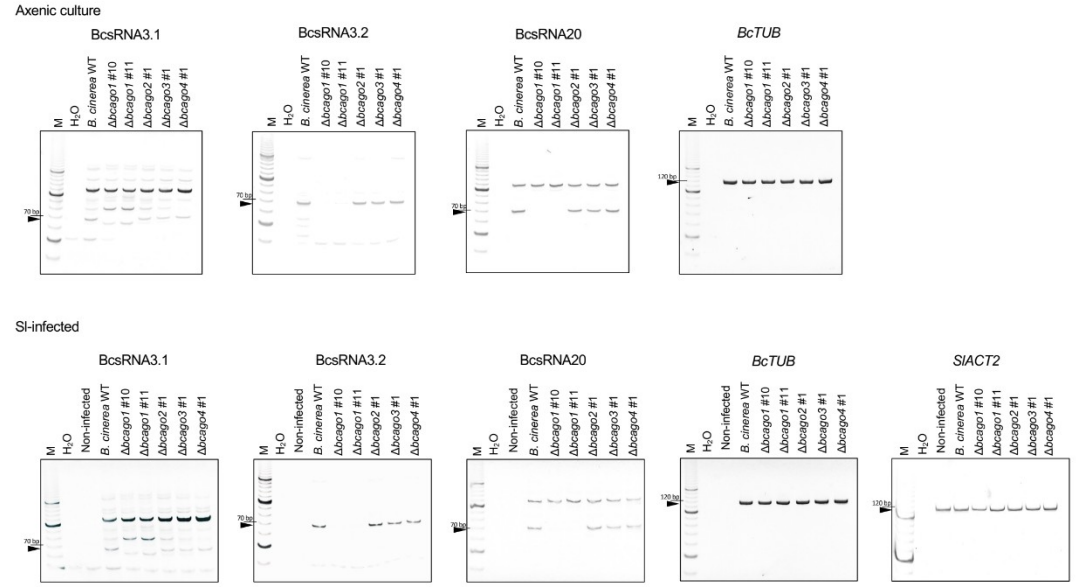

Figure S5

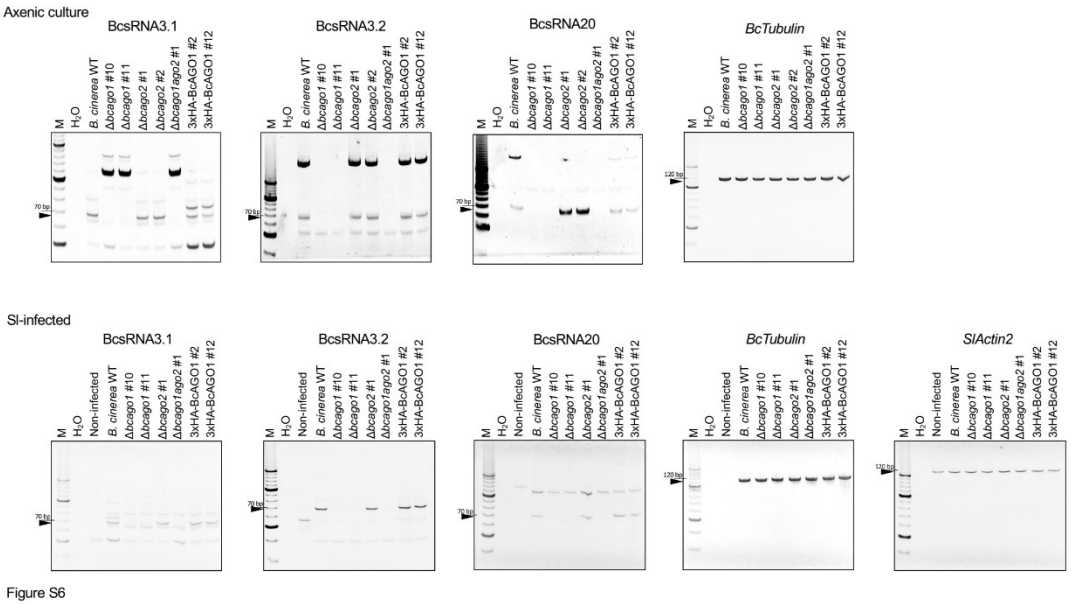

Figure S6

BcsRNA3.1 reverse transcription (RT) primer	GTCGTATCCAGTGCAGGGTCCGAGGTATTCGCACTGGATACGACGCCCAC
BcsRNA3.1 stem-loop PCR forward primer	GCGGCGGTTGTGGATCTTGTA
BcsRNA3.1 small RNA sequence	TTGTGGATCTTGTAGGTGGGC

Cloned sequences

GCGGCGGTTGTGGATCTTGTAGGTGTCGTATCCAGTGCGAATACCTCGGACCCTGCACTGGATAC	
GCGGCGGTTGTGGATCTTGTAGGTGTCGTATCCAGTGCGAATACCTCGGACCCTGCACTGGATAC	
GCGGCGGTTGTGGATCTTGTACTGGATACACCTCGGACCCTGCACTGGATAC	Dimer with self-annealed BcsRNA3.1 RT primer
GCGGCGGTTGTGGATCTTGTACTGGATACACCTCGGACCCTGCACTGGATAC	
GCGGCGGTTGTGGATCTTGTACTGGATACACCTCGGACCCTGCACTGGATAC	
GCGGCGGTTGTGGATCTTGTGGGCGTCGTACCAGTACGAATACCTCGGACCCTGCACTGGATAC	
GCGGCGGTTGTGGATCTTGTGGGCGTCGTACCAGTGCGAAT	
GCGGCGGTTGTGGATCTTGTGGGCGTCGTTCCAGTGCGAATACCTCGGACCCTGCACTGGATAC	Dimer with linear BcsRNA3.1 RT primer
GCGGCGGTTGTGGATCTTGTGGGCGTCGTATCCAGTGCGAATACCTCGGACCCTGCACTGGATAC	
GCGGCGGTTGTGGATCTTGTGGGCGTCGTATCCAGTGCGAATACCTCGGACCCTGCACTGGATAC	

Red: BcsRNA3.1 stem-loop PCR forward primer; Blue: BcsRNA3.1 stem-loop PCR forward primer

Figure S7

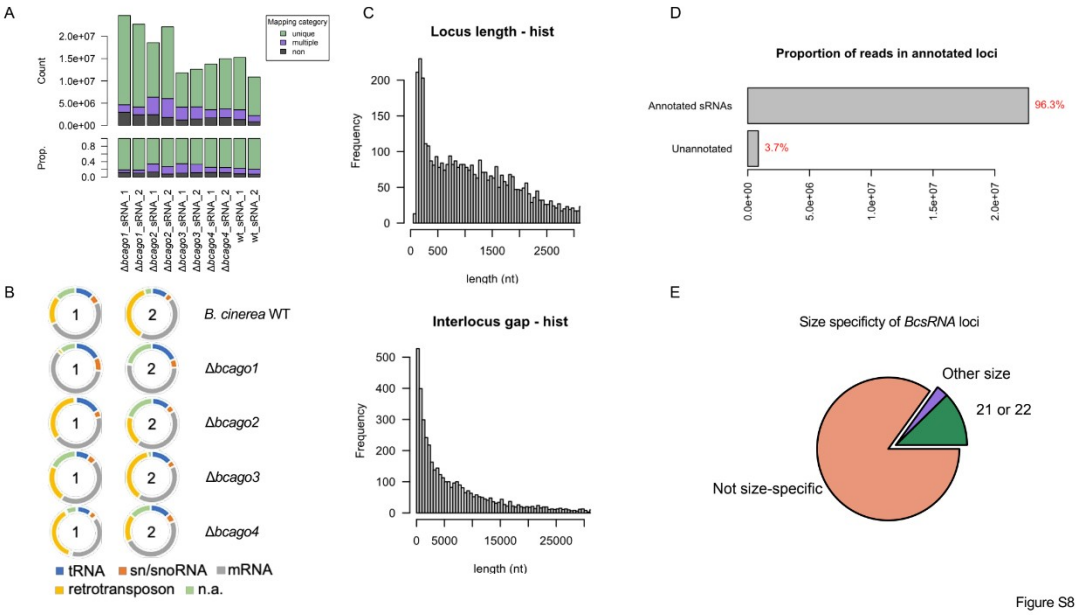

Figure S8

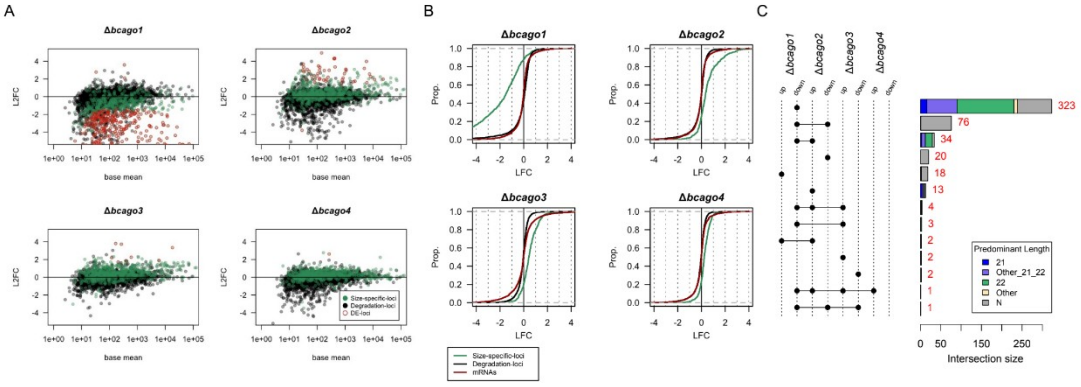

Figure S9

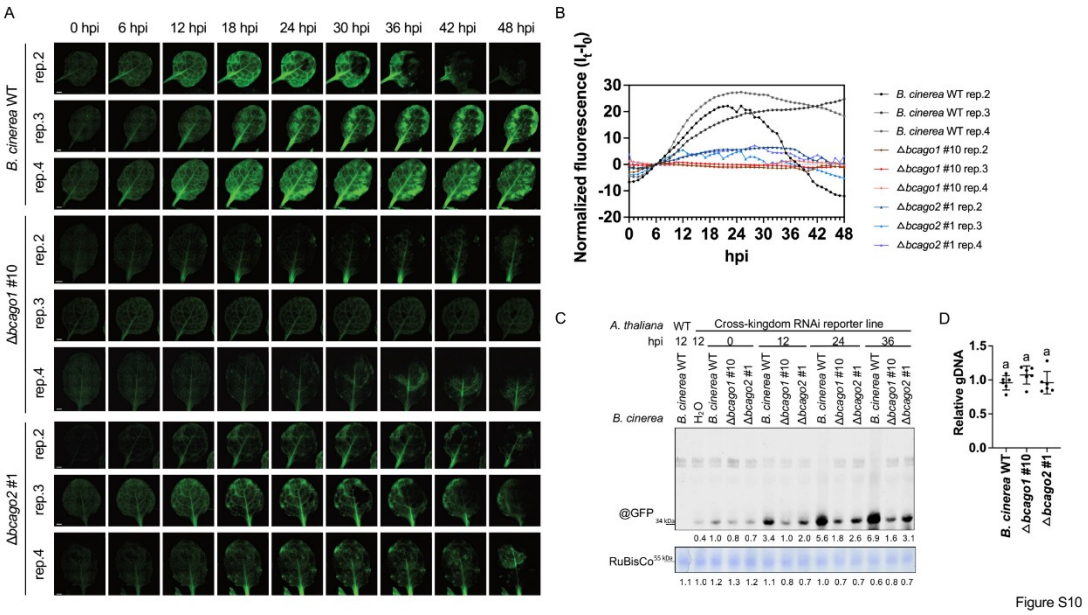

Figure S10

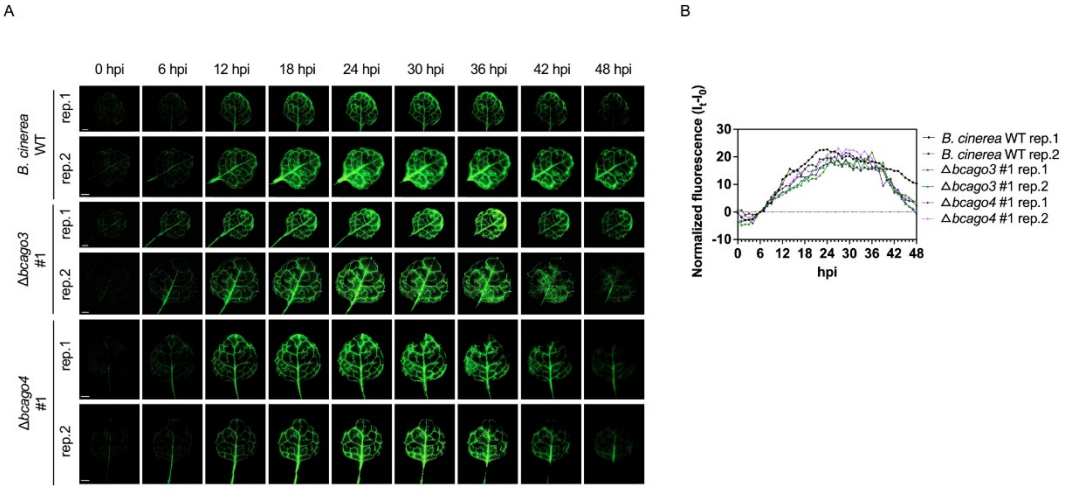

Figure S11

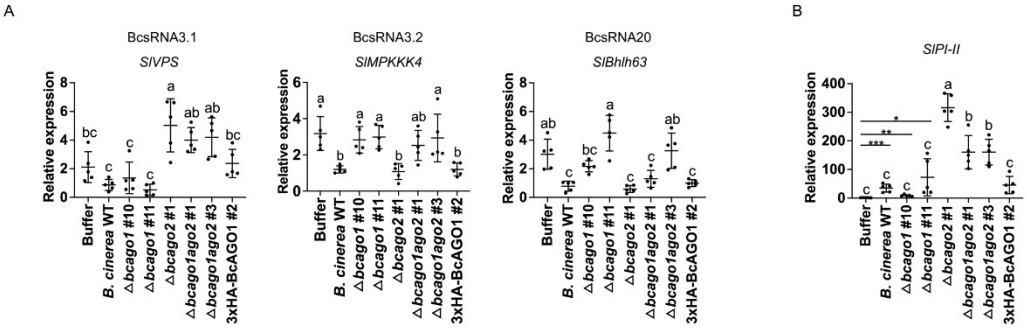

Figure S12

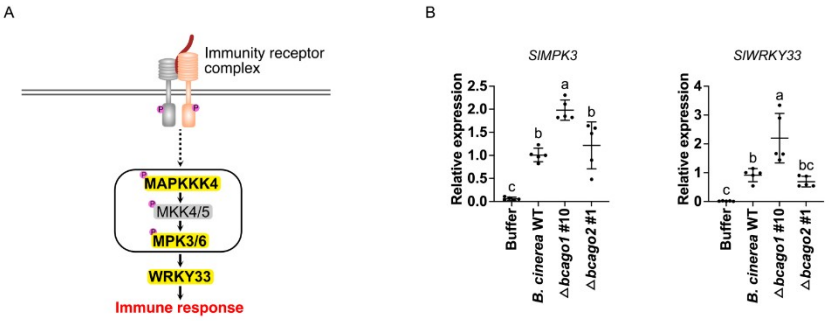

Figure S13

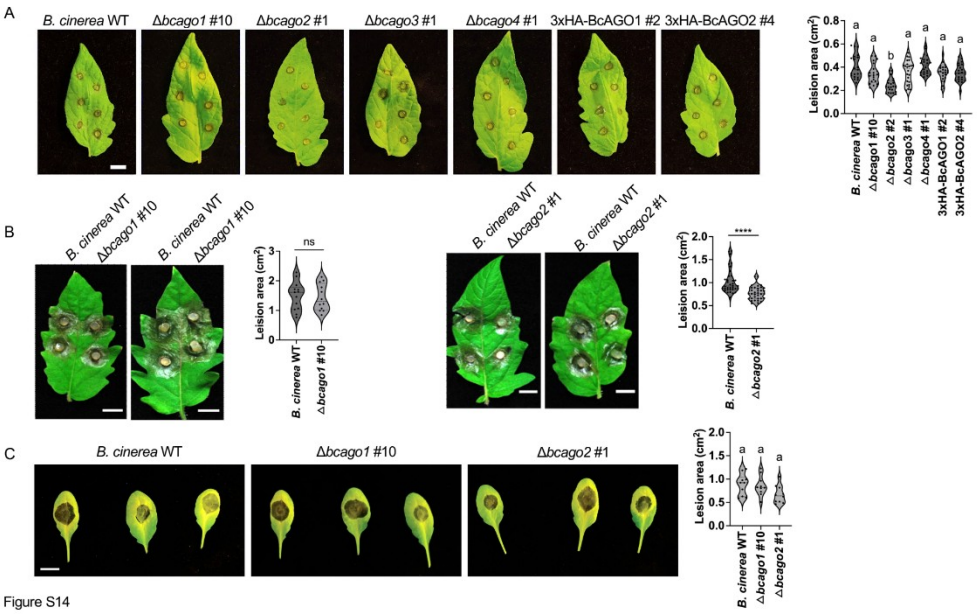

Figure S14

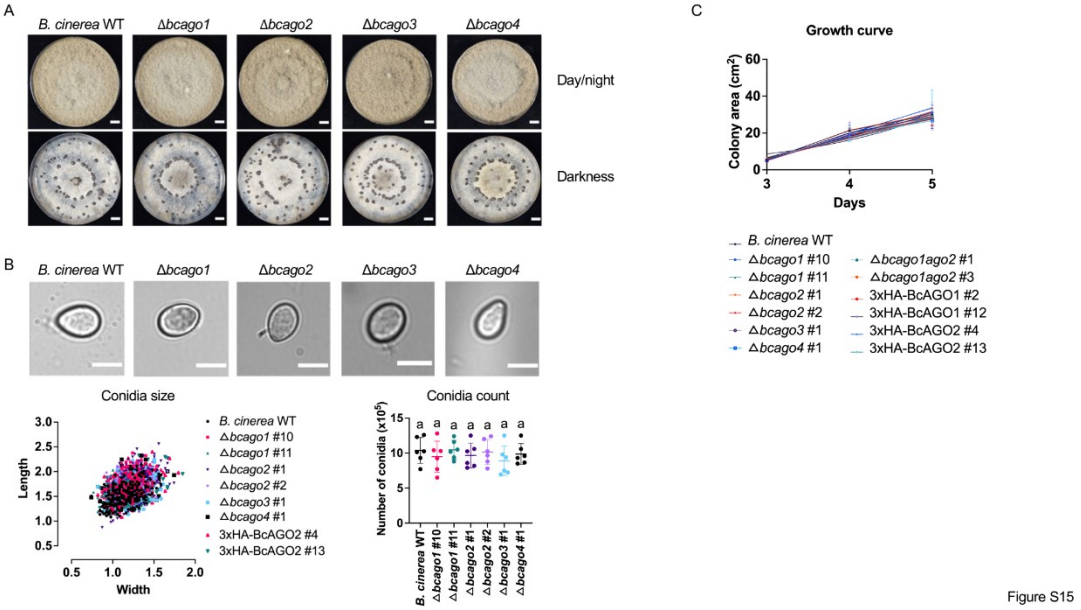

Figure S15

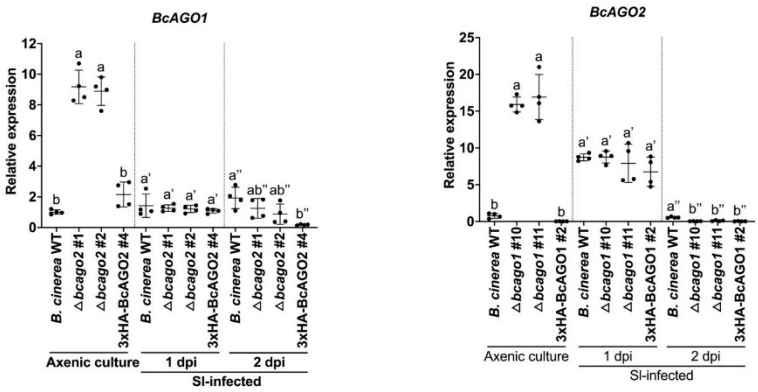

Figure S16

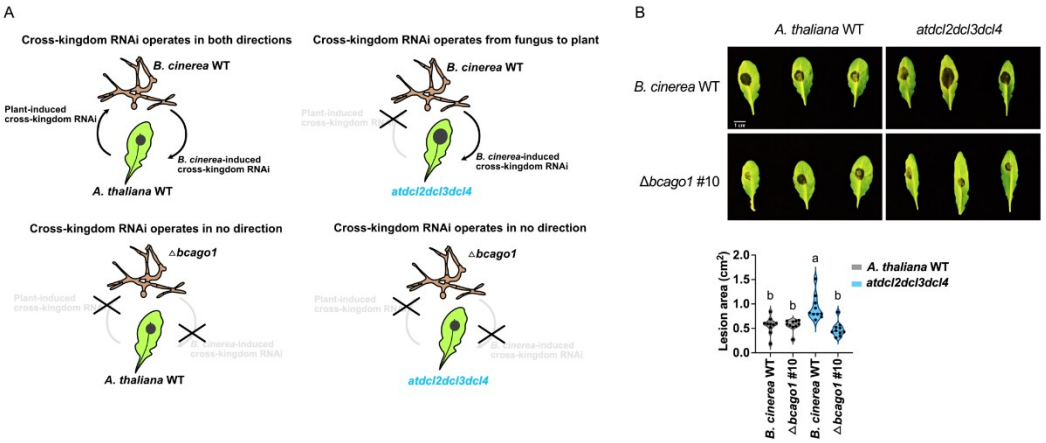

Figure S17

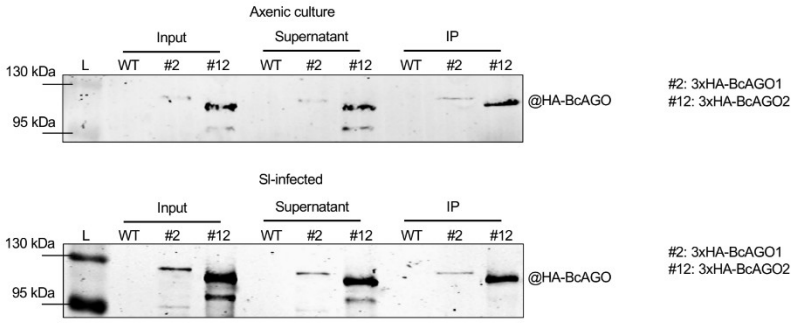

Figure S18

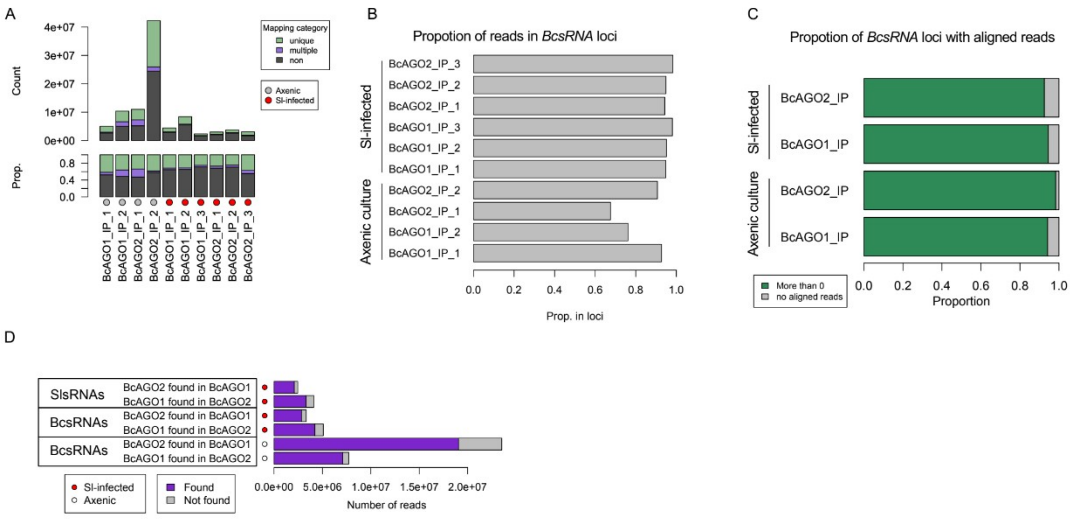

Figure S19

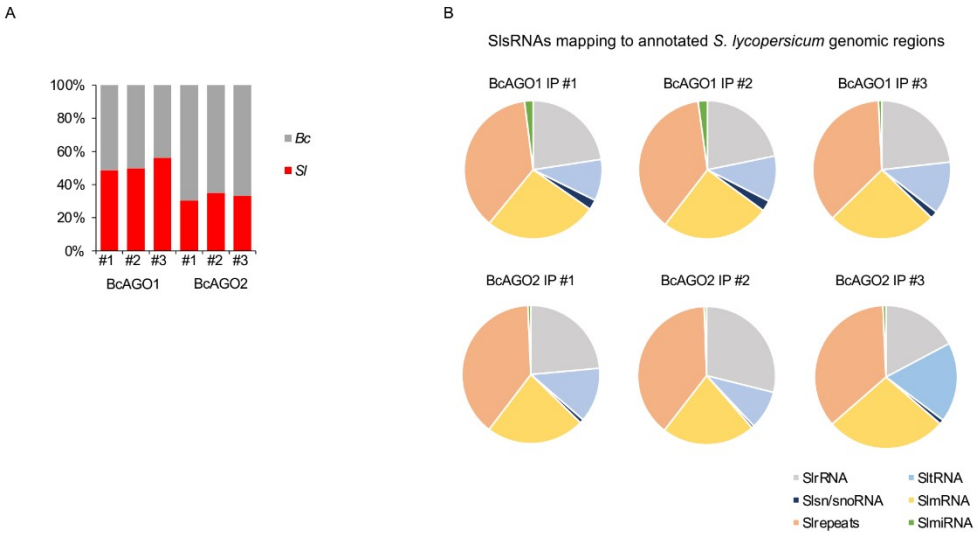

Figure S20

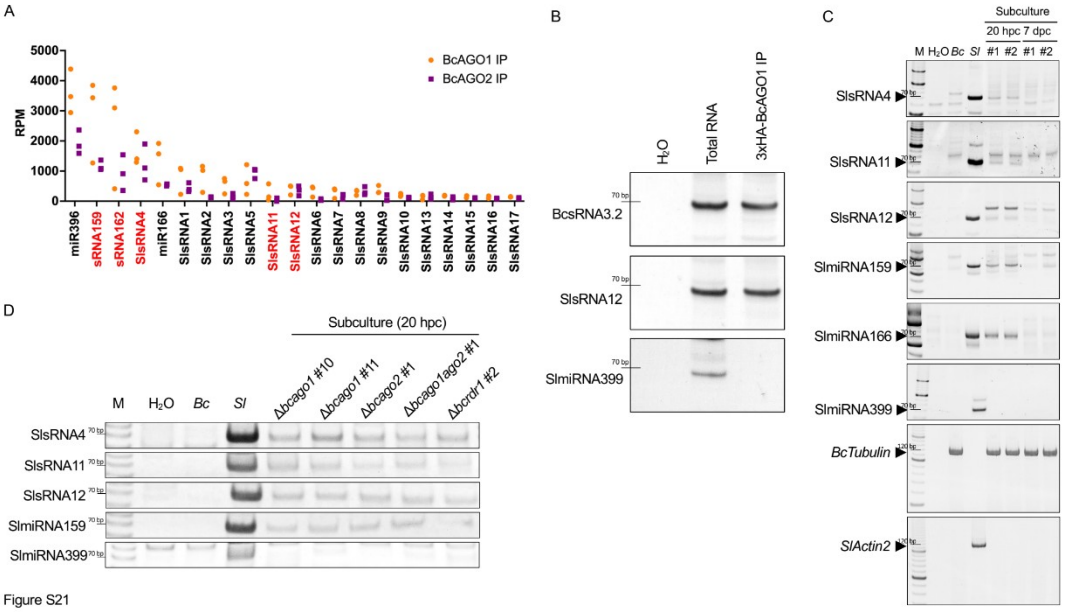

Figure S21

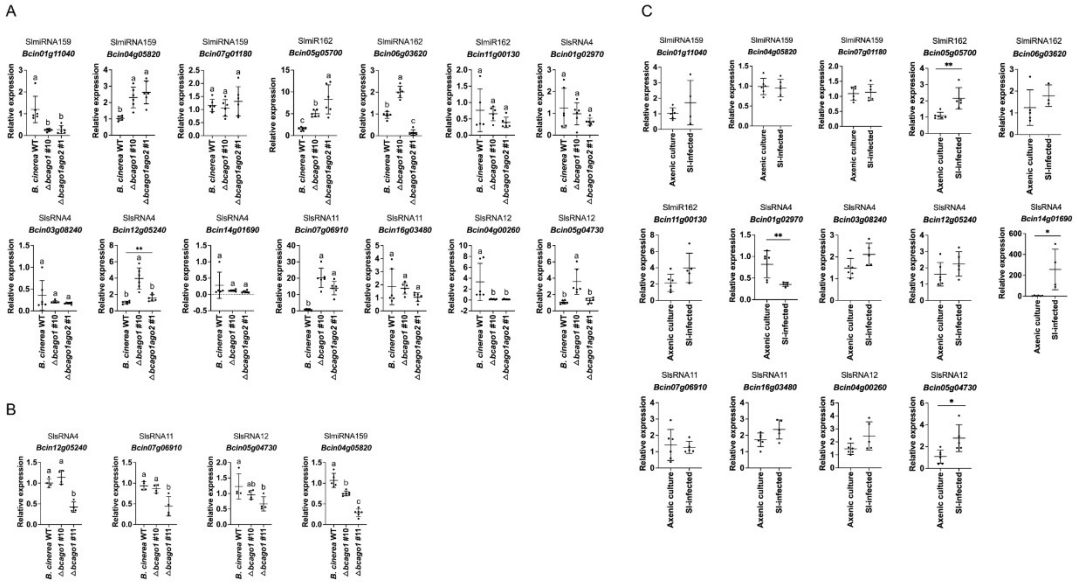

Figure S22

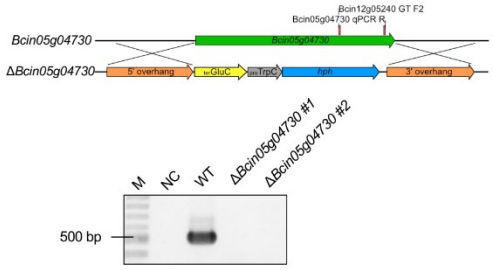

Figure S23

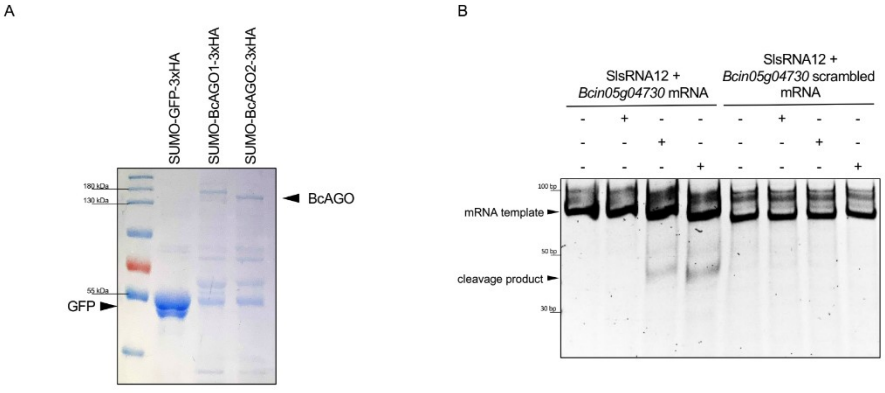

Figure S24

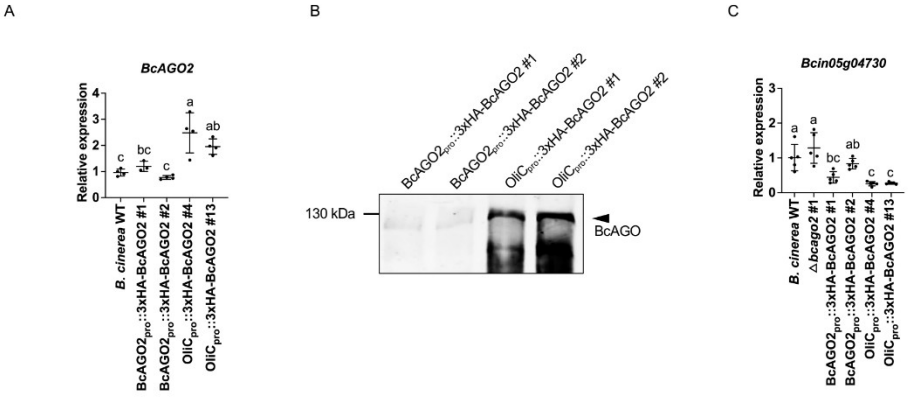
A
BcAGO2
Relative expression
4
3
2
1
0
c
bc
c
a
ab
B. cinerea WT
BcAGO2pro::3xHA-BcAGO2 #1
BcAGO2pro::3xHA-BcAGO2 #2
OliCpro::3xHA-BcAGO2 #4
OliCpro::3xHA-BcAGO2 #13
B
BcAGO2pro::3xHA-BcAGO2 #1
BcAGO2pro::3xHA-BcAGO2 #2
OliCpro::3xHA-BcAGO2 #1
OliCpro::3xHA-BcAGO2 #2
130 kDa
BcAGO
C
Bcin05g04730
Relative expression
3
2
1
0
a
a
bc
ab
c
c
B. cinerea WT
Δbcago2 #1
BcAGO2pro::3xHA-BcAGO2 #1
BcAGO2pro::3xHA-BcAGO2 #2
OliCpro::3xHA-BcAGO2 #4
OliCpro::3xHA-BcAGO2 #13

Figure S25

Supplementary data

Figure S1: Modular structure and phylogenetic relations of BcAGOs. A) Alphafold2 prediction of BcAGOs highlighting PIWI (red), PAZ (green), MID (blue) domains as well as catalytic center (yellow) and 5` small RNA guide strand anchoring site (magenta). B) Phylogenetic tree of different AGO proteins including the fungal species *Magnaporthe oryzae* (Mo), *Neurospora crassa* (Nc), *Fusarium oxysporum* (Fo), *B. cinerea* (Bc), the AGO1 of the plant species *Arabidopsis thaliana* (At), and AGO2 of *Homo sapiens* (Hs). Red area indicates the fungal RNAi quelling clade and blue area the MSUD clade. Numbers indicate bootstrapping values, and the bar represents the phylogenetic distance.

Figure S2: Amino acid sequence alignment of the MID-PIWI motif with BcAGOs. AGO MID-PIWI sequences are given for the fungal species *N. crassa* QDE2, *B. cinerea* BcAGO1, BcAGO2, BcAGO3, BcAGO4, the plant species *A. thaliana* AGO1 and the *Homo sapiens* AGO2. Grey arrow heads indicate the Alanine (D), Glutamic acid (E), D, Histidine (H) amino acids forming the catalytic tetrad within the PIWI domain.

Figure S3: Premature stop codon in the *BcAGO4* sequence. A) Exon/intron structure of the *BcAGO4* in the *B. cinerea* strain B05.10. *BcAGO4* is annotated into two genes, *Bcin15g05050* and *Bc15g05060*, as deposited at the Ensembl genome database. A premature stop codon (STOP) was found in the 3rd exon of the *BcAGO4*. B) DNA sequence alignment at the site of the premature stop codon comparing the *B. cinerea* strains B05.10, T4, and DW1. C) Sanger sequencing of the cloned *BcAGO4* gene confirming the premature stop codon in the strain B05.10. Red arrows in B) and C) indicate the premature stop codon position.

Figure S4: Genotyping of Δ*bcago* ko mutants and 3xHA-BcAGO complementation strains. A) Top, cloning strategy of Δ*bcago* ko cassettes including the positions of genotyping PCR primers. Bottom, PCR results of identified Δ*bcago* ko mutant strains. B) Top, cloning strategy of 3xHA-BcAGO gene complementation cassettes including the position of genotyping PCR primers. Bottom, RT-PCR results of identified 3xHA-BcAGO genetic complementation.

Figure S5: Stem-loop RT-PCR of BcsRNAs in Δ*bcago* mutants: Whole gel images of the stem-loop RT-PCR, according to Figure 1A.

Figure S6: Stem-loop RT-PCR of BcsRNAs in Δ*bcago* mutants and complementation strains. Stem-loop RT-PCR was performed including 3xHA-BcAGO complementation strains.

Figure S7: BcsRNA3.1 RT-PCR artifact in the Δ*bcago1* ko. Sanger sequencing of individual clones representing the lower BcsRNA3.1 PCR band in the Δ*bcago1* ko samples, as indicated in the Figure 1A, revealed no sequence relation to BcsRNA3.1.

Figure S8: Small RNA sequencing analysis of *B. cinerea* WT and Δ*bcago* ko mutants. A) Total read counts and proportional small RNA read numbers that mapped never, one or multiple times to the *B. cinerea* reference genome. B) Distribution of BcsRNAs that mapped to different annotated regions in the *B. cinerea* reference genome; tRNA: transfer RNA, sn/snoRNA: small nuclear/nucleolar RNA, mRNA: messenger RNA, RT: retrotransposon-associated RNA, n.a. not annotated. The number in the circle graphs indicate biological replicates. C) Distribution of the length in nucleotides for the 4,397 defined *BcsRNA* loci and the interlocus gaps. D) The proportion of BcsRNAs mapping to the defined *BcsRNA* loci. E) The proportion of 21-22 nt-, other size-, or no size-specific *BcsRNA* loci. C) - E) are based on a *B. cinerea* WT sequencing dataset.

Figure S9: Normalization of *BcsRNA* loci expression. A) Scatter plots showing differential expression of small RNA read counts at the 4,397 *BcsRNA* loci in the Δ*bcago* ko mutant samples. Points are colorized to show those which were specific for a BcsRNA size (green) or not size-specific (black), additionally showing differentially expressed loci with a red outline (padj <= 0.1, lfc >= 0.58). B) Proportion of log changefold factors considering small RNA (size-specific- or size-unspecific) or mRNA read counts in the Δ*bcago* ko mutant samples. C) Upset plot showing the size-specificity categories for differentially expressed *BcsRNA* loci in the Δ*bcago* ko mutant samples compared to *B. cinerea* WT.

Figure S10: GFP signal intensity in cross-kingdom RNAi reporter plant seedlings infected with Δ*bcago1* or Δ*bcago2*. A) Fluorescence microscopic images from GFP reporter plant seedlings infected with Δ*bcago1* or Δ*bcago2* at different time points representing independent inoculation experiments (rep.2-rep.4). The scale bars represent 1 mm. B) GFP quantification in infected seedling leaves from 0 – 48 hpi. For normalization, GFP fluorescence signal intensity at different time points (I_t) was

subtracted with the initial GFP signal intensity (I_0). C) Immunoblot analysis showing GFP expression in cross-kingdom RNAi reporter plants at four time points of *B. cinerea* infection using a @GFP antibody. RuBisCo signal detected by Coomassie Brilliant Blue (CBB) staining was used as a loading control. Numbers indicate GFP and RuBisCo signal intensities estimated by the FIJI software. D) *B. cinerea* genomic DNA was quantified in GFP reporter plant seedlings at 48 hpi by qRT-PCR. Data points represent biological replicates and error bars indicate the standard deviation. The letters indicate significant difference using one-way ANOVA and Tukey test with $p<0.05$.

Figure S11: GFP signal intensity in cross-kingdom RNAi reporter plant seedlings infected with Δ*bcago3* and Δ*bcago4.* A) Two biological replicates of fluorescence microscopy images from GFP reporter plant seedlings infected with Δ*bcago3* and Δ*bcago4* at different time points. The scale bars represent 1 mm. B) GFP quantification in infected seedling leaves from 0 – 48 hpi. For normalization, GFP fluorescence signal intensity at different time points (I_t) was subtracted with the initial GFP signal intensity (I_0).

Figure S12: Tomato mRNA expression of predicted target genes for BcsRNAs. A) Relative mRNA expression of known tomato target genes measured at 24 hpi by qRT-PCR. B) Relative mRNA expression level of the immunity marker gene *S. lycopersicum SI Proteinase Inhibitor (PI)-II*. In A-B), the tomato *SlActin2* was used as a housekeeping gene. Data points represent biological replicates and error bars indicate the standard deviation. The letters indicate significant difference using one-way ANOVA and Tukey test with $p<0.05$.

Figure S13: Tomato immune response upon infection with Δ*bcago* ko mutants. A) Schematic model of the MPKKK4-MPK3/6-WRKY33 immune signalling pathway. B) Relative mRNA expression of immunity genes *SlMPK3* and *SlWRKY33* was measured in Sl-infected samples at 24 hpi by qRT-PCR. Buffer treatment was used as a non-infected control sample. *SlActin2* was used as a housekeeping gene. Data points represent biological replicates. Error bars indicate the standard deviation of biological replicates. Letters indicate significant difference using one-way ANOVA and the Tukey test or the two-sided Students` t-test, respectively, with $p<0.05$.

Figure S14: Tomato infection assays with *B. cinerea* WT, Δ*bcago* ko mutants, and complementation strains. A) Spore drop inoculation method using 5x10exp4

conidia/ml and 6 times 10 microliter drops per leaf. Lesion area was measured at 48 hpi using the FIJI software. At least 21 lesions were measured per strain. Letters indicate significant difference using one-way ANOVA and the Tukey test with $p<0.05$. B) Agar plug inoculation placing 4 times agar plugs of the same size per leaf. Lesion area was measured at 48 hpi using the FIJI software. Error bars indicate the standard deviation and letters indicate significant difference using the two-sided Students` t-test with $p<0.05$. C) Spore drop inoculation method using 2x10exp5 conidia/ml and 20 microliter drops per leaf. Lesion area was measured at 72 hpi using the FIJI software. 10 lesions were measured per strain. Letters indicate no significant difference using one-way ANOVA and the Tukey test with $p<0.05$.

Figure S15: Growth, colony morphology, and development of *B. cinerea* WT, Δ*bcago* ko mutants, and complementation strains. A) Colony growth, morphology and sclerotia formation of *B. cinerea* strains under day/night light rhythm (top) or in constant dark (bottom). B) Shape and numbers of conidia of *B. cinerea* grown on complete HA agar medium. C) Time course of the colony area of *B. cinerea* strains grown on agar plates. Error bar indicates standard deviation of three biological replicates.

Figure S16: Gene expression of BcAGO1 and BcAGO2 in the Δ*bcago* ko mutant background.

Relative mRNA expression of *BcAGO*s in axenic culture or in SI-infected samples at 24 or 48 hpi measured by qRT-PCR. *B. cinerea BcTubulin* was used as a housekeeping gene. Data points represent biological replicates and error bars indicate the standard deviation. The letters indicate significant difference using one-way ANOVA and Tukey test with $p<0.05$.

Figure S17: *A. thaliana* infection assays with *B. cinerea* WT and Δ*bcago1*. A) Scenarios of functional or blocked bidirectional cross-kingdom RNAi and expected infection outcome. B) Lesion area analysis of *A. thaliana* WT and *atdcl2dcl3dcl4* mutants upon infection with *B. cinerea* WT or Δ*bcago1* ko mutant was measured at 72 hpi in at least 10 leaves per genotype combination. Scale bar represents 1 cm. Letters indicate significant difference using one-way ANOVA and the Tukey test with $p<0.05$.

Figure S18: BcAGO IP immunoblot analysis. Immunoblot analysis of 3xHA-BcAGO1 and 3xHA-BcAGO2 IP from axenic culture and SI-infected samples using

anti-HA antibody-coated beads. PL: protein ladder, WT: *B. cinerea* WT strains, #2: 3xHA-BcAGO1 strains, #12: 3xBcAGO2 strain.

Figure S19: Read depth and *BcsRNA* loci coverage of BcAGO IP samples. A) Total counts and proportional small RNA read numbers mapped never, one, or multiple times to the *B. cinerea* reference genome. B) Proportion of small RNAs mapping to *BcsRNA* loci. C) Total proportion of *BcsRNA* loci which have reads mapping to them from the BcAGO IP samples. D) Numbers of BcsRNA or SlsRNA reads bound to an BcAGO which were also bound to a different BcAGO in the same conditions.

Figure S20: Numbers and origin of SlsRNAs binding to BcAGOs during infection. A) Relative BcsRNA and SlsRNA fractions binding to BcAGO1 or BcAGO2 in Sl-infected samples in three biological replicates (#). B) Origins of BcAGO1 or BcAGO2-bound SlsRNAs based on annotated regions in the tomato (*S. lycopersicum*) genome; SlrRNA: ribosomal RNA, Slsn(o)RNA: small nuclear and nucleolar RNA, Slrepeats: repeat-associated RNA, SltRNA: transfer RNA, SlmRNA: messenger RNA, SlmiRNA: microRNA. Pie charts show distribution of SlsRNAs in three biological replicates (#1, #2, #3).

Figure S21: Accumulation of BcAGO-bound SlsRNAs in *B. cinerea* WT and Δ*bcago* ko mutants. A) Normalized read numbers (RPM) of the most abundant SlsRNAs bound to BcAGO1 and BcAGO2. B) Stem-loop RT-PCR of BcsRNA3.2 and SlsRNA12 from Sl-infected samples using total RNA or RNA upon BcAGO1 IP. SlmiR399 was used as an internal control that did not bind to BcAGO1.C) Whole gel images of SlsRNA stem-loop RT-PCRs, according to Figure 5C. D) Stem-loop RT-PCR of SlsRNAs from re-isolated *B. cinerea* Δ*bcago* ko mutant samples. Re-isolated mycelium of *B. cinerea* was grown for 20 hours on agar plates when RNA was isolated for analysis. The SlmiR399 served as a negative control, as it was never detected in the BcAGO IP small RNA-seq datasets. *Bc* represented RNA samples collected from *B. cinerea* that was not re-isolated from infected tomato, and *Sl* samples were collected from non-infected tomato.

Figure S22: *B. cinerea* mRNA expression of predicted target genes for SlsRNAs. A) Relative mRNA expression was measured in Sl-infected samples at 48 hpi by qRT-PCR and was compared between *B. cinerea* WT, Δ*bcago1* and Δ*bcago1ago2* ko mutant strains. Relative mRNA expression was measured in axenic cultures samples

by qRT-PCR. C) Relative mRNA expression was measured in *B. cinerea* WT comparing axenic culture and Sl-infected samples at 48 hpi by qRT-PCR. In A-C), *BcActin* was used as a housekeeping gene. Data points represent biological replicates. Error bars indicate the standard deviation of biological replicates. Letters and asterisks indicate significant difference using one-way ANOVA and the Tukey test or the two-sided Students` t-test, respectively, with $p<0.05$.

Figure S23: Generation of Δ*Bcin05g04730* ko mutants. Top, cloning strategy of ko cassette including the positions of genotyping PCR primers. Bottom, genotyping PCR of two identified ko mutant strains.

Figure S24: *In vitro Bcin05g04730* RNA cleavage. A) SDS-PAGE of total purified recombinant BcAGO or GFP protein. Gel was stained with Coomassie Brilliant Blue. B) Polyacrylamide gel electrophoresis image upon ethidium bromide staining of the *Bcin05g04730* RNA cleavage assay. Arrows indicate template RNA and cleavage products.

Figure S25: BcAGO2 overexpression led to *Bcin05g04730* suppression. A) *BcAGO2* mRNA expression level in *B. cinerea* WT and a Δ*bcago2* ko mutant complemented with either native $BcAGO2_{pro}$-3xHA-BcAGO2 or overexpressing $OliC_{pro}$-3xHA-BcAGO2. # indicates individual complementation strains. B) Immunoblot analysis of $BcAGO2_{pro}$-3xHA-BcAGO2 and $OliC_{pro}$-3xHA-BcAGO2 strains using an anti-HA antibody. C) *Bcin05g04730 mRNA* expression analysis during tomato infection comparing *B. cinerea* WT, Δ*bcago2*, and $BcAGO2_{pro}$-3xHA-BcAGO2 or $OliC_{pro}$-3xHA-BcAGO2 complementation strains.

Discussion

This thesis investigates the molecular mechanisms of cross-kingdom RNA interference (ckRNAi) interaction between the necrotrophic fungal pathogen *Botrytis cinerea* and its plant hosts. According to the two complementary studies, I elucidated the distinct and cooperative roles of fungal RNA interference components, specifically RNA-dependent RNA polymerase 1 (BcRDR1) and Argonaute proteins (BcAGO1 and BcAGO2), in facilitating pathogenicity through small RNA (sRNA)-mediated gene silencing across species. These findings contribute substantially to the understanding of fungal virulence strategies and establish ckRNAi as a central mechanism of pathogenic success of *B. cinerea (Cheng et al., 2025; Cheng et al., 2023b)*.

Botrytis RDR1 serves as a central regulator of small RNA biogenesis and pathogenicity

The RNA interference (RNAi) pathway plays a fundamental role in regulating gene expression and maintaining genomic stability in eukaryotes. Across a variety of fungal species, RNAi has been involved in the silencing of transposable elements, defense against viruses, and developmental regulation (Dang *et al.*, 2011; Nicolás & Garre, 2017). However, in plant pathogenic fungi, the role of RDRs in virulence remained unknown until recent discoveries demonstrated that pathogens exploit sRNAs for cross-kingdom communication. *Botrytis cinerea* is one of the best models for studying these interactions due to its ability to infect a broad range of plant species and to produce sRNAs that target host immunity genes (Weiberg *et al.*, 2013).

The identification of BcRDR1 as a key component in cross-kingdom communication was a substantial breakthrough. My work pointed out that *bcrdr1* knockout mutants were not only deficient in producing key classes of *Botrytis* small RNAs but also showed a reduction in virulence. This finding builds on and expands on previous studies on RDRs in fungi, such as SAD-1 in *Neurospora crassa*, which is involved in meiotic silencing of unpaired DNA, and QDE-1, which regulates transgene-induced gene silencing (Catalanotto *et al.*, 2002; Shiu *et al.*, 2001). In contrast to these more traditional roles in endogenous genome defense, BcRDR1 functions at the host-pathogen interface, converting retrotransposon transcripts into double-

stranded RNA (dsRNA) precursors for small interfering RNAs (siRNAs) that target host transcripts.

The sRNA sequencing results revealed that BcRDR1 mainly governs the generation of 21–22 nt sRNAs, especially those with a 5' uracil bias, a signature feature of functional siRNAs that are preferentially loaded into Argonaute proteins (Mi *et al.*, 2008). This complements findings from Weiberg *et al.* (2013), which showed that such sRNAs from *B. cinerea* target host genes like *MPK1* and *WAK*, impairing plant defense signaling pathway. Notably, in the absence of BcRDR1, these key virulence-associated sRNAs are drastically depleted, and target gene silencing is abolished, confirming the upstream roles of BcRDR1 in ckRNAi.

Functionally, these fungal siRNAs hijack the host RNAi machinery by loading into host AGO1. They form RNA-induced silencing complexes (RISCs) that cleave the plant immunity-related mRNAs. Our GFP-based switch-on reporter system, adapted from earlier work with *Hyaloperonospora arabidopsidis,* offered a powerful visual tool to monitor this interaction in vivo (Dunker *et al.*, 2020). In plants infected with *B. cinerea* WT, GFP expression was strongly activated, whereas in *bcrdr1* mutants, this activation was absent. The reporter plants provided direct evidence that BcRDR1-generated sRNAs are necessary for effective ckRNAi in real-time.

The findings extend to the epigenetic regulation of retrotransposons within the fungal genome. Previous study showed RDRs act to silence transposons in many species (Ghildiyal & Zamore, 2009), in *B. cinerea* these elements are additionally function as a source of sRNAs to target the host genes. This improves our understanding of transposon utility, aligning with evolutionary models that posit the co-option of mobile genetic elements in host-pathogen co-evolution.

My results on the other hand highlighted the potential of BcRDR1 for disease control. Transgenic Arabidopsis plants expressing STTMs (short tandem target mimics) were found to be effectively neutralizing *Botrytis* sRNAs, resulting in the de-silenced of host immunity genes and reduced fungal colonization. This approach was first validated in plants for endogenous microRNA knockdown and evolved into a strategy for pathogen resistance validation (Cai *et al.*, 2018b; Tang *et al.*, 2012). The capacities of BcRDR1 to biosynthesize pathogenic sRNA, coupled with its non-essential role in vegetative growth, makes it a high-value target for future host induced gene silencing-based studies.

To conclude, my study identified BcRDR1 as a central node in the ckRNAi pathway of *B. cinerea*. BcRDR1 is involved in the production of sRNAs from transposons which silence host immune response genes. My study provides new insights between plants and pathogens and identifies practical potentials for controlling disease.

Functional diversification of *Botrytis* Argonautes in bidirectional cross-kingdom RNAi

Apart from BcRDR1 that initiates small RNA biogenesis, the delivery and functionality of these small RNAs depend critically on AGO proteins in both fungal and plant systems. My study present detailed functional analyses of the AGO proteins in *B. cinerea*, particularly BcAGO1 and BcAGO2, demonstrating their distinct but complementary roles in ckRNAi during plant infection. I found that BcAGO1 primarily promotes sRNA stabilization and loading within the fungal cytoplasm, consistent with typical AGO functions seen in other eukaryotes. For instance, AGO1 in *Neurospora crassa* (QDE-2), is essential for quelling and transgene-induced RNAi (Catalanotto *et al.*, 2002). I discovered BcAGO1 facilitates 21–22 nt small RNAs accumulation, which many of which are derived from transposons. Interestingly, although these functional small RNAs were drastically reduced in *bcago1* mutants, they did not exhibit reduced virulence. This indicates that fungal sRNA accumulation, may not be the only factor for pathogenicity.

On the other hand, BcAGO2 appears to be specifically responsible for the translocation of small RNAs. My study showed that although *bcago2* mutants maintained a normal sRNA profile, they were significantly reduced in virulence and were unable to trigger our GFP reporter plants as well as WT. The results showed that Bc-sRNAs have difficulties being loaded into tomato AGO1 in the absence of BcAGO2, indicating that BcAGO2 is essential for the delivery of fungal sRNAs into the host AGO/RISC complex. This supports findings in *Magnaporthe oryzae*, where AGO3 is involved in small RNA export and targeting to host components (Raman *et al.*, 2017).

BcAGO2 as a virulence factor may reflect an AGO evolution among fungal pathogens for infection. While the majority of the AGO functions are intracellular silencing and stabilization, certain members, such as BcAGO2, have evolved to directly mediate host-pathogen communication. This difference was confirmed by phylogenetic analysis, which assigned

BcAGO1 to a repression-related clade, whereas BcAGO2 was consistent with AGOs involved in the meiotic silencing process (Cheng *et al.*, 2025; Shiu *et al.*, 2001).

Importantly, my infection assays showed that *bcago2* mutants produced smaller lesions and reduced fungal biomass, revealing the impact of sRNA delivery on disease progression. Furthermore, while *bcago1* mutants failed to accumulate specific virulence-associated Bc-sRNAs (e.g., BcsRNA3.1, BcsRNA3.2 and BcsRNA20), *bcago2* mutants failed to translocate them into the host. This resulted in the silencing of target genes such as *SlMPKKK4* and *SlVPS*, which are central to defense signalling and vacuolar trafficking (Wang *et al.*, 2016; Weiberg *et al.*, 2013).

The discovery of the bidirectional sRNA communication is not unique to *B. cinerea*. Recent study in *Fusarium oxysporum* demonstrated the uptake of host-derived miRNAs which silenced fungal virulence factors (Zhou *et al.*, 2022). Similarly, report showed *plants* send sRNAs through extracellular vesicles to silence target fungal mRNAs, which are mediated by *Botrytis* AGOs (Cai *et al.*, 2018b). Together, these studies suggest that AGOs play a key role not only in intracellular silencing but also in ckRNAi.

Furthermore, BcAGOs appear to be limited in functional redundancy. Interestingly, we found BcAGO4 contains a premature stop codon in the B05.10 strain, which may reflect strain-specific evolution or pseudogenization. This genetic variation can be further explored to understand the evolutionary pressures on AGO diversification in pathogenic fungi.

In summary, my study shows the functional differences of fungal AGOs in ckRNAi. BcAGO1 promotes sRNA biogenesis and stabilization within fungal cells, whereas BcAGO2 acts downstream to mediate sRNA translocation and host gene silencing. BcAGO1 and BcAGO2 form a coordinated system that helps *B. cinerea* suppress plant immunity and enhance colonization. My study expands the understanding of ckRNAi and highlights the potential of targeting Argonautes to treat fungal diseases.

Implications for host immunity and cross-kingdom communication

My studies identified BcRDR1, BcAGO1, and BcAGO2 as components of the fungal ckRNAi machinery. I not only revealed the intracellular regulation in *B. cinerea* but also highlighted the

molecular interactions with its plant host. The interaction is mediated through the bidirectional movement and functional activities of small RNAs. The findings in my two papers build on the growing number of literatures, showing that hosts and pathogens exchange RNA-based signals that affect host-pathogen dynamics. These findings confirm that *B. cinerea* delivers fungal sRNAs into host plant cells, where they hijack host RNAi machinery to silence defense-related genes. We believe this is a targeted manipulation that results in the suppression of plant immune pathways. In tomato, genes such as *SlMPKKK4*, *SlVPS*, and *SlBhlh63* are downregulated after infection with wild-type *B. cinerea*. The missing suppression in *bcago2* and *bcrdr1* mutants emphasizes the pathogen's reliance on its own RNAi machinery for successful infection (Cheng *et al.*, 2025; Cheng *et al.*, 2023b).

The phenomenon of cross-kingdom gene silencing is not unique to *Botrytis*. It has been demonstrated that analogous patterns have been observed in other pathosystem. *Fusarium graminearum* has been observed to deliver a specific sRNA into wheat, thereby targeting a resistance-related gene (Jian & Liang, 2019). In contrast, *Sclerotinia sclerotiorum* has been demonstrated to induce host miRNAs, leading to their misregulation and facilitating infection (Derbyshire *et al.*, 2019). In contrast, plants do not merely passively receive these interactions. Recent studies have demonstrated that both Arabidopsis and cotton secrete extracellular vesicles (EVs) containing endogenous small RNAs (sRNAs) into fungal pathogens such as *Verticillium dahliae*. These EVs have been found to target fungal virulence genes and suppress infection (Cai *et al.*, 2018b; Zhang *et al.*, 2022).

Cross-kingdom communication is an exciting new frontier. It opens the door to a new layer of host-pathogen co-evolution. It is indeed surprising that both pathogens and hosts engage in a molecular dialogue mediated by mobile sRNAs. The host's ability to produce and export antifungal sRNAs constitutes a layer of innate immunity. In contrast, pathogens have the ability to evolve mechanisms to deliver and protect their own sRNAs during infection. This interaction exerts strong selective pressure on both partners, influencing the evolution of RDR and AGO proteins, RNA loading preference, and even EV biogenesis.

Traditionally, plant defense has been studied conceptually through the lens of recognition (PAMP-triggered immunity and effector-triggered immunity) and response (reactive oxygen species, pathogenesis-associated proteins). The role of RNA-based regulation has introduced a new category, sRNA-mediated immunity, in which gene silencing is not just a downstream

effect but also a front-line defense and offense strategy. This development reveals new prospects for disease resistance engineering beyond the traditional paradigms that rely on R genes or chemical interventions.

In my study, I showed that plants expressing STTM, which is designed to reduce the impact of fungal sRNAs, exhibited less disease symptoms. The phenotypes validate the importance of certain Bc-sRNAs in virulence and suggest that resistance can be engineered by disabling the pathogen from suppressing host immunity. Similarly, it is possible that targeting BcAGO2 through host-induced gene silencing (HIGS) could defect sRNA delivery, making pathogens unable to suppress host genes even when the pathogen sRNAs are present. The strategy could be extended to target conserved AGO or RDR components in multiple fungal pathogens, which could potentially lead to broad-spectrum of plant resistance.

From a practical standpoint, the translation of these findings into crop improvement must contend with delivery efficiency, expression stability, and regulatory considerations. The use of endogenous plant promoters, tissue-specific expression systems, or synthetic biology approaches could improve the specificity and efficacy of sRNA-based resistance. Furthermore, environmental RNAi (exogenously applied RNA molecules) provides a non-genetic approach for RNA-based plant protection. Spraying of double-stranded RNAs has been successfully demonstrated against *Botrytis cinerea* and *Fusarium graminearum*, thereby reducing infection severity (Cai *et al.*, 2018a; Koch *et al.*, 2016; Wang *et al.*, 2016).

It is interesting to note that the evolutionary convergence in sRNA transport between pathogens and hosts suggests the presence of conserved transport mechanisms. It is believed that EVs could be prime candidates. Recent studies in plant biology have identified tetraspanin-like proteins and PATELLIN proteins as important mediators of vesicle formation and RNA cargo loading (Cai *et al.*, 2018b; Rutter & Innes, 2017). It would be interesting to know whether *B. cinerea* and other fungi use similar systems and, if so, whether these systems could be targeted to block sRNA export or import.

For the ecological and evolutionary aspects, RNA trafficking has a dual impact: it influences the outcome of a single infection and affects interactions within the wider microbiota. For example, plants colonized by beneficial microorganisms may modulate their sRNA output to selectively suppress pathogens while maintaining symbiosis. Additionally, pathogens may

evolve strategies to intercept or degrade host sRNAs, similar to the case with viral RNAi inhibitors in animal and plant system.

In conclusion, the impact of cross-kingdom RNA interference goes way beyond molecular plant pathology. They challenge long-standing assumptions about how genes are controlled, redefine the relationship between host and pathogen, and provide new ways to protect crops. The results of my doctoral study show that sRNA-based communication is an important and useful part of how plants and microbes interact. This has applications in agriculture, biotechnology and basic science.

Potential and Future Directions

The project in this thesis breaks new ground for translational applications in permaculture by exploiting the molecular mechanism of cross-kingdom RNA interference (ckRNAi). The identification and characterization of fungal RNAi components, including BcRDR1, BcAGO1, and BcAGO2 strengthen our understanding of the mechanisms of host-pathogen communication. They also provide a potential avenue for disease management that differs from traditional pesticides and transgenic resistance genes.

One of the developed strategies is host-induced gene silencing (HIGS), a technique that using transgenic plants to express double-stranded RNA (dsRNA) which target specific pathogen genes. HIGS has been shown to successfully silence fungal effectors in *Fusarium graminearum*, *Verticillium dahliae* and *Blumeria graminis* (Koch *et al.*, 2013; Nowara *et al.*, 2010; Song & Thomma, 2018). In my study, transgenic Arabidopsis expressing STTM in sequestering Bc-sRNA and reducing *B. cinerea* virulence suggests that HIGS can be adapted to specifically disrupt the ckRNAi pathway. Targeting genes such as *BcRDR1* or *BcAGO2* may make pathogens unable to deliver sRNA effectors efficiently into the plant, allowing host immunity to remain active.

Apart from transgenic approaches, direct application of RNA-based molecules is a non-GMO alternative. It has been demonstrated that the direct application of dsRNAs or small RNA, known as spray-induced gene silencing (SIGS), has the potential to enhance plants' resistance to pathogens such as *Botrytis cinerea*, *Fusarium* spp., and *Sclerotinia sclerotiorum* (McLoughlin *et al.*, 2018; Qiao *et al.*, 2021; Wang *et al.*, 2016). This strategy has the added advantage of being temporally controllable and potentially specific to pathogens if the RNA

sequences are well-designed. My findings indicate that selecting RNA targets with high specificity to pathogen virulence genes, such as Bc-sRNAs associated with ckRNAi, while minimizing off-target effects in the host plant or non-target organisms, could be advantageous.

The modular nature of the ckRNAi machinery in *B. cinerea* also presents opportunities to develop multi-targeted control strategies. It is possible that by combining STTM constructs or RNA sprays that neutralize multiple components (e.g., BcRDR1, BcAGO1, and BcAGO2), we could construct a layered defense that prevents both sRNA biogenesis and delivery. Such multiplexed approaches might help mitigate the risk of pathogen adaptation or resistance development, which is a common concern with single-gene resistance strategies.

Synthetic biology tools may further enhance these RNA-based interventions. The development of promoter engineering, inducible expression systems, and tissue-specific expression allow for precise delivery of HIGS or STTM. The methods can reduce the metabolic burden on the plants and ensuring targeted and precise timing of defense activation. The use of synthetic RNA aptamers can also be considered for binding and inhibiting pathogen sRNAs in plants without the need to express full-length transgenes.

Although many promising strategies have been developed in present days, several challenges remain before they can be applied in the field. First of all, the stability of applied RNA under environmental conditions (e.g. UV irradiation, rain, temperature, microbial degradation) needs to be improved. Research is currently underway to explore the use of nanoparticle encapsulation and formulation additives to extend the shelf life and absorption efficiency of RNA-based sprays (Mitter *et al.*, 2017; Rank & Koch, 2021). Secondly, the legal rules for RNA bio-pesticides are different in each country and are still being discussed and developed. People have a more positive view of RNA technology than they do of GMO crops. This view must be addressed through education and clear communication.

More studies are needed to understand how ckRNAi mechanisms function in fungal pathogens. If RDR and AGO proteins have similar roles in different species, we may be able to design universal or clade-specific RNA-based interventions. To find conserved sRNA effectors and mechanistic components that can be used against a wide range of targets, it's crucial to compare genomes and analyze all RNA from different pathogens.

Another frontier in the field that may be worth exploring is the diagnostic and predictive potential of ckRNAi. It has been suggested by several studies that sRNAs accumulated in plant tissues during the early stages of infection may serve as biomarkers of the pathogen's presence or its virulence potential. It is possible that by combining RNA analysis with machine learning, we could create predictive models of infection severity or disruption to resistance that could inform precision agriculture interventions.

Last but not the least, it is important to carefully consider the ecological consequences of manipulating sRNA communication. While our research is primarily focused on pathogenic fungi, scientists also looked into the communication between beneficial microorganisms and plants via small RNAs (Silvestri *et al.*, 2025). It is essential to understand the specificity and collateral effects of RNA-based treatment. The understanding is crucial to avoid accidental breakage of beneficial microbiota or plant symbionts.

Together, the mechanistic insights gained in this thesis redefine the molecular dialogue between *B. cinerea* and its host and point the way forward for innovative and sustainable crop protection strategies. From my understanding, the targeting of ckRNAi offers a promising framework for precise, durable, and ecologically safe control of fungal diseases.

References

Amselem, Joelle, Christina A Cuomo, Jan AL van Kan, Muriel Viaud, Ernesto P Benito, Arnaud Couloux, Pedro M Coutinho, Ronald P de Vries, Paul S Dyer, and Sabine Fillinger. 2011. 'Genomic analysis of the necrotrophic fungal pathogens *Sclerotinia sclerotiorum* and *Botrytis cinerea*', *PLoS genetics*, 7: e1002230.

Bartel, David P. 2004. 'MicroRNAs: genomics, biogenesis, mechanism, and function', *Cell*, 116: 281-97.

Baulcombe, David. 2004. 'RNA silencing in plants', *Nature*, 431: 356-63.

Bi, Kai, Yong Liang, Tesfaye Mengiste, and Amir Sharon. 2023. 'Killing softly: a roadmap of *Botrytis cinerea* pathogenicity', *Trends in plant science*, 28: 211-22.

Cai, Qiang, Baoye He, Karl-Heinz Kogel, and Hailing Jin. 2018a. 'Cross-kingdom RNA trafficking and environmental RNAi—nature's blueprint for modern crop protection strategies', *Current opinion in microbiology*, 46: 58-64.

Cai, Qiang, Lulu Qiao, Ming Wang, Baoye He, Feng-Mao Lin, Jared Palmquist, Sienna-Da Huang, and Hailing Jin. 2018b. 'Plants send small RNAs in extracellular vesicles to fungal pathogen to silence virulence genes', *Science*, 360: 1126-29.

Carthew, Richard W, and Erik J Sontheimer. 2009. 'Origins and mechanisms of miRNAs and siRNAs', *Cell*, 136: 642-55.

Catalanotto, Caterina, Gianluca Azzalin, Giuseppe Macino, and Carlo Cogoni. 2002. 'Involvement of small RNAs and role of the qde genes in the gene silencing pathway in Neurospora', *Genes & development*, 16: 790-95.

Chang, Shwu-Shin, Zhenyu Zhang, and Yi Liu. 2012. 'RNA interference pathways in fungi: mechanisms and functions', *Annual review of microbiology*, 66: 305-23.

Cheng, An-Po, Lihong Huang, Lorenz Oberkofler, Nathan R Johnson, Adrian-Stefan Glodeanu, Kyra Stillman, and Arne Weiberg. 2025. 'Fungal Argonaute proteins act in bidirectional cross-kingdom RNA interference during plant infection', *Proceedings of the National Academy of Sciences*, 122: e2422756122.

Cheng, An-Po, Seomun Kwon, Trusha Adeshara, Vera Göhre, Michael Feldbrügge, and Arne Weiberg. 2023a. 'Extracellular RNAs released by plant-associated fungi: from fundamental mechanisms to biotechnological applications', *Applied microbiology and biotechnology*, 107: 5935-45.

Cheng, An-Po, Bernhard Lederer, Lorenz Oberkofler, Lihong Huang, Nathan R Johnson, Fabian Platten, Florian Dunker, Constance Tisserant, and Arne Weiberg. 2023b. 'A fungal RNA-dependent RNA polymerase is a novel player in plant infection and cross-kingdom RNA interference', *PLoS pathogens*, 19: e1011885.

Choquer, Mathias, Elisabeth Fournier, Caroline Kunz, Caroline Levis, Jean-Marc Pradier, Adeline Simon, and Muriel Viaud. 2007. '*Botrytis cinerea* virulence factors: new insights into a necrotrophic and polyphageous pathogen', *FEMS microbiology letters*, 277: 1-10.

Colombo, Marina, Graça Raposo, and Clotilde Théry. 2014. 'Biogenesis, secretion, and intercellular interactions of exosomes and other extracellular vesicles', *Annual review of cell and developmental biology*, 30: 255-89.

Dang, Yunkun, Qiuying Yang, Zhihong Xue, and Yi Liu. 2011. 'RNA interference in fungi: pathways, functions, and applications', *Eukaryotic cell*, 10: 1148-55.

Dean, Ralph, Jan AL Van Kan, Zacharias A Pretorius, Kim E Hammond-Kosack, Antonio Di Pietro, Pietro D Spanu, Jason J Rudd, Marty Dickman, Regine Kahmann, and Jeff Ellis. 2012. 'The Top 10 fungal pathogens in molecular plant pathology', *Molecular plant pathology*, 13: 414-30.

Derbyshire, Mark, Malick Mbengue, Marielle Barascud, Olivier Navaud, and Sylvain Raffaele. 2019. 'Small RNAs from the plant pathogenic fungus *Sclerotinia sclerotiorum* highlight host candidate genes associated with quantitative disease resistance', *Molecular plant pathology*, 20: 1279-97.

Dunker, Florian, Adriana Trutzenberg, Jan S Rothenpieler, Sarah Kuhn, Reinhard Pröls, Tom Schreiber, Alain Tissier, Ariane Kemen, Eric Kemen, and Ralph Hückelhoven. 2020. 'Oomycete small RNAs bind to the plant RNA-induced silencing complex for virulence', *Elife*, 9: e56096.

Elmer, PAG, and T Reglinski. 2006. 'Biosuppression of *Botrytis cinerea* in grapes', *Plant Pathology*, 55: 155-77.

Ender, Christine, and Gunter Meister. 2010. 'Argonaute proteins at a glance', *Journal of cell science*, 123: 1819-23.

Espino, José, Mario González, Celedonio González, and Nélida Brito. 2014. 'Efficiency of different strategies for gene silencing in *Botrytis cinerea*', *Applied microbiology and biotechnology*, 98: 9413-24.

Fulci, Valerio, and Giuseppe Macino. 2007. 'Quelling: post-transcriptional gene silencing guided by small RNAs in *Neurospora crassa*', *Current opinion in microbiology*, 10: 199-203.

Galagan, James E, and Eric U Selker. 2004. 'RIP: the evolutionary cost of genome defense', *TRENDS in Genetics*, 20: 417-23.

Ghildiyal, Megha, and Phillip D Zamore. 2009. 'Small silencing RNAs: an expanding universe', *Nature Reviews Genetics*, 10: 94-108.

Greenshields, David L, and Jonathan DG Jones. 2008. 'Plant pathogen effectors: getting mixed messages', *Current Biology*, 18: R128-R30.

He, Baoye, Qiang Cai, Lulu Qiao, Chien-Yu Huang, Shumei Wang, Weili Miao, Tommy Ha, Yinsheng Wang, and Hailing Jin. 2021. 'RNA-binding proteins contribute to small RNA loading in plant extracellular vesicles', *Nature plants*, 7: 342-52.

He, Baoye, Huan Wang, Guosheng Liu, Angela Chen, Alejandra Calvo, Qiang Cai, and Hailing Jin. 2023. 'Fungal small RNAs ride in extracellular vesicles to enter plant cells through clathrin-mediated endocytosis', *Nature communications*, 14: 4383.

Honda, Shinji, Ana Eusebio-Cope, Shuhei Miyashita, Ayumi Yokoyama, Annisa Aulia, Sabitree Shahi, Hideki Kondo, and Nobuhiro Suzuki. 2020. 'Establishment of N*eurospora crassa* as a model organism for fungal virology', *Nature communications*, 11: 5627.

Hutvagner, Gyorgy, and Martin J Simard. 2008. 'Argonaute proteins: key players in RNA silencing', *Nature reviews Molecular cell biology*, 9: 22-32.

Jeblick, Tanja, Thomas Leisen, Christina E Steidele, Isabell Albert, Jonas Müller, Sabrina Kaiser, Florian Mahler, Frederik Sommer, Sandro Keller, and Ralph Hückelhoven. 2023. '*Botrytis* hypersensitive response inducing protein 1 triggers noncanonical PTI to induce plant cell death', *Plant physiology*, 191: 125-41.

Jian, Jiao, and Xu Liang. 2019. 'One small RNA of *Fusarium graminearum* targets and silences CEBiP gene in common wheat', *Microorganisms*, 7: 425.

Jones, Jonathan DG, and Jeffery L Dangl. 2006. 'The plant immune system', *Nature*, 444: 323-29.

Jones, Jonathan DG, Brian J Staskawicz, and Jeffery L Dangl. 2024. 'The plant immune system: from discovery to deployment', *Cell*, 187: 2095-116.

Jones-Rhoades, Matthew W, David P Bartel, and Bonnie Bartel. 2006. 'MicroRNAs and their regulatory roles in plants', *Annu. Rev. Plant Biol.*, 57: 19-53.

Katiyar-Agarwal, Surekha, Rebekah Morgan, Douglas Dahlbeck, Omar Borsani, Andy Villegas Jr, Jian-Kang Zhu, Brian J Staskawicz, and Hailing Jin. 2006. 'A pathogen-inducible endogenous siRNA in plant immunity', *Proceedings of the National Academy of Sciences*, 103: 18002-07.

Koch, Aline, Dagmar Biedenkopf, Alexandra Furch, Lennart Weber, Oliver Rossbach, Eltayb Abdellatef, Lukas Linicus, Jan Johannsmeier, Lukas Jelonek, and Alexander Goesmann. 2016. 'An RNAi-based control of *Fusarium graminearum* infections through spraying of long dsRNAs involves a plant passage and is controlled by the fungal silencing machinery', *PLoS pathogens*, 12: e1005901.

Koch, Aline, Neelendra Kumar, Lennart Weber, Harald Keller, Jafargholi Imani, and Karl-Heinz Kogel. 2013. 'Host-induced gene silencing of cytochrome P450 lanosterol C14α-demethylase–encoding genes confers strong resistance to *Fusarium* species', *Proceedings of the National Academy of Sciences*, 110: 19324-29.

Kong, Xiuzhen, Meng Yang, Brandon H Le, Wenrong He, and Yingnan Hou. 2022. 'The master role of siRNAs in plant immunity', *Molecular plant pathology*, 23: 1565-74.

Kwon, Seomun, Oliver Rupp, Andreas Brachmann, Christopher Frederik Blum, Anton Kraege, Alexander Goesmann, and Michael Feldbrügge. 2021. 'mRNA inventory of extracellular vesicles from *Ustilago maydis*', *Journal of Fungi*, 7: 562.

Laluk, Kristin, and Tesfaye Mengiste. 2010. 'Necrotroph attacks on plants: wanton destruction or covert extortion?', *The arabidopsis Book/American society of plant biologists*, 8: e0136.

Liu, Peng, Xiaoxiang Zhang, Fan Zhang, Miaoze Xu, Zhuangxin Ye, Ke Wang, Shuang Liu, Xiaolei Han, Ye Cheng, and Kaili Zhong. 2021. 'A virus-derived siRNA activates plant immunity by interfering with ROS scavenging', *Molecular Plant*, 14: 1088-103.

Lovelace, Amelia H, Sara Dorhmi, Michelle T Hulin, Yufei Li, John W Mansfield, and Wenbo Ma. 2023. 'Effector identification in plant pathogens', *Phytopathology®*, 113: 637-50.

Luo, Changxin, Nawaz Haider Bashir, Zhumei Li, Chao Liu, Yumei Shi, and Honglong Chu. 2024. 'Plant microRNAs regulate the defense response against pathogens', *Frontiers in Microbiology*, 15: 1434798.

Mallory, Allison C, and Hervé Vaucheret. 2006. 'Functions of microRNAs and related small RNAs in plants', *Nature genetics*, 38: S31-S36.

McLoughlin, Austein G, Nick Wytinck, Philip L Walker, Ian J Girard, Khalid Y Rashid, Teresa de Kievit, WG Dilantha Fernando, Steve Whyard, and Mark F Belmonte. 2018. 'Identification and application of exogenous dsRNA confers plant protection against *Sclerotinia sclerotiorum* and *Botrytis cinerea*', *Scientific reports*, 8: 7320.

Mi, Shijun, Tao Cai, Yugang Hu, Yemiao Chen, Emily Hodges, Fangrui Ni, Liang Wu, Shan Li, Huanyu Zhou, and Chengzu Long. 2008. 'Sorting of small RNAs into *Arabidopsis* argonaute complexes is directed by the 5′ terminal nucleotide', *Cell*, 133: 116-27.

Mitter, Neena, Elizabeth A Worrall, Karl E Robinson, Peng Li, Ritesh G Jain, Christelle Taochy, Stephen J Fletcher, Bernard J Carroll, GQ Lu, and Zhi Ping Xu. 2017. 'Clay nanosheets for topical delivery of RNAi for sustained protection against plant viruses', *Nature plants*, 3: 1-10.

Nicolás, Francisco E, and Victoriano Garre. 2017. 'RNA interference in fungi: retention and loss', *The Fungal Kingdom*: 657-71.

Nowara, Daniela, Alexandra Gay, Christophe Lacomme, Jane Shaw, Christopher Ridout, Dimitar Douchkov, Götz Hensel, Jochen Kumlehn, and Patrick Schweizer. 2010. 'HIGS: host-induced gene silencing in the obligate biotrophic fungal pathogen *Blumeria graminis*', *The Plant Cell*, 22: 3130-41.

Oliveira-Garcia, Ely, Tej Man Tamang, Jungeun Park, Melinda Dalby, Magdalena Martin-Urdiroz, Clara Rodriguez Herrero, An Hong Vu, Sunghun Park, Nicholas J Talbot, and Barbara Valent. 2023. 'Clathrin-mediated endocytosis facilitates the internalization of *Magnaporthe oryzae* effectors into rice cells', *The Plant Cell*, 35: 2527-51.

Peláez, Pablo, and Federico Sanchez. 2013. 'Small RNAs in plant defense responses during viral and bacterial interactions: similarities and differences', *Frontiers in plant science*, 4: 343.

Porquier, Antoine, Constance Tisserant, Francisco Salinas, Carla Glassl, Lucas Wange, Wolfgang Enard, Andreas Hauser, Matthias Hahn, and Arne Weiberg. 2021. 'Retrotransposons as pathogenicity factors of the plant pathogenic fungus *Botrytis cinerea*', *Genome biology*, 22: 1-19.

Qiao, Lulu, Chi Lan, Luca Capriotti, Audrey Ah-Fong, Jonatan Nino Sanchez, Rachael Hamby, Jens Heller, Hongwei Zhao, N Louise Glass, and Howard S Judelson. 2021. 'Spray-induced gene silencing for disease control is dependent on the efficiency of pathogen RNA uptake', *Plant Biotechnology Journal*, 19: 1756-68.

Raman, Vidhyavathi, Stacey A Simon, Feray Demirci, Mayumi Nakano, Blake C Meyers, and Nicole M Donofrio. 2017. 'Small RNA functions are required for growth and

development of *Magnaporthe oryzae*', *Molecular plant-microbe interactions*, 30: 517-30.

Rank, Aline Pereira, and Aline Koch. 2021. 'Lab-to-field transition of RNA spray applications–how far are we?', *Frontiers in plant science*, 12: 755203.

Ren, Bo, Xutong Wang, Jingbo Duan, and Jianxin Ma. 2019. 'Rhizobial tRNA-derived small RNAs are signal molecules regulating plant nodulation', *Science*, 365: 919-22.

Rocafort, Mercedes, Isabelle Fudal, and Carl H Mesarich. 2020. 'Apoplastic effector proteins of plant-associated fungi and oomycetes', *Current opinion in plant biology*, 56: 9-19.

Rutter, Brian D, and Roger W Innes. 2017. 'Extracellular vesicles isolated from the leaf apoplast carry stress-response proteins', *Plant physiology*, 173: 728-41.

Selin, Carrie, Teresa R De Kievit, Mark F Belmonte, and WG Dilantha Fernando. 2016. 'Elucidating the role of effectors in plant-fungal interactions: progress and challenges', *Frontiers in Microbiology*, 7: 600.

Shiu, Patrick KT, Namboori B Raju, Denise Zickler, and Robert L Metzenberg. 2001. 'Meiotic silencing by unpaired DNA', *Cell*, 107: 905-16.

Silvestri, Alessandro, William Conrad Ledford, Valentina Fiorilli, Cristina Votta, Alessia Scerna, Jacopo Tucconi, Antonio Mocchetti, Gianluca Grasso, Raffaella Balestrini, and Hailing Jin. 2025. 'A fungal sRNA silences a host plant transcription factor to promote arbuscular mycorrhizal symbiosis', *New Phytologist*, 246: 924-35.

Song, Yin, and Bart PHJ Thomma. 2018. 'Host-induced gene silencing compromises *Verticillium* wilt in tomato and Arabidopsis', *Molecular plant pathology*, 19: 77-89.

Tanaka, Shigeyuki, and Regine Kahmann. 2021. 'Cell wall–associated effectors of plant-colonizing fungi', *Mycologia*, 113: 247-60.

Tang, Guiliang, Jun Yan, Yiyou Gu, Mengmeng Qiao, Ruiwen Fan, Yiping Mao, and Xiaoqing Tang. 2012. 'Construction of short tandem target mimic (STTM) to block the functions of plant and animal microRNAs', *Methods*, 58: 118-25.

Tang, Jun, Xueting Gu, Junzhong Liu, and Zuhua He. 2021. 'Roles of small RNAs in crop disease resistance', *Stress Biology*, 1: 6.

van Kan, Jan AL. 2006. 'Licensed to kill: the lifestyle of a necrotrophic plant pathogen', *Trends in plant science*, 11: 247-53.

Van Niel, Guillaume, Gisela d'Angelo, and Graça Raposo. 2018. 'Shedding light on the cell biology of extracellular vesicles', *Nature reviews Molecular cell biology*, 19: 213-28.

Veloso, Javier, and Jan AL van Kan. 2018. 'Many shades of grey in *Botrytis*–host plant interactions', *Trends in plant science*, 23: 613-22.

Voinnet, Olivier. 2009. 'Origin, biogenesis, and activity of plant microRNAs', *cell*, 136: 669-87.

Wang, Haixia, Ely Oliveira-Garcia, Petra C Boevink, Nicholas J Talbot, Paul RJ Birch, and Barbara Valent. 2023. 'Filamentous pathogen effectors enter plant cells via endocytosis', *Trends in plant science*, 28: 1214-17.

Wang, Ming, Arne Weiberg, Feng-Mao Lin, Bart PHJ Thomma, Hsien-Da Huang, and Hailing Jin. 2016. 'Bidirectional cross-kingdom RNAi and fungal uptake of external RNAs confer plant protection', *Nature plants*, 2: 1-10.

Weiberg, Arne, Marschal Bellinger, and Hailing Jin. 2015. 'Conversations between kingdoms: small RNAs', *Current opinion in biotechnology*, 32: 207-15.

Weiberg, Arne, Ming Wang, Feng-Mao Lin, Hongwei Zhao, Zhihong Zhang, Isgouhi Kaloshian, Hsien-Da Huang, and Hailing Jin. 2013. 'Fungal small RNAs suppress plant immunity by hijacking host RNA interference pathways', *Science*, 342: 118-23.

Williamson, Brian, Bettina Tudzynski, Paul Tudzynski, and Jan AL Van Kan. 2007. '*Botrytis cinerea*: the cause of grey mould disease', *Molecular plant pathology*, 8: 561-80.

Wong-Bajracharya, Johanna, Vasanth R Singan, Remo Monti, Krista L Plett, Vivian Ng, Igor V Grigoriev, Francis M Martin, Ian C Anderson, and Jonathan M Plett. 2022. 'The ectomycorrhizal fungus *Pisolithus microcarpus* encodes a microRNA involved in cross-kingdom gene silencing during symbiosis', *Proceedings of the National Academy of Sciences*, 119: e2103527119.

Zhang, Bo-Sen, Ying-Chao Li, Hui-Shan Guo, and Jian-Hua Zhao. 2022. '*Verticillium dahliae* secretes small RNA to target host MIR157d and retard plant floral transition during infection', *Frontiers in plant science*, 13: 847086.

Zhou, Xin, Jinting Wang, Fang Liu, Junmin Liang, Peng Zhao, Clement KM Tsui, and Lei Cai. 2022. 'Cross-kingdom synthetic microbiota supports tomato suppression of Fusarium wilt disease', *Nature communications*, 13: 7890.

Acknowledgment

I would first like to thank my supervisor Prof. Dr. Arne Weiberg for offering me the opportunity to work on this fascinating project. Your technical and knowledgeable support means a lot to me. I enjoyed all of our discussions, which I could always feel your passion for science. It was really my pleasure working with you. I learned a lot from you in the past five years. You have been as a great mentor and I am very happy that you are now being as a professor in the new university.

I would like to thank my TAC members Prof. Dr. Martin Parniske and Prof. Dr. Michael Feldbrügge. You always brought valuable points to my project and gave me many constructive career suggestions during our discussion.

I would like to thank the members of AG Weiberg over the past five years, especially to Florian, Constance, Bernhard, Lorenz, and Ronald. We had an awesome collaboration and great relationship in the lab. We had a great time and I believe that we elevated the Weiberg lab to the next level. The past five years with you are memorable to me.

I want to thank my talented students Fabian, Theresa, Kyra, and Adrian. It was my pleasure doing experiments and discussing with you. The projects were running well because of your participation.

I would like to thank members in the Genetics for so many interesting communication, discussion, and events. I enjoy a lot working in this environment.

I would like to thank our collaborators who provided strong support and input. Dr. Nathan R. Johnson for the bioinformatic analysis. Dr. Stefan Krebs for Illumina sequencing. Dr. Ignasi Forné for the MS spec analysis.

I would like to thank my family for fully supporting the idea of me coming far away to study for my doctorate.

Lastly, I would like to especially thank my partner Jingli Lao for her strong mental support over the years. My achievement in science and living life here in Germany is really count on you. Your contribution to my daily life is priceless.